PHD

Studies on insulin-stimulated GLUT4 vesicle fusion with plasma membrane using in vitro fusion systems

Jin, Bo

Award date:
2007

Awarding institution:
University of Bath

Studies of insulin-stimulated GLUT4 vesicle fusion with plasma membrane using *in vitro* fusion systems

Bo Jin

A thesis submitted for the degree of Doctor of Philosophy

University of Bath

Department of Biology and Biochemistry

May 2007

ProQuest LLC
789 East Eisenhower Parkway
P.O. Box 1346
Ann Arbor, MI 48106-1346

Abstract

GLUT4 is the main insulin-regulated glucose transporter, which is present in insulin-responsive tissues. In the un-stimulated cells, GLUT4s are localized in intra-cellular GLUT4 storage vesicles (GSV). In response to insulin stimulation, GSVs rapidly translocate, dock and fuse with the plasma membrane in order to expose GLUT4 to the extra-cellular glucose. The insulin-stimulated GLUT4 vesicle translocation is a multi-step exocytotic process but the crucial regulated and rate determining step along this process has been previously difficult to resolve.

The work described in this thesis investigates the fusion process in the exocytotic limb of the GLUT4 translocation pathway using two *in vitro* systems. The first of these assays used plasma membrane reconstituted into liposomes and studied their fusion with immuno-isolated GLUT4 vesicles. To aid the isolation of biologically active GLUT4 vesicles in the first fusion system, the maltose-binding protein-protein A fusion protein were cloned and expressed.

In this system, fusion is SNARE proteins and cytoplasm dependent but not cytoskeleton dependent. The rate of the fusion activity is stimulated 8-fold by the insulin activated plasma membrane fraction. Both the magnitude and time course of stimulated fusion recapitulate the insulin response of intact cells. Akt from the cytoplasm fraction is required for fusion. However the participation of Akt in the stimulation of fusion is dependent on its *in vitro* recruitment onto the insulin-activated plasma membrane. These data reveal that insulin activation of the plasma membrane fraction of the fusion reaction is an essential step in regulation. Inhibition of fusion was found using a Ca^{2+} chelator and a V-ATPase inhibitor, suggesting roles of Ca^{2+} and the V-ATPase in the fusion mechanism.

The second fusion assay system used only recombinant SNAREs reconstituted into liposomes. Experiments using the second fusion system show that fusion is cytoplasm and Ca^{2+} dependent. The kinetics and characteristics of this fusion system have been studied and have been compared with the more complex system utilizing components obtained from insulin sensitive cells.

Acknowledgements

I would like to express my deepest gratitude to my supervisor Professor Geoffrey D. Holman (University of Bath) for his constant help, encouragement, patience, comments and for his great guidance throughout the research, to make this research work possible. It has been my greatest pleasure and honor to be his student and work with him.

I would like to thank Dr. Francoise Koumanov for her selfless guidance and help in my research work at University of Bath. I also would like to thank Dr. Paul R. Whitley, my internal examiner for his guidance.

I wish to thank all the staffs, students and friends (Jing, Scott, Judith, Amelia, Sunil, Joe, Huailo, David et al) I have worked with in Lab 1.37, who share much of their talents, knowledge and research experience with me. It is really a great pleasure to work in this environment. Thank you all!

I wish to thank the ORS and the Department of Biology and Biochemistry in University of Bath, who funded this research. I also wish to thank all the staffs in the animal house for their help.

A special gratitude should be expressed to my parents and Yanwu Guo. Throughout my study in the University of Bath, they provided me with the firmest support. A big "thank you" should also go to all my friends and families in China, who are always believing in me and giving me the best wishes.

Table of content

Abbreviations

A23187	A mobile ion-carrier that forms stable complexes with divalent cations, also known as Calcimycin, calcium ionophore
Ab	Antibody
AEBSF	[4-(2-Aminoethyl)benzenesulfonylflouride, HCl]
AMP	Adenosine 5'-monophosphate
AMPK	AMP activated protein kinase
APS	ammonium persulphate
AS160	Akt substrate of 160 kDa
ATP	adenosine 5'-triphosphate
BAPTA	1,2- bis(o-aminophenoxy)ethane-N,N,N',N'-tetraacetic acid, sodium
BAPTA-AM	1,2- bis(o-aminophenoxy)ethane-N,N,N',N'-tetraacetic acid tetrakis (acetoxymethyl ester)
bp	Base pair
BSA	Bovine Serum Albumin
BoLC/B BoNT/B	Botulinum neurotoxin light chain/B protease
cpm	Counts per minute
C-term	C-terminal
Da	Daltons
dH_2O	Single distilled water
ddH_2O	Double distilled water
DMSO	Dimethyl Sulfoxide
DPA	Dipicolinic Acid
DTT	$_{DL}$-Dithiothreitol
E. coli	Escherichia coli
ECL	Enhanced chemiluminescence
EDTA	Diaminoethanetetra-acetic acid disodium salt
EGTA	Ethylene Glycol-bis(β-aminoethylether) N, N, N', N'-tetraacetic acid
ELISA	Enzyme-Linked Immuno-sorbent Assay
ERC	Endosomal recycling compartment
Eu	Europium
FFP18	Fluorescent dye which selectively monitors near membrane calcium and has low calcium affinity
g	Gram
g	Gravity
GDI1	GDP dissociation inhibitor 1
GLUT	Glucose Transporter
GLUT4	Glucose Transporter 4

GST	Glutathione S-transferase
GSV	GLUT4 Storage Vesicle
h	Hour
HA	Haemagglutinin
HDM	High density microsomes
HEPES	N-[2-Hydroxyethyl]piperazine-N'-[2-ethenesulfonic acid]
HRP	Horseradish peroxidase
IC_{50}	The half maximal inhibitory concentration, represents the concentration of an inhibitor that is required for 50 % inhibition of its target
IgG	Immunoglobulin G
IPTG	Isopropyl-β-D-thiogalactopyranoside
IRAP	Insulin-responsive aminopeptidase
IRS	Insulin receptor substrate
kbp	Kilo base pairs
kDa	Kilo daltons
KRH	Krebs-Ringer-HEPES
LB	Luria Broth
LDM	Low density microsomes
LDS	Lithium dodecyl sulfate
MBS	m-Maleimidobenzoyl-N-Hydroxysuccinimide ester
MCS	multiple cloning site
MES	2-(N-morpholino)ethane sulfonic acid
min	Minutes
MOPS	3-(N-Morpholino)propanesulfonic acid
mTORC2	mammalian target of rapamycin complex-2
NSF	N-ethylmaleimide sensitive factor
N-term	N-terminal
O.D.	Optical density
PBS	Phosphate Buffered Saline
PC	1-Palmitoyl-2-Oleoyl-sn-Glycero-3-Phosphocholine
PCR	Polymerase Chain Reaction
PDK1	3'-phosphoinositide-dependent kinase-1
PE	L-α-Phosphatidylethanolamine
Pi	Inorganic phosphate
PI	Phosphatidylinositol
PI3K	Phosphatidylinositol 3-Kinase
PIKfyve	Phosphoinositide kinase for five position containing a fyve finger
PH domain	Pleckstrin-homology domain
PKA	Protein Kinase A
PKB	Protein Kinase B
PKC	Protein Kinase C
PM	Plasma Membrane

PS	1, 2-Dioleoyl-sn-Glycero-3-[Phospho-L-Serine] (Sodium Salt)
PTPases	Protein tyrosine phosphatases
PTB domain	Phosphotyrosine binding domain
rpm	Revolutions per minutes
rcf	Relative centrifugation force = "*g*"
SA	Streptavidin
SDS	Sodium Dodecyl Sulphate
SDS-PAGE	Sodium Dodecyl Sulphate-Polyacrylamide Gel Electrophoresis
sec	Seconds
SH2	Src homology 2
SH3	Src homology 3
siRNA	Small interfering RNA
SNAP	Soluble *N*-ethylmaleimide sensitive factor attachment protein
SNARE	soluble *N*-ethylmaleimide sensitive factor attachment protein receptor
Spa	*Staphylococal* protein A
TAE	Tris-acetate EDTA
TBS	Tris-buffered Saline
TBS-T	Tris-buffered Saline containing Tween-20
TE	t-SNARE reconstituted Europium encapsulated liposome
TEMED	N, N, N', N'-tetramethylethylenediamine
TES	Tris-EDTA Sucrose
TfR	Transferrin receptor
TGN	Trans-Golgi Network
Thesit	Nonaethylene glycol monododecyl ether
Tris	Tris(hydroxymethyl)methylamine
t-SNARE	SNARE proteins present on the plasma membrane
Tween-20	Polyoxyethylene sorbitan monolaureate
U	Units
UV	Ultra Violet
V	Volts
VAMP	Vesicle-associated membrane protein
VD	v-SNARE reconstituted DPA encapsulated liposomes
v-SNARE	SNARE proteins present on the vesicle membrane
X-gal	5-bromo-4-chloro-3-indolyl-b-D-galactopyranoside
W13	N-(4-aminobutyl)-5-chloro-2-naphthalenesulfonamide

List of figures

List of tables

Chapter 1 Introduction

1.1 Glucose homeostasis

Glucose is one of the main sources of energy in eukaryotic organisms. It plays a central role in metabolism and cellular homeostasis. Therefore the level of glucose in the blood is very tightly regulated. Most mammalian cells are dependent on a continuous supply of glucose, which acts as one of the primary sources for the generation of adenosine-5'-triphosphate (ATP) (Gould and Holman, 1993). In normal individuals, the blood glucose level is normally in a range of 3.5 - 5.5 mM (0.63 - 1 mg/ml) (Tuch et al., 2000).

Glucose homeostasis is maintained by the coordinated regulation of 3 processes: glucose absorption *via* the small intestine, glucose production in the liver, and consumption of glucose by nearly all tissues. These three processes are regulated by two hormones: insulin and glucagon. In response to elevated circulating glucose (e.g. after a meal), insulin is secreted into the bloodstream by the pancreatic β cells and promotes glucose uptake in insulin responsive tissues. By contrast, when blood glucose concentration is low (e.g. periods between meals), glucagon is secreted and stimulates the breakdown of glycogen from liver and the release of glucose into the blood.

Abnormal levels of blood glucose cause severe problems to health. Low blood glucose concentrations (hypoglycemia) can cause seizures, loss of consciousness, and irreversible cell damage. Excessive blood glucose concentrations (hyperglycemia) have a detrimental effect referred to as "glucotoxicity", which can result in blindness, renal failure, cardiac and peripheral vascular disease, and neuropathy (Scheepers et al., 2004). In

addition, as glucose is the main regulator of insulin secretion and production, excessive amounts of glucose over a prolonged period have negative effects on pancreatic β cell function, resulting in increased basal insulin release, reduced maximal secretory response, and a gradual depletion of insulin stores (Kaiser et al., 2003). Thus, blood glucose concentrations need to be maintained within narrow limits and kept at a steady level.

1.1.1 Diabetes

The disease diabetes mellitus constitutes a vast majority of pathological cases of abnormality in glucose homeostasis. The International Diabetes Federation estimated that the global number of people with diabetes will rise from 194 million in 2003 to 333 million by 2025 (Zimmet et al., 2003). This will be an overall increase of 72 %, while in Africa, Asia and Middle East the expected increase is 90 - 100 % (Jenkins and Campbell, 2004). Diabetes results from a deficiency of insulin or a loss of response to insulin. The resulting elevated blood glucose causes the kidneys to excrete glucose in the urine. When the cells, which normally use glucose as energy supply, are lacking in glucose, fat becomes the main source of energy for cellular respiration. However, breakdown of fat causes the accumulation of acidic metabolites in the blood which is harmful to eyes, brains and can be life threatening.

There are mainly two classifications of diabetes mellitus. Type 1, insulin dependent diabetes mellitus, is a type of organ-specific autoimmune disorder characterized by the destruction of pancreatic β cells which consequently impairs insulin secretion. Type 2, non insulin dependent diabetes mellitus, which makes up about 90 % of the patients suffering from diabetes mellitus (Bennett, 1994), is mostly a result of faulty insulin action rather than the consequence of alterations in the levels of insulin in the

blood (as is the case for type 1). In other words, in type 2 diabetes mellitus, insulin is present in the blood, but the body's cells no longer react properly to insulin and therefore cannot use it. This phenomenon is generally referred to as "insulin resistance". This is usually due to abnormalities on the cell surface of insulin responsive cells or within the cell, or both.

1.2 The glucose transporter families

Since glucose plays a central role in cellular metabolism, the transport of glucose across the plasma membrane of mammalian cells is one of the most important cellular nutrient transport events. Because the lipid bilayer of the eukaryotic plasma membrane is impermeable for hydrophilic molecules, glucose is transported across the plasma membrane by membrane associated carrier proteins, glucose transporters. The three processes to maintain glucose homeostasis mentioned earlier (section 1.1) are accomplished with the help of the glucose transporter proteins. They are divided into two main groups: the facilitative glucose transporters (GLUT) and the sodium/glucose co-transporters (SGLT) (Bell et al., 1990; Carruthers, 1990). The plasma membranes of virtually all mammalian cells contain GLUT proteins. The GLUT transport system for glucose is the facilitative diffusion type: these transporters allow the movement of glucose across the plasma membrane down a chemical gradient either into or out of cells. These transporters are specific for the D-enantiomer of glucose and are not coupled to any energy-requiring components, such as ATP hydrolysis or a H^+ gradient (Gould and Holman, 1993). In contrast, the sodium/glucose co-transporters (SGLT), mainly expressed in intestine and kidney, actively accumulate glucose into the cells against its concentration gradient and across the luminal surface. The glucose concentrated inside the cells by them moves outward *via* GLUT proteins which are located mainly at the basolateral surface (Scheepers et al., 2004).

1.2.1 The tissue expression and function of glucose transporters

The human GLUT family consists of 14 members, 11 of which have been shown to catalyze sugar transport (Fig 1.1). Their genes appear to belong to the family of solute carriers 2A (*SLC2A*). The individual isoforms exhibit different substrate specificities, kinetic characteristics, and expression profiles, thereby allowing a tissue-specific adaptation of glucose uptake through regulation of their gene expression.

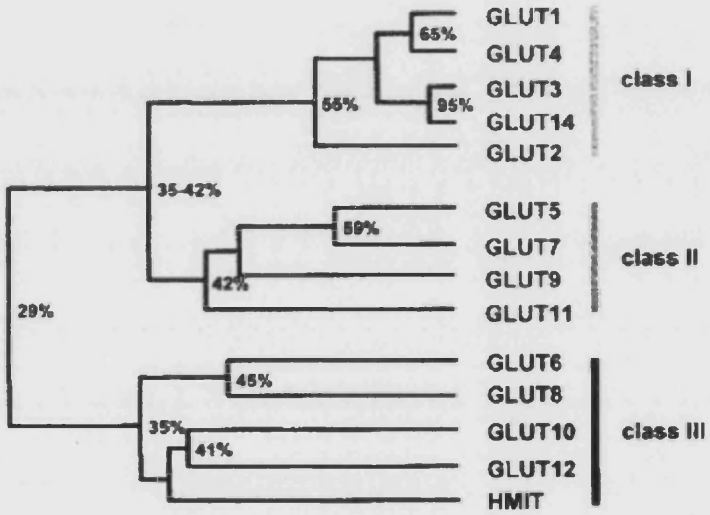

Fig 1.1 Dendrogram of the family of human sugar transporters. The alignment was performed with the CLUSTAL program. Numbers at the branches of the tree indicate percentage of identity (Scheepers et al., 2004).

According to sequence similarities and characteristic elements, they are divided into three subfamilies (Joost and Thorens, 2001).

The class I GLUTs comprise GLUT1 to 4 and the recently identified GLUT14. GLUT1 to 4 are thoroughly characterized isoforms. GLUT1 is ubiquitously expressed and responsible for the basic supply of cells with glucose. It exhibits highest expression levels in erythrocytes and endothelial cells of the

brain (Mueckler et al., 1985). GLUT2 is predominantly expressed in pancreatic β cells, liver, kidney, and small intestine (basolateral membrane). It transports fructose, glucosamine and glucose (Fukumoto et al., 1988; Uldry et al., 2002; Wood and Trayhurn, 2003). GLUT3 is a high-affinity glucose transporter with predominant expression in tissues with a high glucose requirement such as brain (Kayano et al., 1988). GLUT4 is a high-affinity glucose transporter expressed in insulin-sensitive tissues (heart, skeletal muscle, adipose tissue) (Fukumoto et al., 1989). Insulin stimulates the translocation of GLUT4 from intracellular compartments to the plasma membrane, resulting in an approximate 20-30-fold increase in glucose transport in rat adipocytes (Holman et al., 1990b; Taylor and Holman, 1981), 2-4-fold in human adipocytes (Pedersen and Gliemann, 1981), 7-fold in rat muscle (Ploug et al., 1987) and 2-fold in human muscle (Dohm et al., 1988). The values for the fold changes are approximate and can vary depending on the tissue preparation for experiment. In addition, in skeletal muscle translocation of GLUT4 can be induced by muscle contraction and hypoxia (Cartee et al., 1991; Lund et al., 1995). GLUT14 is exclusively expressed in testis. The amino acid sequence of GLUT14 is 95 % identical with GLUT3 (Wu and Freeze, 2002).

The class II GLUTs include the fructose-specific transporter GLUT5 and three related isoforms, GLUT7, GLUT9, and GLUT11. GLUT5 exhibits virtually no glucose transport activity and is responsible for the uptake of fructose in small intestine, testis, and kidney (Kayano et al., 1990). GLUT7 is a high-affinity transporter for glucose and fructose in small intestine, colon, testis, and prostate (Li et al., 2004). GLUT9, which is suggested to be critical for early pre-implantation development (Carayannopoulos et al., 2004), is a glucose transporter highly expressed in kidney and liver, lowly expressed in small intestine, placenta, lung, and leukocytes (Phay et al., 2000). GLUT11 is a fructose transporter with low affinity for glucose, expressed

predominantly in pancreas, kidney but also moderately in heart and skeletal muscle (Doege et al., 2001).

Class III GLUTs comprise the transporter isoforms GLUT6, GLUT8, GLUT10, GLUT12, and HMIT. GLUT6 is a low-affinity glucose transporter, predominantly expressed in brain, spleen, and peripheral leukocytes (Doege et al., 2000a). GLUT8 and GLUT12 are glucose transporters whose activity can be inhibited by D-fructose and D-galactose, indicating that they might be multifunctional transporters (Ibberson et al., 2000; Rogers et al., 2003). GLUT8 is predominantly expressed in testis (Doege et al., 2000b) and GLUT12 in heart and prostate (Rogers et al., 2003). GLUT10 is predominantly expressed in the liver and pancreas but its substrate specificity is not clear (Andersen et al., 2003; McVie-Wylie et al., 2001). The H^+-coupled *myo*-inositol transporter (HMIT) is expressed predominantly in the brain. It specifically transports *myo*-inositol and related stereoisomers but lacks any glucose transport activity (Uldry et al., 2001).

These different characteristics allow a complex and specific regulation of glucose uptake according to the cellular requirements and the physiologic conditions of substrate supply (Joost and Thorens, 2001). Table 1.1 summaries the characteristics of all the GLUT isoforms.

Table 1.1 Summary of tissue distribution, substrate specificity and other characteristics for GLUT isoforms. (N/A: data not available)

Class	Name	Tissue distribution	Substrate specificity	Characteristics
I	GLUT1	Erythrocytes, Brain endothelial cells (blood-brain barrier)	Glucose	Basic supply for cells
	GLUT2	Pancreas, liver, kidney, small intestine	Glucose (low), Fructose, Glucosamine (high)	Glucose uptake totally depends on blood glucose concentration
	GLUT3	Brain (neuronal), Testis	Glucose (high)	N/A
	GLUT4	Heart, Skeletal muscle, Adipose tissue	Glucose (high)	Insulin-responsive translocation
	GLUT14	Testis	N/A	N/A
II	GLUT5	Small intestine, Testis, Kidney	Fructose (specific)	No glucose transport activity
	GLUT7	Small intestine, Colon, Testis, Prostate	Glucose (high) Fructose (high)	N/A
	GLUT9	Kidney, liver (high), small intestine, placenta, lung, and leukocytes (low)	glucose	N/A
	GLUT11	pancreas, kidney, and placenta (high), heart and skeletal muscle (moderate)	Fructose, Glucose (low)	N/A
III	GLUT6	brain, spleen, and peripheral leukocytes	Glucose (low)	N/A
	GLUT8	Testis	Glucose (high)	N/A
	GLUT10	liver and pancreas	N/A	N/A
	GLUT12	heart and prostate	Glucose	N/A
	HMIT	brain	*myo*-inositol and related stereoisomers	No glucose transport activity

1.2.2 The structure of glucose transporters

Although the overall sequence homology between the members of GLUTs family is less than 30 % (Fig 1.1) (Scheepers et al., 2004), there is a much

higher degree of structural similarity. The common features revealed by sequence alignment and analysis of all the above-mentioned transporters include (Joost and Thorens, 2001): (1) 12 transmembrane hydrophobic helices as secondary structure with both the N- and C-termini at the cytoplasmic surface, (2) seven conserved glycine residues in the helices (1, 2, 4, 5, 7, 8 and 10) as *Sugar/polyol transporter signatures*, (3) several basic and acidic residues at the intracellular surface of the proteins, whose interaction mediates the conformational alteration of the transporter during the translocation of the substrate (Schurmann et al., 1997) and provide the proper membrane topology (Sato and Mueckler, 1999), (4) two conserved tryptophan residues in helices 6 and 11 which have been shown to be essential for both transport activity and ligand (cytochalasin B, forskolin) binding (Garcia et al., 1992; Schurmann et al., 1993), and (5) two conserved tyrosine residues in helices 4 and 7 which have also been shown to be important for the function of GLUT1 and GLUT4 (Mori et al., 1994; Wandel et al., 1994).

The three classes of GLUTs also have their specific features. Residues that appear specific for the class I transporters are a glutamine in helix 5 (QL motif corresponding with Q161 in GLUT1; (Mueckler et al., 1994)) and the STSIF-motif in the extracellular loop 7 (Doege et al., 1998). The specific characteristic of class II transporters is the lack of the tryptophan following the conserved GPXXXP motif in helix 10 (corresponding with tryptophan 388 in GLUT1, which is shown to be important for cytochalasin B and forskolin binding, but not for glucose transport activity) (Garcia et al., 1992; Schurmann et al., 1993). Class III GLUTs are characterized by a shorter extracellular loop 1 that lacks a glycosylation site, and by the presence of such a site in the larger loop 9 (Joost and Thorens, 2001).

1.3 GLUT4: the insulin-regulated glucose transporter

Glucose transporter 4 (GLUT4) is the major glucose transporter of muscle, adipose cells and cardiac cells. It is unique amongst other members of the GLUT family because it is mainly present on insulin-sensitive cells and is delicately regulated by insulin through posttranslational events. Insulin maintains glucose homeostasis largely by enhancing glucose uptake into insulin-sensitive fat and muscle tissues. GLUT4 is responsible for insulin-stimulated glucose transport into the cells of these targeted tissues.

Observations have indicated that GLUT4 plays a crucial role in whole-body glucose homeostasis. Firstly, insulin-stimulated glucose transport is an important rate-limiting step for glucose metabolism in both muscle and fat tissue, and is severely disrupted in type 2 diabetes (Bryant et al., 2002). Secondly, GLUT4 knock-out mice show mild or strong insulin resistance (Watson et al., 2004b). In contrast, over expression of the human GLUT4 in muscle and fat tissue in the diabetic DB/DB mouse model protect these animals from insulin resistance or diabetes (Watson et al., 2004b). Accordingly, understanding the molecular and cellular characteristics and mechanisms of GLUT4 and its regulation could possibly yield new targets for therapeutic interventions for diabetes, one of the most prevalent diseases that we will have to confront in the near future.

1.3.1 GLUT4 in insulin-sensitive cells

In 1980, Cushman's group and Kono's group independently found insulin caused the redistribution of "glucose transport activity" from intracellular membrane compartments to the cell surface (Cushman and Wardzala, 1980; Suzuki and Kono, 1980). By measuring glucose binding and transport activity in membrane fractions isolated from rat adipocytes, they found that insulin resulted to a decrease of this activity in the intracellular membrane

fraction but at the same time caused a simultaneous increase in the plasma membrane fraction. This specific "glucose transport activity" was confirmed to be one isoform of the GLUTs family in 1989, when five independent groups reported the cloning of the cDNA encoding this isoform - GLUT4 (Birnbaum, 1989; Charron et al., 1989; Fukumoto et al., 1989; James et al., 1989; Kaestner et al., 1989). This allowed the generation of the GLUT4 antibodies which provided an important tool for further study of this protein.

Like all the GLUTs proteins, the structure of GLUT4 also contains 12 transmembrane domains with the N- and C- terminus facing the cytoplasm (Fig 1.2). A number of sorting signals are present in the structure. These include a FQQI motif at the N-terminus and a dileucine motif with an acidic cluster downstream at the C-terminus. The FQQI motif functions in the GLUT4 endocytosis from the plasma membrane and the trafficking from endosomal compartments into the insulin responsive perinuclear storage compartment (Al Hasani et al., 2002; Garippa et al., 1994; Melvin DR et al., 1999). The dileucine motif acts during the endocytosis of GLUT4 from the plasma membrane and exit of GLUT4 from the trans-Golgi network (TGN) (Garippa et al., 1996; Palacios et al., 2001; Subtil et al., 2000). The C-terminal acidic cluster appears to function in the targeting of GLUT4 from endosomes to a subdomain of the TGN enriched in the t-SNARE (SNARE stands for soluble *N*-ethylmaleimide sensitive factor attachment protein receptor) proteins syntaxin 6 and 16 (Shewan et al., 2003).

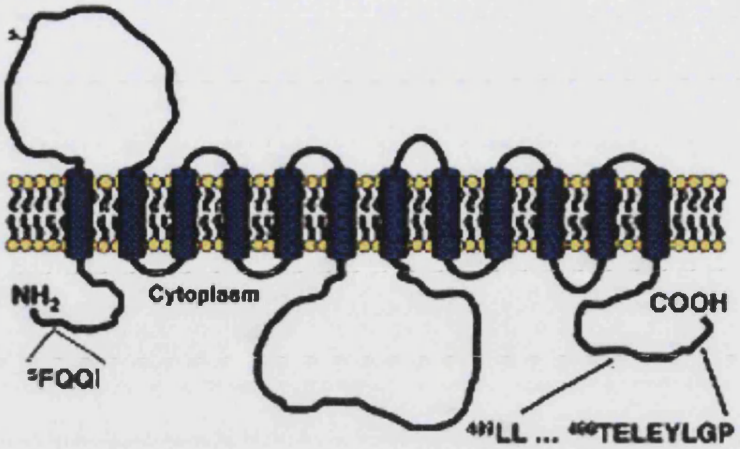

Fig 1.2 Schematic diagram of the predicted transmembrane topology of GLUT4. See text for details (Watson et al., 2004b).

Muscle and adipose cells are the major tissues displaying insulin-dependent glucose uptake. Although GLUT1 expresses at low level in those tissues and is insulin-sensitive to some extent (Rudich A et al., 2003), it is not the major player in this event. Insulin increases glucose uptake primarily *via* GLUT4 rather than GLUT1. In the basal state, approximately 5 - 10 % of the GLUT4 is located at the cell surface and > 90 % in intracellular compartments. This steady-state distribution is resulted from the fast endocytosis and slow exocytosis of the GLUT4 (Patel et al., 2005; Yang and Holman, 1993). When cells are stimulated with insulin, GLUT4 proteins rapidly translocate from the intracellular compartments to the plasma membrane and become exposed to the outside of the cells so as to be able to transport glucose into the cells. It can be readily visualized by using a fluorescent tag (Fig 1.3), or by photo-labeling and protein pull-down techniques. GLUT4 vesicle movement can also be recorded under microscopy once GLUT4 is labeled (Lizunov et al., 2005; Oatey et al., 1997).

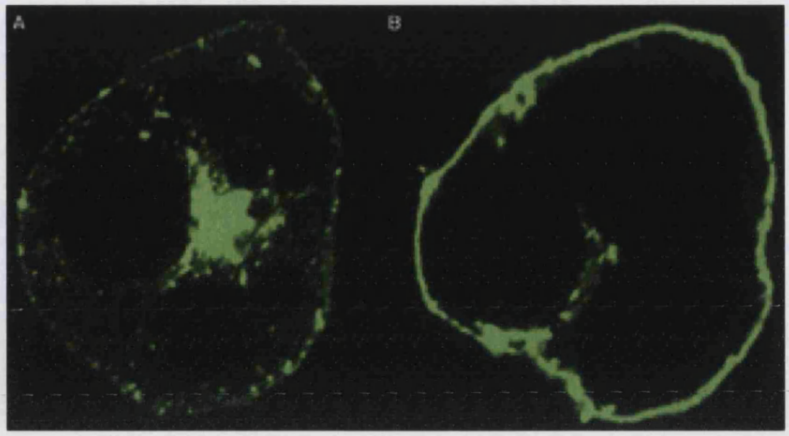

Fig 1.3 Insulin stimulation results in the translocation of GLUT4 from intracellular storage sites to the plasma membrane. Differentiated 3T3-L1 adipocytes were transfected with a GLUT4-enhanced green fluorescent protein fusion construct and then incubated in the absence (A) or presence (B) of insulin for 30 min. The cells were fixed and subjected to confocal fluorescent microscopy (Watson et al., 2004b).

1.3.2 Intracellular GLUT4 compartments

In basal state GLUT4s sequester in the intracellular compartments. The understanding of these compartments helps in figuring out the whole picture of GLUT4 translocation. There are three classifications for intracellular GLUT4 compartments. One is by Klip's group (Dugani and Klip, 2005), namely "ERC pool" and "non-ERC pool" respectively where ERC stands for endosomal recycling compartment. This denomination comes from the study using chemical ablation of transferrin receptor (TfR) - containing compartments. TfR, an ERC marker, identifies two populations of GLUT4 pools: one overlapping with TfR (ERC pool), and one separating away from it (non-ERC pool) (Martin et al., 1996). The non-ERC pool is thought to be the compartment that insulin stimulates to translocate, therefore recognized as the "GLUT4 storage vesicle (GSV)" compartment. The second classification is by James' group (Larance et al., 2005). They claim in the

basal state GLUT4 is localized in three kinds of compartments: the endosomal system, the trans-Golgi network (TGN) and the highly insulin-responsive GLUT4 storage vesicle (GSV). The third classification is by Kandror's group (Xu et al., 2006). They indicate that there are at least two GLUT4 vesicular populations: ubiquitous cellugyrin-positive transport vesicles and specialized cellugyrin-negative insulin-responsive GLUT4 storage vesicles (GSV). Cellugyrin is a four transmembrane domain containing protein, representing a ubiquitous analogue of the major synaptic vesicle protein - synaptogyrin. Cellugyrin-positive vesicles are not enriched in GLUT4 and do not translocate to plasma membrane. It is suggested that they may represent intracellular transport vesicles en route to GSVs.

The characteristics of GSV have been studied extensively. James' group concludes that the major membrane proteins in GSVs are GLUT4, IRAP and VAMP2 (Larance et al., 2005). IRAP is an insulin-responsive aminopeptidase. It co-segregates with GLUT4 and undergoes the same insulin-stimulated redistribution. It is thought to move with GLUT4 across the different compartments in parallel (Dugani and Klip, 2005). VAMP2 is the vesicle-associated protein 2, a vesicular soluble N-ethylmaleimide-sensitive factor attachment protein receptor (v-SNARE). It is recognized to be the protein that is more likely to mark the GSV. It is required for the GLUT4 fusion with the plasma membrane in insulin stimulated state (Koumanov et al., 2005). However, stimuli apart from insulin such as hypertonic shock and platelet-derived growth factor do not require VAMP2 to increase GLUT4 levels on plasma membrane, but depends on another v-SNARE VAMP7 (Bryant et al., 2002; Watson et al., 2004b). This raises the question of whether GSV includes a sub-class of VAMP2 positive vesicles or whether VAMP2 joins the GSVs when cells are stimulated by insulin. The remaining proteins are probably endosomal or TGN-derived. They include the Rab proteins which are associated with insulin signalling cascade, assistant

proteins for SNARE-mediated membrane fusion and so on. By using protein mass spectrometry, a full screen of the proteins on GSV has been analysed (Larance et al., 2005).

Recently it has been found that GSVs are formed in a series of sorting events of GLUT4. The GLUT4 sorting from the TGN to the GSVs requires a Golgi-localized γ-ear-containing Arf-binding protein (GGA) (Watson et al., 2004a). GGA interacts with sortilin, a TGN and endosomal membrane protein which is thought to be necessary for the formation of small GLUT4 enriched vesicles (Shi and Kandror, 2005). Whether these vesicles bear other characteristics of the GSVs is still under investigation.

1.3.3 Regulation of GLUT4 trafficking

Kinetic studies identify that it is the exocytosis process that is stimulated by insulin (Satoh et al., 1993; Yang and Holman, 1993). Recently McGraw's group indicates that GLUT4 distribution between the plasma membrane and the intracellular compartments is maintained by an insulin-modulated bipartite dynamic mechanism (Martin et al., 2006). In other words, in basal state the GLUT4s undergo slow efflux and rapid internalization dynamically and attain equilibrium; insulin stimulates this exchange rate to break the equilibrium and realize the GLUT4 translocation.

Apart from the insulin signalling cascade, in skeletal and cardiac myocytes, muscle contraction also induces an increase in glucose transport. The acute effect of muscle contractions on glucose transport is independent of insulin and reverses rapidly after cessation of exercise.

For both of those stimuli, there have been extensive but not yet completed studies.

A) Insulin

A complicated signalling cascade is involved in insulin-stimulated glucose transport, the full extent of which has not been identified. The translocation of GLUT4 to the plasma membrane following stimulation with insulin may require regulation at various steps. There has been at least two pathways identified or postulated: the phosphatidylinositol (PtdIns) 3-kinase (PI 3-kinase) pathway (Kanzaki and Pessin, 2003) (Fig 1.4) and the Rho-family GTPase TC10 pathway (Baumann et al., 2000). The former is well established and the latter remains controversial.

The PI 3-kinase pathway involves a series of activation cascades. The interaction of insulin with the insulin receptor (IR) on the outer surface of the plasma membrane activates the protein tyrosine-kinase activity that is associated with the β-subunit of the receptor. The receptor then phosphorylates itself and IR substrate-1 (IRS1). Phosphorylated IRS1 binds to phosphatidylinositol (PtdIns) 3-kinase (PI 3-kinase), which is recruited to the plasma membrane and converts the inositol phospholipid PtdIns-4,5-bisphosphate (PtdIns(4,5)P2) to PtdIns-3,4,5-trisphosphate (PIP3). The increased amount of PIP3 results in its interaction with Akt/protein kinase B (PKB) at the pleckstrin homology (PH) domain, thereby recruiting Akt/PKB to the plasma membrane. At the plasma membrane, phosphorylation of Akt/PKB at Thr308 by PIP3-bound 3-phosphoinositide-dependent protein kinase-1 (PDK1) results in Akt/PKB activation. PIP3 also triggers the activation of the mammalian target of rapamycin complex-2 (mTORC2) by an unknown mechanism, allowing mTORC2 to phosphorylate Akt/PKB at Ser473 for maximal activation. These phosphorylated upstream molecules are directly or indirectly inducing GLUT4 translocation from the GSV compartment to the plasma membrane. The cascade until Akt/PKB activation is well established.

Akt/PKB then phosphorylates downstream proteins. The cascade downstream of Akt/PKB activation is still under investigation. Of many of Akt/PKB substrates, three have been identified as being involved in insulin-stimulated glucose transport (Watson and Pessin, 2006): AS160 (Akt substrate of 160 kDa) (Kane et al., 2002), PIKfyve (phosphoinositide kinase for five position containing a fyve finger) and synip.

AS160 consists of two phosphotyrosine binding (PTB) domains, a Rab-GAP domain (GAP stands for GTPase-activating protein) and five PKB phosphorylation sites (Sano et al., 2003). Rab proteins are small G-proteins involved in vesicle trafficking (section 1.4.1). In their GTP-bound form, the Rab protein is involved in vesicle movement and fusion. The Rab-GAP stimulates the intrinsic GTPase activity of the Rab to generate the inactive GDP-bound form of the Rab. AS160 is specific for Rabs 2A, 8A, 10 and 14 which are present on the GLUT4 vesicles (Kessler et al., 2000; Larance et al., 2005; Miinea et al., 2005). It is shown to be associated with GLUT4 vesicles in the basal state but not with insulin-stimulated GLUT4 vesicles (Larance et al., 2005). A mechanism involving AS160 and GLUT4 translocation to the plasma membrane has been addressed. It suggests that the insulin-stimulated translocation of GLUT4 requires a Rab to be in its active GTP form. In basal cells, the Rab involved in translocation is maintained in its inactive GDP form by the GAP domain of AS160. When AS160 is phosphorylated by insulin-activated Akt, the GAP activity of AS160 is inhibited. This increases the level of the active GTP form of a Rab and thus GLUT4 vesicle translocation is triggered (Sano et al., 2003). This theory has further been confirmed by the use of short-hairpin RNA (shRNA) to knockdown the AS160 protein (Eguez et al., 2005). Results confirmed that the AS160 GAP activity was required for the basal retention of GLUT4.

PIKfyve is the second protein identified as being downstream of Akt/PKB and involved in insulin-stimulated GLUT4 translocation. It co-localizes with a highly motile subpopulation of GLUT4 vesicles. Akt/PKB phosphorylates PIKfyve at serine 318 and this phosphorylation stimulates the PI(3)P 5-kinase activity of the enzyme. It then catalyses the synthesis of PI(5)P and PI(3,5)P2. PIKfyve was first reported to have a role in insulin-stimulated glucose transport by the use of dominant-negative kinase-dead PIKfyve (Ikonomov et al., 2002). Expression of a PIKfyve construct mutated at the Akt/PKB phosphorylation site enhances insulin-stimulated GLUT4 translocation (Berwick et al., 2004). This gives evidence for the role of PIKfyve in GLUT4 trafficking. However, further experiments are needed to determine if PIKfyve is an important signalling molecule in this process.

Another recently identified Akt substrate involved in GLUT4 translocation is the SNARE (soluble *N*-ethylmaleimide sensitive factor-attachment receptor)-associated protein synip (Yamada et al., 2005). Synip was originally identified to interact with syntaxin4 (Min et al., 1999). Syntaxin4 is a t-SNARE localized to the cell surface, whereas another SNARE molecule, VAMP2, is localized to GLUT4 vesicles (sections 1.4.2, 1.4.3). Interactions between syntaxin4 and VAMP2, together with other fusogenic molecules, are thought to drive the fusion of GLUT4 vesicle with the plasma membrane. As a working model, synip binds to syntaxin4 in the basal state and blocks the ability of VAMP2 to interact productively with syntaxin4 (Min et al., 1999). Although several other syntaxin-binding proteins including tomosyn and Munc18c have also been reported to prevent the translocation of GLUT4 by interfering with the SNARE-dependent fusion mechanism (Tamori et al., 1998; Tellam et al., 1997; Thurmond and Pessin, 2000; Widberg et al., 2003), synip is the only one that is observed to be under regulation by insulin. Insulin induces the dissociation of synip from syntaxin4, thus enabling productive SNARE pairing between syntaxin4 and VAMP2 (Min et

al., 1999). Insulin stimulation results in the Akt phosphorylation of synip at Ser99, leading to the dissociation of the synip-syntaxin4 complex (Yamada et al., 2005). Mutation of Ser99 prevents the dissociation of synip from syntaxin4 and inhibits GLUT4 translocation in a dominant interfering manner. Thus, the insulin-stimulated phosphorylation of synip by Akt might provide a mechanism for insulin to regulate the docking or fusion of GLUT4 vesicles with the cell surface. However, this hypothesis is still controversial, because other results suggest that phosphorylation of synip at Ser99 is not necessary for GLUT4 translocation (Sano et al., 2005).

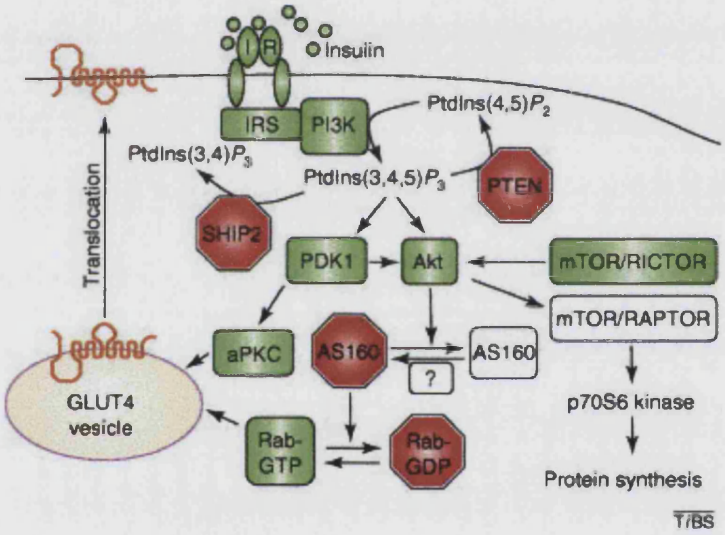

Fig 1.4 Schematic diagram showing the relation between insulin-signaling and GLUT4 vesicles translocation through PI3-kinase pathway. See text for details (Watson RT and Pessin JE., 2006).

The TC10 pathway is known as a PI 3K-independent signalling pathway. It was only identified in adipose cells but not muscle cells (Baumann et al., 2000). This pathway originates in caveolae or in lipid rafts, involves tyrosine phosphorylation of the proto-oncogene c-Cbl and results in the activation of a small GTP-binding protein, TC10, a member of the Rho family GTPases. To date this pathway remains controversial as some groups found that this

pathway has no effect on insulin signalling to GLUT4 (Zhou et al., 2004).

B) Contraction and exercise

Independent of insulin, the contraction-stimulated GLUT4 translocation in muscle cells is believed to be the result of the activation of a different pathway. It involves the AMP-activated protein kinase (AMPK), which is activated by a contraction-induced rise in AMP (Adenosine 5'-monophosphate) and a concomitant drop in ATP. The downstream targets of AMPK that are involved in GLUT4 translocation await their identifications. Some chemical inhibitors suggest one or more protein kinase C (PKC) isoforms are involved (Luiken et al., 2004). It also has been found that contraction increases the insulin sensitivity in those cells. However, the basic mechanism underlying this phenomenon still remains a mystery (Holloszy, 2005).

1.4 Membrane fusion

The fusion of GLUT4 vesicles with the plasma membrane is an important step in exposing GLUT4 to the exterior of the cell, thus enabling it to transport its hexose substrate into and out of the cell. There is evidence that insulin, as well as stimulating translocation of GLUT4 vesicles to the plasma membrane, also directly promotes the docking and fusion of vesicles to the plasma membrane (Inoue et al., 1999; Timmers et al., 1996). This up-regulation by insulin occurs both on the plasma membrane and on GLUT4 vesicles. Insulin treatment affects intracellular pH (Yang et al., 2002b; Yang et al., 2002a), interaction of SNAREs with proteins such as synip (Min et al., 1999; Tellam et al., 1997; Watson and Pessin, 2006), and calcium ion concentration (Whitehead et al., 2001), all of which affect membrane fusion.

In general, membrane fusion is a universal reaction with great diversities. It occurs in all life forms, from the extra- and intra-cellular fusion of viral pathogens with host cells, the extra-cellular fusion of eukaryotic cells, to the intra-cellular fusion of organelles. Despite the diversity, all fusion reactions embody a fundamental process which includes membrane contact, membrane merger and the opening of an aqueous fusion pore (Jahn et al., 2003) (Fig 1.5).

Two models are widely involved to describe the fusion: the "proximity" model and the "protein-pore" model. The "proximity" model shows a fusion pore lined by lipids. According to the stalk hypothesis (Chernomordik et al., 1987; Kozlov and Markin, 1983), counteracting electrostatic forces are overcome, lipids of the proximal leaflets interact, thus membranes are brought to close proximity, which is termed as "tethering" or "docking". Then the boundary between the hydrophilic and hydrophobic portion of the bilayer is destabilized, the proximal monolayers merge to form a stalk, then the fusion pore open. The "protein-pore" model shows a fusion pore formed from transmembrane segments of proteins. When the fusion pore dilates, the transmembrane segments separate laterally, lipids are incorporated into the pore, and the bilayers merge. Normally the opening of the fusion pore is followed by an irreversible gradual expansion of the fusion pore, and it causes full fusion (Lindau and Almers, 1995). In some cases, the initial fusion pore is followed by its rapid closure in a kiss-and-run event (Fisher et al., 2001; Lindau and de Toledo, 2003).

Although fusion can be demonstrated in pure lipid vesicles free of protein (Chanturiya et al., 1997), in most of the cases fusion is strongly influenced by certain proteins, which include Rab proteins, SNARE proteins, and a variety of assisting proteins.

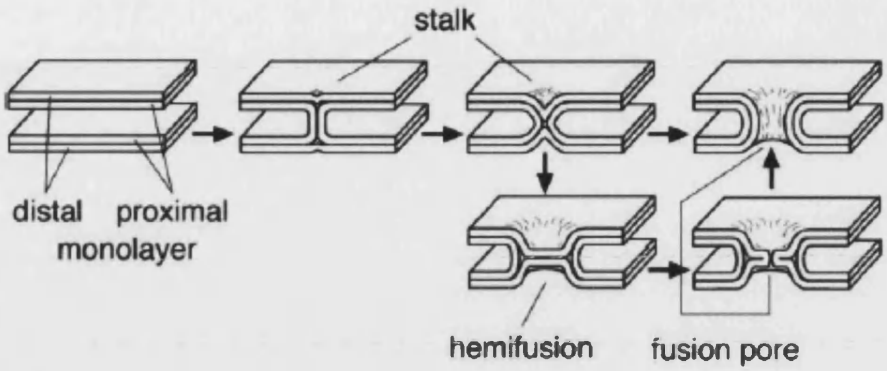

Fig 1.5 Hypothetical formation of a fusion pore (Jahn et al., 2003).

1.4.1 Rab proteins

When an intracellular transport vesicle ("donor") is destined to fuse with an "acceptor" membrane, it first needs to recognize its partner membrane by physical contact in a specific location, which is termed as "tethering" or "docking". This provides specificity to the fusion reactions. Tethering or docking is thought to be mediated by the Rab family of small GTPase proteins. They shuttle between a soluble GDP bound form that is inactive and a membrane bound GTP bound form that is active. In most fusion reactions, active Rabs on the donor membrane recruit effectors (often by assembly of multimeric complexes) that are present in the acceptor membrane, thereby tethering the two membranes together (Jahn et al., 2003). During or after fusion, Rab proteins are inactivated by GTPase-activating proteins (GAPs), and dissociated from the respective membrane to initiate a new cycle of fusion. As mentioned earlier, several isoforms of Rab proteins have been identified on GLUT4 vesicles and a mechanism has been raised to bridge insulin signalling and GLUT4 translocation through AS160 and Rab (section 1.3.3.A).

1.4.2 SNARE hypothesis

SNARE proteins (soluble *N*-ethylmaleimide-sensitive factor attachment protein receptor) are thought to act following the tethering of transport vesicles and target membrane. Since the late 1980s, when SNARE proteins were first characterized, rapid progress has identified SNAREs as key elements in membrane fusion.

SNAREs were originally identified in synaptic vesicles, and are a super family of small proteins with 25 members in yeast, 36 members in human and 54 members in plant (Jahn and Scheller, 2006). They have a simple domain structure. A characteristic of SNAREs is the SNARE motif: an evolutionarily conserved stretch of 60 - 70 amino acids that are arranged in heptad repeats. At their C-terminal ends, most SNAREs have a single transmembrane domain that is connected to the SNARE motif by a short linker. Many SNAREs have independently folded domains that are positioned N-terminal to the SNARE motif and that vary between the subgroups of SNAREs (Fasshauer, 2003; Hong, 2005).

SNARE proteins can be functionally classified as vesicular (v-SNARE) and target (t-SNARE) SNAREs according to the membrane on which they are present. The best characterized SNARE proteins are those involved in synaptic transmission. They are the t-SNAREs syntaxin1 and SNAP25, which reside on the plasma membrane, and the v-SNARE VAMP2 (vesicle-associated membrane protein, also known as synaptobrevin), which is present on synaptic vesicles. Following the tethering, SNAREs engage in trans-complexes that bridge the fusion membrane. When the membranes fuse, the SNAREs align with each other to form cis-complexes (Fig 1.6). After fusion SNARE complexes are dissociated so that the individual SNARE proteins can be recycled with their resident membranes.

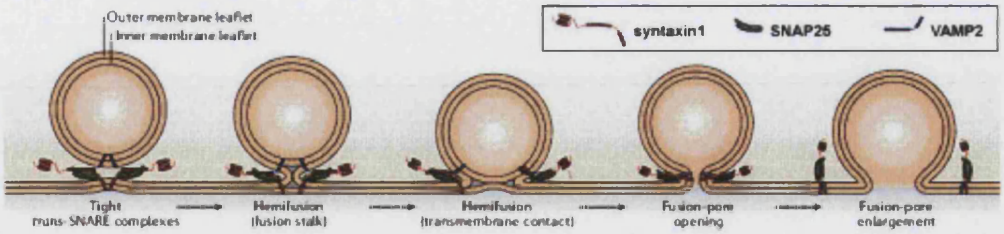

Fig 1.6 Hypothetical transition states in SNARE-mediated fusion according to the stalk hypothesis. The SNAREs form trans-complex to tether the vesicle in close proximity. Then by either bent (possibly strained), or the C-terminal ends pulled into the hydrophobic core of the bilayer, the SNAREs form *cis* complexes before fusion is complete. In this case, the assembly of at least some SNARE complexes might therefore be complete before fusion-pore opening (Jahn and Scheller, 2006).

1.4.3 SNARE in GLUT4 exocytosis

Membrane fusion displays selectivity among different pairs of v- and t-SNARE proteins (McNew et al., 2000; Whyte and Munro, 2002). Earlier it has been mentioned that GLUT4 traffics through a series of intracellular compartments (section 1.3.2). The v-SNARE VAMP2 is a selective marker for GLUT4 Storage Vesicles (GSV), a subset of GLUT4 vesicles that largely segregate from TfR and which are the most competent for insulin-stimulated GLUT4 vesicle fusion with plasma membrane (Bryant et al., 2002; Watson et al., 2004b). The t-SNAREs in the target plasma membrane are syntaxin4 and SNAP23. The insulin signalling can target components of the vesicle-PM fusion machinery through the mechanism described earlier on (section 1.3.3). Other proteins like tomosyn and munc18c can bind syntaxin4 to modulate the insulin-dependent gain in surface GLUT4 (Hodgkinson et al., 2005; Widberg et al., 2003). Although Rab-mediated tethering typically occurs *via* an intermediate tethering complex rather than directly to SNARE proteins, Rab4 is found to interact with the SNARE protein syntaxin4 in an insulin dependent manner (Li et al., 2001). This

finding suggests that Rab4 may directly link long and short range transport of GLUT4 vesicles in the exocytic pathway under insulin regulation.

1.4.4 Methods to study membrane fusion

There are various methods to study membrane fusion. In living cells, organelles are stained with fluorescent or luminescent markers and the process is monitored under microscopy (Lizunov et al., 2005). The living-cell fusion assays exactly represent the event happening in cells in real time. The drawbacks are that the assays are normally hard to manipulate. There are enormous interference factors in living cells, which would affect the event that is studied. Hence, many groups have set up cell-free fusion assays to study versatile fusion events in organisms. In the yeast system, yeast vacuoles are isolated by density gradient centrifugation and are applied directly in fusion reactions (Mayer et al., 1996; Rothman and Orci, 1992). In various cells, endosomes are harvested, labeled and mixed together *in vitro* to check the endocytic fusion events (Luzio et al., 2005; Rizzoli et al., 2006). In 1990s, fusion of lysosomes and late endosomes has been shown in a cell-free system and proved to be ATP, cytosol and temperature dependent (Mullock et al., 1994; Mullock et al., 1998). This fusion requires the presence of NSF (*N*-ethylmaleimide sensitive factor) and SNAPs (soluble NSF attachment proteins) and is inhibited by Rab-GDI (GDP dissociation inhibitor), which implies a need for a Rab GTPase. These characteristics are consistent with the action of the fusion machinery used at many other sites on the secretory and endocytic pathways and are in accordance to the tenets of the SNARE hypothesis (Rothman, 1994). An *In vitro* assay has also been set up to reconstitute mitochondria inner and outer membrane fusion (Meeusen et al., 2004). Not only vesicles directly purified from cells, but also artificial liposomes are used in numerous studies to investigate the functions of proteins of interest. Using the reconstituted

liposomes fusion assay, SNARE proteins have been confirmed as the minimal machinery to drive membrane fusion (Weber et al., 1998).

In the reconstituted liposome fusion assay, fluorometric methods exploit processes, such as nonradioactive energy transfer, fluorescence quenching and pyrene excimer formation, which are dependent on probe concentration (Blumenthal et al., 2002; Duzgunes and Wilschut, 1993; Hoekstra D., 1990; Hoekstra, 1990; Stegmann et al., 1989). Assays of membrane fusion report either the mixing of membrane lipids (lipid mixing) or the mixing of the aqueous contents of the fused entities (content mixing). There are also additional methods for detecting membrane fusion based on image analysis (Yates and Rampersaud, 1998) or carbon-fiber amperometry (Graham et al., 2002).

A) Lipid Mixing

Struck, Hoekstra and Pagano introduced lipid-mixing assays based on NBD-rhodamine energy transfer (Struck et al., 1981). In this method, membranes labeled with a combination of fluorescence energy transfer donor and acceptor lipid probes - typically NBD-PE and *N*-Rhodamin-PE, respectively - are mixed with unlabeled membranes. Fluorescence resonance energy transfer (FRET) is detected as rhodamine emission at ~585 nm resulting from NBD excitation at ~470 nm. The fluorescence decreases when the average spatial separation of the probes is increased upon fusion of labeled membranes with unlabeled membranes (Fig 1.7). This assay has been successfully used in the study of membrane fusion (Wilschut et al., 1992). The reverse detection scheme has also proven to be a useful lipid-mixing assay (Uster, 1993; Weber et al., 1998).

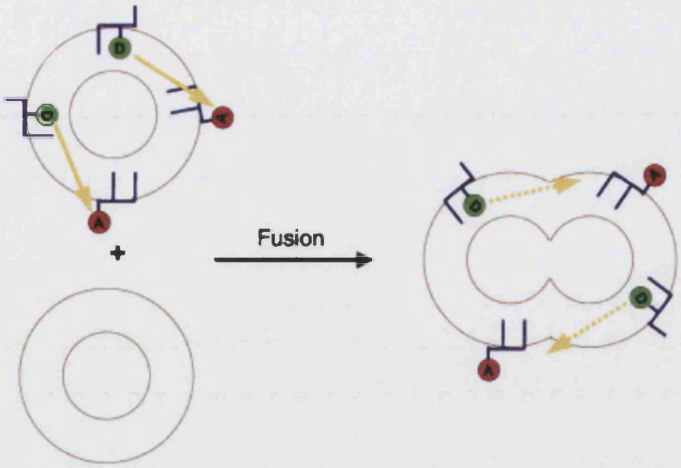

Fig 1.7 Pictorial representation of a lipid-mixing assay based on fluorescence resonance energy transfer (FRET). The average spatial separation of the donor (D) and acceptor (A) lipid probes increases upon fusion of labeled membranes with unlabeled membranes. This results in decreased efficiency of proximity-dependent FRET (represented by yellow arrows). Decreased FRET efficiency is registered by increased donor fluorescence intensity and decreased acceptor fluorescence intensity.

Lipid mixing assays can also be based on self-quenching of octadecyl rhodamine B fluorescence (Hoekstra et al., 1984). Fusion increases the space between octadecyl rhodamine B so as to decrease self-quenching and increase fluorescence. This assay is extensively used for detecting virus fusion with cells (Cheetham et al., 1994; Srinivasakumar et al., 1991). Another lipid mixing assay, based on pyrene excimer formation (Bron et al., 1993), has also been applied to study membrane fusion (Bron et al., 1994).

A drawback of the lipid mixing assay is that incomplete fusion can produce a positive signal. In the hemi-fusion step (Fig 1.6, Fig 1.5), the fluorescent probe can move through the phospholipid bilayer bridge. In this case a positive signal can be detected although fusion is not complete.

B) Content Mixing

Leakage of aqueous contents from cells or vesicles as a result of lysis, fusion or a change in physiological permeability can be detected fluorometrically using low molecular weight soluble tracers. Assays designed to detect solution mixing often rely on a fluorophore and quencher pair, and this provide a technique to monitor content mixing.

Wilschut and Papahadjopoulos originally described a content mixing assay of fluorescent enhancement with Tb^{3+}/dipicolinic acid (DPA) (Wilschut et al., 1980). In this assay, separate vesicle populations are loaded with $TbCl_3$ or DPA. Vesicle fusion results in formation of Tb^{3+}/DPA chelates that are ~10,000 times more fluorescent than free Tb^{3+} (Wilschut et al., 1980). Fluorescence of the chelates is detected at 490 nm or 545 nm, following excitation at 276 nm. Including Ca^{2+} and EDTA in the external medium inhibits formation of the complex outside the fused vesicles. The Tb^{3+}/DPA fluorescence enhancement assay has been used to investigate the role of phospholipid conformation in vesicle fusion (Glaser and Gross, 1994) and the interaction of cardiotoxin with phospholipid vesicles (Chien et al., 1994).

There are also other assays for content mixing. Fluorescence quenching assays with ANTS/DPX were originally developed by Smolarsky and co-workers to follow complement-mediated immune lysis (Smolarsky et al., 1977). This assay is based on the collisional quenching of the polyanionic fluorophore ANTS by the cationic quencher DPX. The ANTS/DPX fluorescence quenching assay has since been widely used to detect membrane fusion (Bailey and Cullis, 1994; Epand et al., 1995).

1.4.5 Role of Ca^{2+} in membrane fusion and insulin-stimulated GLUT4 exocytosis

The hypothesis that SNAREs form the basic molecular apparatus that forces lipid bilayers to fuse is widely supported (Jahn, 2004; Sorensen, 2004).

However, this does not imply that SNAREs alone are required to induce vesicle exocytosis in organisms. SNAREs alone are sufficient to induce fusion of liposomes, but the kinetics of these events does not mimic the kinetics that has been observed in synaptic vesicle fusion *in vivo* (Hu et al., 2003; Weber et al., 1998). Additional accessory proteins must serve to regulate the fusion reaction. In the most extensively studied vesicle exocytosis and membrane fusion event, the neuronal transmitter release, Ca^{2+} triggers exocytosis from neurons and neuroendocrine cells. The delay between a rapid rise in Ca^{2+} and a postsynaptic response can be as short as 60 to 200 μsec, placing strong kinetics constraints on the transduction pathway that culminates in secretion (Llinas et al., 1981; Sabatini and Regehr, 1996). Therefore one particularly important accessory protein is needed to sense Ca^{2+}.

A protein has been found to work in this process. Strong evidences support that synaptotagmin functions as the Ca^{2+} sensor which regulates SNARE-mediated exocytosis in neurotransmitter release (Augustine, 2001; Chapman, 2002; Tucker et al., 2004). Upon binding Ca^{2+}, the loop domains of the synaptotagmin partially penetrate into lipid bilayers that contain anionic phospholipids (Bai et al., 2004a; Chapman and Davis, 1998; Davis et al., 1999), which has been proved essential for the action of Ca^{2+}-synaptotagmin during fusion (Bhalla et al., 2005). Some isoforms of synaptotagmin oligomerize in the presence of Ca^{2+}, providing another route through which Ca^{2+} could regulate exocytosis (Tucker and Chapman, 2002). In addition, synaptotagmin binds to the t-SNAREs syntaxin and SNAP25 (Davis et al., 1999; Tucker et al., 2004). Mutations that selectively disrupt this binding reduce the rate of secretion and destabilize fusion pores in PC12 cells (Bai et al., 2004b). Together these findings suggest that synaptotagmin acts on a state of vesicles in which SNARE complexes have fully assembled. The SNARE complex assembly creates a metastable

fusion intermediate. The Ca^{2+}-triggered synaptotagmin insertion and its interaction with the t-SNAREs destabilize the intermediate and regulate the opening and closing of fusion pores.

The role of Ca^{2+} in membrane fusion has also been studied from another perspective. In yeast vacuole fusion, Ca^{2+} efflux from vacuole has been found critical (Peters and Mayer, 1998). Ca^{2+} concentration inside of yeast vacuole is > 2 mM, accumulated by active transport through an ATP-driven Ca^{2+} pump and a Ca^{2+}/H^{+} exchanger. In the studies, the Ca^{2+} ionophore ionomycin and Ca^{2+}-ATPase inhibitors strongly inhibited fusion. Strong Ca^{2+} chelator 1,2-bis(o-aminophenoxy)ethane-N,N,N',N'-tetraacetic acid (BAPTA) was also found inhibiting if present in the whole fusion process, but not if removed before the fusion initiated. All these facts suggest that the process relevant to fusion is the Ca^{2+} efflux from the vacuole lumen. The inhibitors were added to ongoing fusion at different time points, from the beginning of fusion to the time point of full resistance, ie, when fusion was not inhibited any more. The inhibitory time course of ionomycin and BAPTA was much longer than the one of GDP dissociation inhibitor 1 (GDI1). GDI1 is a docking marker (Mayer and Wickner, 1997). The longer inhibitory effect means that when docking is completed, fusion is still inhibited by ionomycin and BAPTA. This finding indicates that Ca^{2+} is required in the post-docking phase. The conclusion is remarkably similar with the finding in synaptic vesicle fusion. In synaptic vesicle fusion calmodulin was required as the receptor for the Ca^{2+} signal. But unlike synaptotagmin, which interferes with fusion at low Ca^{2+} concentrations, calmodulin exerts an active, promoting effect on the post-docking events (Peters and Mayer, 1998).

Ca^{2+} has already found to be involved in insulin action and glucose transport (Youn et al., 1994). Although insulin treatment does not elevate the intracellular concentration of free Ca^{2+} (Kelly et al., 1989; Klip and Ramlal,

1987), the treatment of 3T3-L1 adipocytes with the Ca^{2+} chelator BAPTA-AM markedly inhibits insulin-stimulated GLUT4 translocation (Whitehead et al., 2001; Worrall and Olefsky, 2002). In addition it has been reported that elevated concentrations of cytosolic Ca^{2+} that are induced by exercise lead to an increase in glucose transport (Holloszy, 2003; Pereira and Lancha, 2004). So far there has not been a clear suggested mechanism for how Ca^{2+} affects glucose transport. It has been suggested that Ca^{2+} plays a minimal or permissive role on this event (Whitehead et al., 2001).

1.4.6 Role of pH in membrane fusion and insulin-stimulated GLUT4 exocytosis

Apart from the commonly accepted model for the general membrane fusion machinery in which membranes are forced into close proximity by the action of SNAREs, various studies have shown that membrane protein exocytosis and membrane fusion are related to certain pH conditions. Analysis of transferrin receptor (TfR) recycling (Johnson et al., 1993; Presley et al., 1997) has revealed that reduced endosome acidification results in a reduced rate of exit of TfRs from the recycling compartment to the plasma membrane. The vesicle coating and budding of secretory vesicles which requires the redistribution of ADP ribosylation factor (ARF) to the cytoplasmic face of the trans-Golgi network, is a pH-dependent process (Zeuzem et al., 1992). In adrenal chromaffin cells, the intragranular pH rapidly modulates exocytosis and it has been suggested that the gradient of pH is the main driving force that maintains secretory vesicles accumulation and membrane fusion (Camacho et al., 2006). In addition, pH-dependent fusion steps are known to be involved in virus-induced fusion involving hemagluttinin (Stegmann, 2000).

In GLUT4 translocation, cytosol pH has been found to be important in

glucose transport activity in rat adipocytes (Yang et al., 2002b). Insulin-stimulated cytosol alkalinization has also been revealed to facilitate the optimal activation of glucose transport in cardiomyocytes (Yang et al., 2002a). The intra-cellular or intra-vesicular pH is normally created by H^+ pumps including the Na^+/H^+ exchanger and the vacuolar H^+-ATPase. Inhibition of these proteins has blocked the glucose transport and GLUT4 exocytosis.

There are two hypotheses raised to explain the pH effects on membrane fusion and protein exocytosis: 1) the electrochemical gradient of pH is utilized as a driving force, 2) the V-ATPase acts as a fusion pore.

For various organelles *in vivo* (lysosomes, endosomes, trans-Golgi cisternae, secretory granules, etc), acidification of the organelles is required for many cellular processes including receptor-ligand dissociation, degradation pathways. The generation of intercompartment proton motive forces by gradient of H^+ is utilized as driving forces for numerous secondary transport processes including exocytosis and membrane fusion (Nelson, 2003; Nishi and Forgac, 2002). V-ATPases translocate protons across the membrane of these organelles to realize acidification and electrochemical gradient of pH (Nelson and Harvey, 1999; Nishi and Forgac, 2002).

V-ATPases are large multimeric enzymes made up of several different subunits. These subunits are organized in two complexes: a cytoplasmic complex V1 that hydrolyzes ATP and a membrane complex V0 involved in proton translocation. V1 is composed of eight different subunits (A-H). V0 contains four to five proteolipid subunits c and single copies of subunits a, d, and c" (Nelson and Harvey, 1999; Nishi and Forgac, 2002). The a subunit of V0 is a 110-kDa integral membrane protein, with nine transmembrane domains located in its C-terminal half and a large N-terminal sector in the cytoplasm (Leng et al., 1999). Several isoforms of the a subunit have been

identified. In yeast there are two isoforms associated to vacuolar and Golgi/endosomal membranes, respectively (Kawasaki-Nishi et al., 2001) and in mice, four (a1-a4) (Nishi and Forgac, 2000; Oka et al., 2001; Toyomura et al., 2000). Except a4, which is specifically expressed in kidney, all the others are expressed to various extents in all tissues. In neurons, the V1 and V0 complexes are transported independently in the axon and assemble once arrived in nerve terminals (Morel et al., 1998). V-ATPase is present both in the presynaptic plasma membrane and in the membrane of synaptic vesicles. The large electrochemical H^+ gradient generated by this enzyme, pH 5.2 - 5.5 inside the synaptic vesicles (Fuldner and Stadler, 1982; Michaelson and Angel, 1980), is used by specific vesicular transporters to accumulate the neurotransmitter.

Although "pore models" for membrane fusion have been suggested repeatedly in the past, it has been difficult to gather compelling data to verify the presence of a proteolipid pore during membrane fusion (Jahn, 2004; Jena, 2004; Lindau and Almers, 1995; Mayer, 2002; Morel, 2003; Weimer and Jorgensen, 2003). The existence of a proteinaceous pore capable of releasing neurotransmitter has first been proposed for vesicles isolated from electroplaques of the electric organ of *Torpedo marmorata*. Israel *et al.* reported the isolation of a proteolipid pore complex from synaptosomes from electroplaques of *Torpedo*, named the "mediatophore" (Israel et al., 1986). This pore complex was later shown to contain a subunit of the V0 complex of V-ATPase and transfection of this component in some cells allowed quantal release of neurotransmitter (Falk-Vairant et al., 1996). But these studies failed to demonstrate the role of V0 proteins at the synapse *in vivo* because it was difficult to mimic a complex event such as synaptic vesicle exocytosis by transfecting a single protein in cells (Falk-Vairant et al., 1996). The *Torpedo* V0 subunit a1 was only shown to localize specifically to nerve terminals and interact with SNAREs (Morel et al., 2003). A direct

requirement of V0 proteolipids for membrane fusion was demonstrated for a yeast vacuolar fusion assay (Peters et al., 2001). The proteolipid pore-forming V0 complex from V-ATPase was shown to be required downstream of SNARE action (Bayer et al., 2003; Peters et al., 2001).

Although so far the yeast vacuolar fusion assay is the only system in which evidence for an additional component downstream of SNARE function has been identified (Bayer et al., 2003; Peters et al., 2001), the new studies in Drosophila nerve terminals largely showed coincident observations. The V0 subunit a1 was shown to be required for evoked synaptic vesicle exocytotic fusion, independently of proton translocation (Hiesinger et al., 2005). The earlier mentioned fact that subunit a1 was shown to localize to synaptic terminals and interact with the v-SNARE n-Syb (Morel et al., 2003) is in agreement with the findings in *Drosophila* synapses. The selective interactions of the 100 KDa subunit of V0 complex with the t-SNAREs Syntaxin and SNAP-25 are in agreement with the observations made in yeast (Hiesinger et al., 2005; Peters et al., 2001).

Larance *et al.* identified the V-ATPase subunit a is present on GLUT4 vesicles from 3T3-L1 adipocytes using Mass Spectrometry (Larance et al., 2005). This finding leads to the questions as to whether there is acidification in the lumen of GLUT4 vesicles and whether the gradient of H^+ affects the vesicle fusion with plasma membrane and GLUT4 exocytosis. The presence of subunit a also suggests the possibility that it functions as a fusion pore. These findings provide a basis for elucidating whether pH is involved in the mechanism of GLUT4 vesicles fusion with plasma membrane.

1.5 Experimental aims

The work described in this thesis is mainly aimed at elucidating the mechanism involved in insulin-stimulated GLUT4 vesicle fusion with plasma

membrane. Two strategies were tried to reconstitute this event *in vitro*: 1) to immuno-isolate GLUT4 vesicles and reconstitute plasma membrane liposomes for a fusion assay, 2) to use recombinant SNARE proteins in a reconstituted liposome fusion assay.

Investigations were undertaken to determine the factors necessary for immuno-isolation of GLUT4 vesicles and for reconstitution of plasma membrane liposomes for fusion assay. The kinetics of the fusion were determined and compared with those in insulin-stimulated glucose uptake. The relation of insulin signalling to this event was explored by use of PI 3-kinase inhibitors, by immuno-depletion of cytosolic components and by determining factors recruited to the plasma membrane liposomes.

Studies were also undertaken to investigate the roles of Ca^{2+} ions and the V-ATPase protein in GLUT4 vesicles fusion with plasma membrane. To address this aim, specific chelators, ionophores and inhibitors were applied to the membrane and cytosol fractions of the fusion assay. Fusion assays were also carried out at different pH levels to address the question of whether a pH gradient is required.

Recombinant SNARE proteins were reconstituted and used in liposome fusion assays. The aim was to assess the ability of SNARE proteins to drive fusion. In these studies, membrane fusion was observed in the presence of cytosol and Ca^{2+}. Studies which aimed to determine whether this assay measured SNARE-specific fusion were carried out.

Chapter 2 Materials and methods

2.1 Materials

2.1.1 Laboratory chemicals

Unless otherwise stated, all chemical reagents were purchased from Fisher Scientific or Sigma.

Table 2.1 Laboratory chemicals

Reagent	Resource
Enhanced chemiluminescent reagent (ECL)	Amersham Pharmacia Biotech
ECL Advance Western Blotting Detection Kit	Amersham Pharmacia Biotech
SuperSignal West Dura Extended Duration Substrate Kit	Pierce
Monocomponent porcine insulin	gift from Dr. G. Daniellson (Novo Nordisk)
Collagenase Type 1 from *Clostridium histolyticum*	Worthington Biochemical Corporation
Bovine Serum Albumin	Intergen Co.
Biotinylated-Europium(TMT)	in house
Dylight647 conjugated Streptavidin	Pierce
n-octyl glucoside	Melford Laboratories
Protein molecular markers	Sigma or New England Biolabs
1-Palmitoyl-2-Oleoyl-sn-Glycero-3-Phosphocholine (POPC or PC)	Avanti Polar Lipids
1, 2-Dioleoyl-sn-Glycero-3-[Phospho-L-Serine] (Sodium Salt) (DOPS or PS)	Avanti Polar Lipids
L-α-Phosphatidylethanolamine (PE; from porcine brain)	Avanti Polar Lipids
Amylose resin	New England Biolabs
Ni-NTA His-Bind Resin	Novagen
1,2-*bis*(o-Aminophenoxy)ethane-N,N,N',N'-tetraacetic Acid, Sodium (BAPTA)	Calbiochem
1,2-*bis*(o-Aminophenoxy)ethane-N,N,N',N'-tetraacetic Acid Tetra(acetoxymethyl) Ester (BAPTA-AM)	Calbiochem
4-Bromo-A23187	Calbiochem
Concanamycin A	Calbiochem
Acrylamide stock (30 % acrylamide, 0.8 % bis-acrylamide)	Flowgen
Molecular biology grade agarose	Invitrogen
DNA molecular weight markers	Invitrogen
NUPAGE gels	Invitrogen

2.1.2 Buffers

The buffer compositions are stated in the context of their use. For a compiled full description, the buffers are summarised in appendix 1), 2) and 3).

2.1.3 Antibodies

The source of antibodies and their appropriate dilutions for western blotting (section 2.2.4) and immunoprecipitations (section 2.2.1) are shown in the tables below. All antibodies were diluted in Tris-buffered saline (TBS) (10 mM Tris, pH 7.4, 154 mM NaCl).

Table 2.2 Sources and dilutions of antibodies used for Western Blot analysis

Antibody	Polyclonal/ Monoclonal Purified/Serum	Source	Dilution for Western Blotting
Rabbit anti-GLUT4 C-terminus	Polyclonal Serum and purified	In House production (Holman et al., 1990b)	1:10,000
Sheep anti-GLUT4 C-terminus	Polyclonal Purified	In House production	1:1000
Mouse anti-GLUT1 C-terminus	Monoclonal Purified	Biogenesis	1:1000
Rabbit anti-syntaxin4	Polyclonal serum	In House production	1:4000
Rabbit anti-SNAP23	Polyclonal Purified	In House production	1 µg/ml
Rabbit anti-VAMP2	Polyclonal Purified	In House production	1 µg/ml
Mouse anti-VAMP2	Monoclonal	Synaptic System	1:500
Goat anti-Akt1	Polyclonal Purified	Santa Cruz	1:1000
Rabbit anti-Akt2	Monoclonal	Upstate	1:1000
Rabbit anti-phospho-Akt (Ser473)	Monoclonal	Cell signalling	1:1000 (5 % BSA)
Rabbit anti-phospho-Akt (Thr473)	Monoclonal	Cell signalling	1:1000 (5 % BSA)
Rabbit anti-phospho-Akt substrate	Monoclonal	Cell signalling	1:1000 (5 % BSA)
Goat anti-V-ATPase subunit a	Polyclonal	Santa Cruz	1:400

Table 2.3 Sources and dilutions of secondary antibodies used for Western Blot analysis

Antibody	Source	Dilutions
Goat anti-rabbit IgG HRP conjugate	Sigma	1:4000
Goat anti-mouse IgG HRP conjugate	Sigma	1:1000
Goat anti-sheep IgG HRP conjugate	Sigma	1:4000
Rabbit anti-goat IgG HRP conjugate	Sigma	1:4000

Table 2.4 Sources and concentrations of antibodies used for immuno-precipitations

Antibody	Source	Concentration Required for Immuno-precipitation
Rabbit anti-GLUT4 C-terminus	FPLC purified against GLUT4 peptide	100 µg for pHDM of basal adipocytes from 2 rats
Mouse anti-Akt1	Cell signalling	15 µl for 150 µl of concentrated cytosol from rat adipocytes
Rabbit anti-Akt2	Upstate	15 µl for 150 µl of concentrated cytosol from rat adipocytes

2.1.4 Preparation of Bovine Serum Albumin for rat adipocytes

10 g of BSA (Fraction V) per 60 ml of double-distilled water was dissolved overnight at 4 °C. The BSA was filtered through a Millipore type A membrane filter (0.8 µm pore size) under vacuum and the pH of the solution was adjusted to 7.6 with 10 M NaOH. Double distilled water was added to give a final BSA concentration of 10 % (w/v). The BSA was divided in to 40 ml aliquots and stored at -20 °C until required.

2.1.5 Preparation of insulin

Monocomponent porcine insulin was a gift from Dr. G. Daniallson, Novo Nordisk. 1 mg of insulin was dissolved in 1 ml of 0.03 M HCl and the solution made up to 3 ml with double-distilled water. 1 ml of this solution was then diluted to 50 ml with 1 % (w/v) BSA in Krebs-Ringer-HEPES (KRH) buffer

(140 mM NaCl, 4.7 mM KCl, 2.5 mM $CaCl_2$, 1.25 mM $MgSO_4$, 0.2 mM NaH_2PO_4, 10 mM HEPES, pH 7.4). The resulting insulin solution (1 µM) was divided into 500 µl aliquots and stored at -20 °C until required. The solution was not frozen again once it had been thawed.

2.1.6 Protease inhibitors

Unless otherwise stated, the protease inhibitors and the concentrations at which they were used are shown in table 2.5 below.

Table 2.5 Protease inhibitors

Inhibitor		Inhibits	Working concentration
Protease inhibitor cocktail	Antipain	Ser and Cys proteases	1 µg/ml (1.65 µM)
	Aprotinin	Ser proteases	1 µg/ml
	Pepstatin A	Ser and Cys proteases	1 µg/ml (1.46 µM)
	Leupeptin	Acid proteases	1 µg/ml (2.1µM)
AEBSF		Ser proteases	100 µM

2.1.7 Molecular biology reagents

1) Oligonucleotide primers

DNA primers were made to order through Sigma-Aldrich. Primer sequences are shown below:

Table 2.6 Sequences of oligonucleotides

Primer name	Sequence
*BamH*I for (section 3.3.1)	5' - GGG GGA TCC CCA AGC TTA AAA GAT GAC CC - 3'
His for 1st (section 3.3.3)	5' - GGC CGC CAC CAC CAC CAC CAC CAC TGA C - 3'
His for 2nd (section 3.3.3)	5' - GGC CGC CAC CAC CAC CAC CAC CAC TGA G - 3'

2) Vectors and constructs

The plasmid pMBP-Parallel2 was a gift from Dr. Stephan Bagby from University of Bath. The plasmid pAX11 was a gift from Dr. J. Zueco. Plasmid pT7 blue was from Novagen. Thrombin cleavable His-tagged, Nuclease-A-fused full length rat VAMP2 (His-NucA-VAMP2) pDRSN1-VAMP2 and glutathione S-transferase (GST)-fused full length mouse SNAP23 and rat syntaxin4 co-expression construct (GST-SNAP23-syntaxin4) pGEX-tSNAREs were from former PhD student Dr. David Ribe in our laboratory at the University of Bath.

3) Restriction enzymes and ligase

Table 2.7 Restriction enzymes and ligase

Enzyme	Resource
*BamH*I (section 3.3.1, 3.3.3)	Boehringer-Mannheim
*Spe*I (section 3.3.1, 3.3.3)	Sigma
*Not*I (section 3.3.3) and *Xho*I (section 3.3.3)	New England Biolabs (NEB)
*Xba*I (section 3.3.3)	Promega
T4 DNA ligase (section 3.3.1, 3.3.3)	Promega

2.2 Methods

2.2.1 Preparation of rat adipocytes

1) Isolation of rat adipocytes

Isolated adipose cells were prepared from the whole epididymal fat pads of male Wistar rats (180 - 200 g) as described (Simpson et al., 1983; Taylor and Holman, 1981). The rats were stunned and the necks dislocated. The epididymal fat tissue was quickly removed and rinsed in KRH buffer (140 mM NaCl, 4.7 mM KCl, 2.5 mM $CaCl_2$, 1.25 mM $MgSO_4$, 0.2 mM NaH_2PO_4,

10 mM HEPES, pH 7.4) with 1 % (w/v) BSA at 37 °C. The washed tissue was placed in adipocyte digestion buffer (3.5 % (w/v) BSA in KRH supplemented with 5 mM glucose and 500 µg/ml Collagenase type 1 from *Clostridium histolyticum*) in a 23 ml polystyrene flat-bottomed tube (Sarstedt), and minced finely with scissors. Both buffers were supplemented with adenosine at a final concentration of 200 nM. The tissue suspension was shaken rapidly in a shaking water bath at 37 °C for approximately 25 - 26 min until most of the tissue lumps were digested. The resulting cell suspension was filtered through a nylon mesh (250 µm mesh size, Lockertex), into a 23 ml polystyrene flat-bottomed tube (Sarstedt), washed with 1 % BSA/KRH, and returned to 37 °C. The cells were allowed to float. The infranatant buffer was removed using a needle (2 mm diameter X 100 mm) attached to a 20 ml plastic syringe, and 15 - 20 ml 1 % (w/v) BSA/KRH buffer was added. The cells were gently resuspended and then allowed to float. This washing procedure was repeated 3 - 4 times. The cell suspension was adjusted to a cytocrit of 40 % (using a capillary tube which was centrifuged at 1000 *g* for 1 min and expressed as the ratio of the length of the packed cell fraction in the tube to the total length of the suspension in the tube) and ready for further use.

2) Stimulation of rat adipocytes with insulin

Insulin at a final concentration of 20 nM was used to stimulate the isolated rat adipocytes (40 % cytocrit) for 20 min at 37 °C. Basal cells were also maintained at 37 °C during this time.

3) Sub cellular fractionation (subfractionation) of rat adipocytes

Basal or insulin-treated cells were washed once in HEPES-EGTA-Sucrose I (HESI) buffer (250 mM Sucrose, 0.5 mM EGTA, 20 mM HEPES, pH 7.0) (with protease inhibitor cocktail and AEBSF) at 15 - 18 °C. When the cells

floated to the top the excess HESI buffer was removed. The cells were rapidly homogenized (basal first) with 10 strokes of a 55 ml Potter-Elvehjem homogenizer (Thomas Scientific), with a specific clearance of 150 µm. Homogenized cells were transferred to disposable centrifuge tubes and rapidly centrifuged at 1000 *g* for 1 min at 4 °C in a refrigerated Ole Dich centrifuge (Camlab). After that the centrifuge tubes were kept on ice for 10 min to solidify the fat. The homogenizer was washed, cooled and the same procedure was repeated with the insulin stimulated cells. The homogenate (infranatant between top fat layer and bottom pellet) was collected with a 21G needle (TERUMO) and a 2 ml syringe (TERUMO). The following spins were all carried out in a TL-100 bench-top ultracentrifuge (Beckman) using TLA-100.3 rotor at 4 °C unless otherwise stated. The procedure is represented on Fig 2.1. The collected infranatant was centrifuged at 17,500 *g* (18,000 rpm) for 20 min to obtain a crude plasma membrane (PM) pellet containing mitochondria and nuclei, as well as a supernatant containing the microsomal and cytosolic fractions. The PM pellet and the supernatant were prepared separately afterwards. 1) The pellet containing plasma membrane was resuspended in 1 ml HESI buffer and homogenized once again with 5 strokes in a 2 ml homogenizer (Thomas Scientific). The homogenizer was washed out with a further 1 ml HESI which was added to the homogenate and centrifuged at 17,500 *g* (18,000 rpm) for 20 min. The pellet was resuspended in 300 µl HESI, loaded on top of a 600 µl sucrose cushion (1.12 M Sucrose, 1 mM EDTA, 20 mM HEPES, pH 7.0) and centrifuged at 105,000 *g* (35,000 rpm) for 20 min in the TLS-55 swing out rotor. The mitochondria and nuclei were pellet down and purified plasma membrane was recovered at the cushion interface. 700 µl of the interface was harvested, resuspended in 2 ml HESI and centrifuged at 74,000 *g* (37,000 rpm) for 9 min. The plasma membrane pellet was washed with another 2 ml of HESI and re-pelleted at 74,000 *g* (37,000 rpm) for 9 min. The plasma membrane was then resuspended in 150 µl HESI. 2) The supernatant

containing microsomal and cytosolic fractions was centrifuged at 49,000 *g* (30,000 rpm) for 9 min to pellet the high density microsomes (HDM), leaving the low density microsomes (LDM) and cytosol in the supernatant (post HDM supernatant, or pHDM supernatant). The HDM pellet was washed in 2 ml HESI and pelleted again at 49,000 *g* (30,000 rpm) for 9 min. Then the HDM was resuspended in 50 µl HESI. The low density microsomes (LDM) were pelleted by centrifugation at 541,000 *g* (100,000 rpm) for 17 min leaving the cytosol in the supernatant. Then the pellet was washed with 2 ml HESI and pelleted again at 541,000 *g* (100,000 rpm) for 17 min. The low density microsomes were resuspended in 100 µl HESI. All the fractions were assayed for protein content, snap frozen with liquid N_2 and stored at -80 °C.

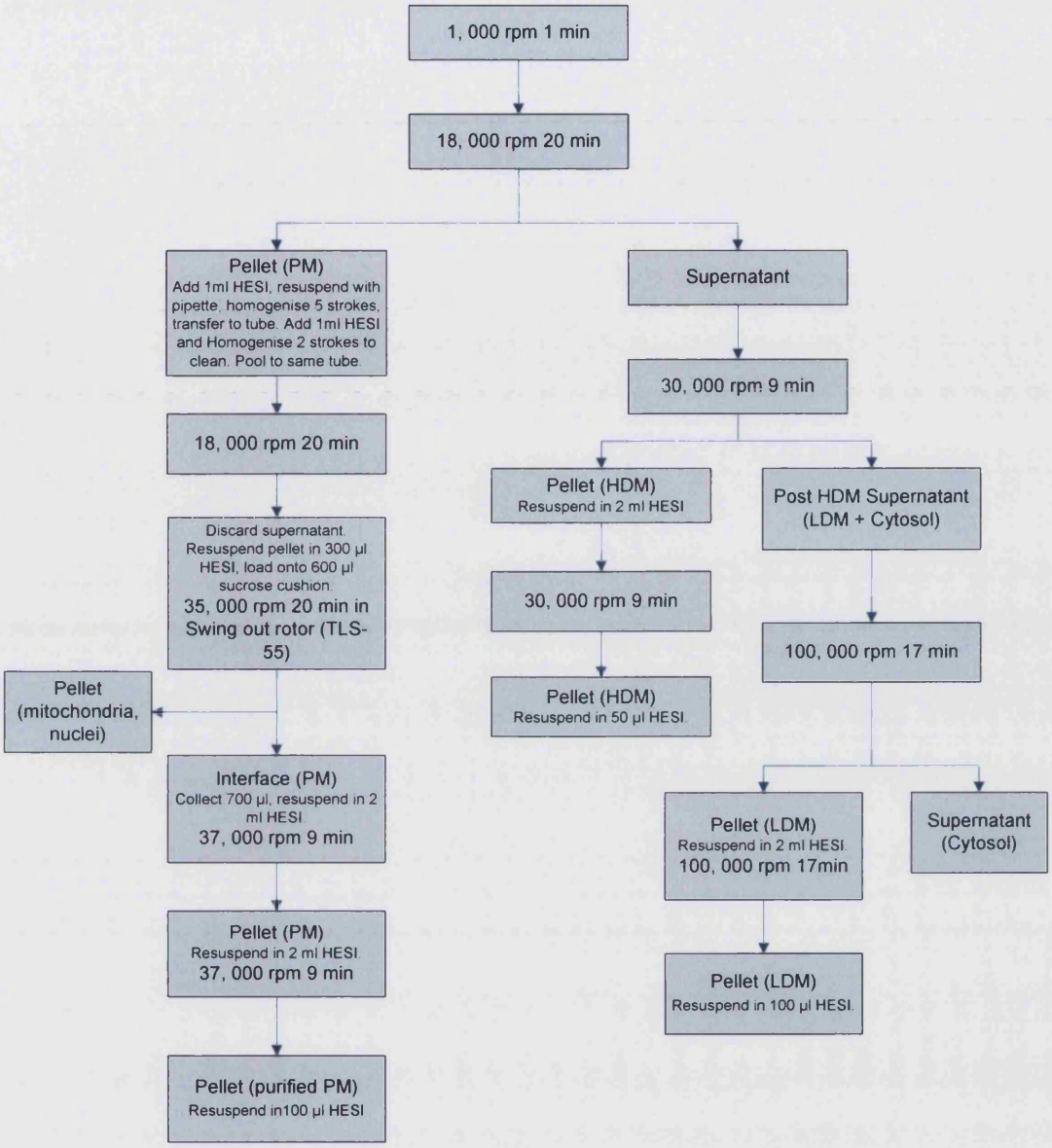

Fig 2.1 Diagram representation of the rat adipocytes sub-cellular fractionation. See texts for details.

4) Concentrated cytoplasm from rat adipocytes

Basal or insulin-stimulated rat adipocytes were washed with KRH without BSA at 37 °C, then with intra-cellular (IC) buffer (20 mM HEPES pH 7.4, 140 mM K-glutamate, 5 mM NaCl, 1 mM EGTA) containing 1 µg/ml of protease

inhibitor cocktail and 100 µM AEBSF (section 2.1.6) at 15 - 18 °C, and then spun briefly to concentrate the cells. The infranatant buffer was discarded with a syringe. The cells were then vortexed vigorously for about 5 - 10 sec, repeated 5 times. The suspension was transferred to a polycarbonate centrifuge tube (Beckman) and spun at 250, 802 *g* using MLA-80 rotor in Beckman Optima MAX Ultracentrifuge for 70 min at 4 °C. After centrifugation, the tubes were left on ice for 10 - 15 min to solidify the fat at the top. The cytoplasm in the middle layer was harvested with a 2 ml syringe and a 21G needle. The protein concentration of cytoplasm was determined. The cytoplasm was aliquoted, snap frozen in liquid nitrogen and then kept at -80 °C.

5) Immuno-precipitations

- Immuno-precipitation of GLUT4 vesicles from rat adipocytes with MBP-Spa and Amylose resin

1 ml of amylose resin slurry (NEB) was loaded on a disposable Talon gravity column (Clontech) resulting in 0.7 ml of bed volume. Resin was washed 3 times with column buffer (20 mM HEPES pH 7.4, 150 mM NaCl) by filling the column with the buffer. One aliquot (500 µl) of recombinant MBP-Spa bacterial lysate was thawed on ice and diluted to 3 ml with high salt column buffer 1 (20 mM HEPES pH 7.4, 500 mM NaCl) with 100 units of α-Amylase inhibitor from *Triticum aestivum* (wheat seed). This was added to column and rotated for 2 h or overnight at 4 °C. The next day (or after 2 h) the column was drained, washed 1 time with high salt column buffer 2 (20 mM HEPES pH 7.4, 1 M NaCl), and 2 times with normal column buffer. 100 µg of rabbit affinity purified anti C-terminal GLUT4 antibody was diluted in 3 ml column buffer with 100 units of α-Amylase inhibitor (for basal GLUT4 vesicles, 100 µg Ab/rat; for fusion assay with 4 rats, 100 µg Ab/fusion assay). This was

rotated in the column for 2 h at 4 °C. After incubation the column was washed 3 times with column buffer. Freshly prepared post HDM supernatant (section 2.2.1.3) and 100 unites of α-Amylase inhibitor were added to the column, and rotated for 2 h at 4 °C. At the end of the incubation the supernatant was drained from the column, and the column was washed with at least 8 ml of the desired buffer (IC buffer for fusion assay in Chapters 4, 5, 6). The efficiency of the washes was monitored by either measuring the absorbance at 280 nm in the UV spectrometer or the fluorescence contained it the vesicles with the FARCyte fluorescent plate reader (Tecan). 40 mM maltose was freshly prepared in 5 ml of the desired buffer (IC buffer for fusion assay in Chapters 4, 5, 6) to be the elution buffer. When the washes finished the column was plugged, 1 ml elution buffer was added to the column and the column was rotated for 10 min at room temperature. This eluate was collected in a tube as elution fraction 1. The rest elution buffer was added to the column and 4 to 6 additional 500 µl fractions were collected. The efficiency of the elutions was monitored by either measuring the absorbance at 280 nm in the UV spectrometer or fluorescence. The ultimate confirmation was to run all the fractions on a gel to confirm the presence of GLUT4.

- Immuno-precipitation of Akt from concentrated cytosol

To immuno-deplete Akt from concentrated cytosol, freshly-made concentrated cytosol from rat adipocytes was incubated overnight with anti-Akt1 antibody clone 5G3 (Cell Signalling Technology) alone or in combination with anti-Akt2 antibody clone AW114 (Upstate). 150 µl of cytosol from insulin-stimulated adipocytes were incubated with 15 µl Akt1 antibody and 15 µl Akt2 antibody. The controls were cytosols with and without 10 µg mouse IgG and 10 µg rabbit IgG. For depletion of Akt1 only, cytosol was incubated with Akt1 antibody only and the controls were with

and without mouse IgG. The antibodies were removed with immobilised ProteinA/G by incubating the cytosol-antibody mixture with 15 µl ProteinA/G beads (Peirce). The cytosol was analysed to assess the amount of depletion by western blot prior to use in the fusion assay.

2.2.2 Rat adipocytes GLUT4 surface photolabeling

Rat adipocytes at 40 % cytocrit were stimulated with 5 nM insulin for 20 min at 37 °C. In a typical experiment 10 ml of cells were used. After cooling the cells to 18 °C the surface GLUT4 was labeled with 500 µM biotinylated photolabel GP15 (Hashimoto et al., 2001). 1 ml cells were transferred to a 35 mm polystyrene dish at 18 °C. 500 µM biotinylated photolabel GP15 was added to the cells and mixed well. The dishes were irradiated for 1 min in a Rayonet RPR-100 photochemical reactor with 300 and 350 nm lamps. Cells were then transferred to 5 polystyrene tubes and washed 5 times with 25 ml KRH buffer at 18 °C.

2.2.3 Rat adipocytes GLUT4 surface DyLight tagging and GLUT4 internalization

Photolabeled rat adipocytes (section 2.2.2) were incubated with 10 µg/ml of cells DyLight647 streptavidin (Pierce) for a further 15 min. Insulin was removed and GLUT4 was internalized (Yang et al., 2002b). Briefly, the cells were washed three times with pH 6.0 KRH buffer at room temperature to remove insulin and 1 time with KRH buffer containing 2 mM glucose. The cells were then kept in KRH buffer containing 2 mM glucose at 37 °C for 45 min to allow GLUT4 internalization and reversal of the cells to basal state.

2.2.4 Protein Biochemistry techniques

1) SDS-polyacrylamide gel electrophoresis

Three-time concentrated SDS sample buffer was prepared and stored at room temperature. At the time of use, reducing agent dithiothreatol (DTT) was added freshly. Protein samples were solubilised in one-time concentrated sample buffer (2 % (w/v) SDS, 62.5 mM Tris HCl pH 6.8, 0.01 % (w/v) bromophenol blue, and 10 % (v/v) glycerol) with 20 mM DTT and heated at 95 - 100 °C for 5 - 10 min in a heating block.

Electrophoresis was carried out using the Laemmli discontinuous buffer system. Slab gels were prepared using either the mini-Protean 3 system (Bio-Rad), mini-Atto system (Atto Corporation), or the CBS system (C.B.S. Scientific Company Inc). 10 or 15 % resolving gels and 6 % stacking gels were prepared. All gels were made to a thickness of 1.5 mm. Gels were prepared according to the manufacturers' instructions, using the following buffer system: acrylamide/bis-acrylamide (30 % (w/v) acrylamide) (National Diagnostics, Flowgen), Resolving gel buffer (1.5 M Tris HCl, 0.4 % (w/v) SDS, pH 8.8), Stacking gel buffer (0.5 M Tris HCl, 0.4 % (w/v) SDS, pH 6.1), 10 % (w/v) ammonium persulphate (APS) and N,N,N,N'-tetramethylethylenediamine (TEMED). The stock solutions were stored up to 1 month at room temperature. Composition of the resolving and stacking gels can be seen in Appendix table 4). Polymerisation was initiated by the addition of TEMED and APS, both to 0.05 % (v/v) final concentration. Gels were run at a constant 200 Volts in electrophoresis running buffer (25 mM Tris HCl, pH 6.3, 0.1 % (w/v) SDS, 0.2 M Glycine) for approximately 1 h until the bromophenol blue dye had just run off the gel.

Molecular weight markers were either High Molecular Weight markers (HMW markers) consisting of myosin (205 kDa), β-galactosidase (116 kDa),

phosphorylase b (97.4 kDa), bovine albumin (66 kDa), ovalbumin (45 kDa) and carbonic anhydrase (29 kDa), or Broad range Protein markers (BMW markers) (New England Biolabs) consisting of myosin (212 kDa), MBP-β-galactosidase (158 kDa), β-galactosidase (116 kDa), phosphorylase b (97 kDa), serum albumin (66 kDa), glutamic dehydrogenase (55.6 kDa), maltose binding protein 2 (42.7 kDa), lactate dehydrogenase (36.4 kDa), triose phosphate isomerase (26.6 kDa), trypsin inhibitor (20 kDa), lysozyme (14 kDa), aprotonin (6.5 kDa) and insulin A, B chain (2.3 - 3.4 kDa).

2) Electrophoretic transfer of proteins to nitrocellulose membrane

Following SDS-PAGE, proteins on the gels were transferred onto nitrocellulose membranes using the Multiphor II Novablot electrophoretic transfer apparatus (Pharmacia) by the semi-dry transfer method. The stacking gel was removed and the resolving gel briefly incubated in SDS-transfer buffer to remove the electrophoresis running buffer. The filter paper and nitrocellulose cut to the size of the gel were also briefly immersed in transfer buffer (39 mM Glycine, 48 mM Tris, 0.0375 % SDS (w/v), 20 % methanol (v/v), pH 8.8 without adjusting). Nine pieces of Whatman paper (3mm) (Munktell, Pharmacia Biotech) were placed on the anode of the transfer apparatus. A piece of nitrocellulose membrane (Gelman Sciences, 45 µm pore size) was placed on the stack, followed by the gel. The final nine pieces of filter paper were placed on the gel and the cathode on top of the stack. All trapped bubbles were removed. The transfer was run at a constant current calculated as follows: (area of the gel cm^2) x 0.8 mili Amps for 1 h 50 min. Following transfer, the nitrocellulose membrane was washed briefly in distilled water, and stained with Ponceau S stain (0.1 % (w/v) Ponceau S in 3 % (v/v) trichloroacetic acid) for 2 - 3 min. Excess stain was washed off with distilled water and the protein bands could be visualised. The nitrocellulose

was left to air dry and the positions of the molecular weight markers were recorded.

3) Western Blotting

The nitrocellulose membrane was washed in Tris-buffered Saline with 0.1 % (v/v) Tween-20 (TBS-T) to re-hydrate and remove the Ponceau S stain. The nitrocellulose was then blocked in 5 % Marvel (dried skimmed milk powder) in TBS-T with gentle rocking for 30 - 60 min at room temperature or overnight at 4 °C, to block non-specific protein binding sites. The membrane was washed 4 times for 15 min in TBS-T followed by incubation with the primary antibody, at the required dilution (section 2.1.3), in TBS-T containing 1 % (w/v) BSA, for 2 h at room temperature. For sheep C-terminal GLUT4, Akt, phosphorylated-Akt and V-ATPase, the incubation was overnight at 4 °C. The nitrocellulose was washed for 6 times for 5 min with TBS-T followed by incubation for 45 min at room temperature with the secondary antibody at the required dilution (section 2.1.3) in blocking solution. Once again the nitrocellulose was washed for 6 times for 15 min in TBS-T.

The nitrocellulose membrane was developed using ECL or ECL Advance (Amersham Pharmacia Biotech) following the manufacturer's guidelines. In brief the two reagents were mixed in a 1:1 ratio and the membrane was incubated for 1 min in ECL or 5 min in ECL Advance. The chemiluminescent signals were detected with an EPI Chemi II darkroom imaging system (UVP). In experiments where protein bands were quantified by densitometry, multiple exposures of the blots were performed to ensure that the analysis was performed in the linear range of signal densities.

4) Coomassie blue staining

Protein bands on the gels were visualised by staining with Coomassie brilliant blue reagent (0.2 % (w/v) Coomassie blue R-250 in 10 % (v/v) glacial acetic acid, 30 % (v/v) MeOH, 60 % (v/v) dH_2O) for 1 h, followed by incubation with destain (30 % (v/v) MeOH, 10 % (v/v) glacial acetic acid, 60 % (v/v) dH_2O). The gels were dried at room temperature between two layers of Biotrace membrane presoaked in destaining solution containing 8.7 % (v/v) glycerol.

5) BCA protein determination

The bicinchoninic acid (BCA) protein assay (Pierce) was used to determine protein concentrations. A standard curve of BSA using a 1 mg/ml BSA stock (in 0.1 M NaOH) was prepared. 10 µl of 1 - 10 µg BSA was added to Microtitre plate (Sterilin) in duplicate. 10 µl of sample was also added to the plate, either undiluted or diluted with 0.1 M NaOH. The BCA working solution was prepared by adding Reagent A (1 % BCA-NO_2, 2 % $Na_2CO_3.H_2O$, 0.16 % Na_2tartarate, 0.4 % NaOH, 0.95 % $NaHCO_3$) and Reagent B (4 % (w/v) $CuSO_4.5H_2O$) together in a ratio of 50:1. 200 µl of this working solution was added to each of the wells containing standard and samples. The plate was incubated at 37 °C for 30 min with the lid in place, allowed to cool and then read on a microplate spectrophotometer (Tecan) at 565 nm.

2.2.5 Molecular Biology and protein expression

Standard molecular biology techniques were used for all DNA manipulation and protein expression (Sambrook et al., 1989).

1) Plasmid miniprep extraction

Plasmid DNA was purified from cultures of *E.coli* cells in 10 ml Luria Broth (LB) medium (1 % (w/v) Bacto™ Tryptone, 0.5 % (w/v) Bacto™ Yeast Extract, 0.5 % NaCl, pH 7.5, autoclaved) using the Wizard Plus SV miniprep DNA purification system (Promega), according to the protocol provided by the manufacturer.

2) Polymerase chain reaction (PCR) for Spa sequence from pAX11

2 µl of pAX11 DNA was amplified in 60 µl of Pfx amplification buffer (Invitrogen) containing 10 mM of dNTP, 50 mM $MgSO_4$, 0.4 µl Platinum Pfx DNA polymerase (Invitrogen) and 10 µM of two primers, M13 Uni 5' GGG TTT TCC CAG TCA and M13 R 5' ATG ACC ATG ATT ACG (Eurogentec). The polymerase chain reaction (PCR) involved 30 cycles of denaturation (92 °C 10 sec), annealing (55 °C 30 sec) and extension (68 °C 1 min) after an initial denaturation step at 92 °C for 2 min. A final extension of 10 min was carried out at 68 °C. Annealing temperature for the subsequent PCR with the new primer (MNG-Biotech AG) was 60 °C.

3) DNA Gel extraction

The DNA gel slices were collected and gel extraction was performed using a commercial kit (Qiagen), according to the protocol provided by the manufacturer.

4) DNA digestion

*BamH*I-*Spe*I double digestion of both the Spa PCR product and pMBP-Parallel2 involved the incubation of 1 µl of DNA, 1.5 µl buffer 2 (Sigma), 1 µl of each of the restriction enzymes *BamH*I and *Spe*I and 1.5 µl

of 10 times concentrated BSA (1 mg/ml) for 1 h at 37 °C. Single digestion of pMBP-Spa with *Xho*I involved the incubation of 26 µl of DNA, 4 µl NEBuffer 3 (New England Biolabs), 4 µl of *Xho*I and 4 µl of 10 times concentrated BSA (1 mg/ml) for 2 h at 37 °C. 20 µl of the *Xho*I single digested pMBP-Spa was then incubated with 3 µl NEBuffer 3 (New England Biolabs), 3 µl of *Not*I and 3 µl of 10 times concentrated BSA for 2 h at 37 °C. Then the *Not*I was heat inactivated by keeping the digest product at 70 °C heating block for 20 min. The digestions were loaded onto a gel and the bands excised quickly under UV light with a razor blade.

5) Cloning

The cohesive ends of the Spa PCR product and pMBP-Parallel2 digestion products were ligated using the LigaFast Rapid DNA ligation system (Promega). The following equation was used to calculate the amount of insert DNA required for the ligation reaction:

$$\frac{100\ ng\ \ plasmid \times insert\ kb \times ratio\ of\ (insert / plasmid)}{plasmid\ kb} = ng\ of\ insert$$

In the case of pMBP-Spa (section 3.3), the insert was $\frac{100 \times 0.47 \times 2}{6.725} = 13.9\ ng$.

100 ng of the digested pMBP-Parallel2 plasmid was mixed with 13.9 ng of the Spa insert and 10 µl of 2 times concentrated rapid ligation buffer. This was heated at 65 °C for 5 min and cooled for a few minutes on ice before the addition of 0.66 µl of ligase. As a control, a perfectly blunt ended cloning kit (Novagen) was also used to ligate the digested insert into a PT7 blue vector (Novagen). Briefly, 5 µl of end conversion mix was added to 13.9 ng of the Spa insert and incubated at 22 °C for 15 min followed by 75 °C for 5 min and cooled on ice for 2 min. 100 ng of the PT7 vector was added with 1 µl of T4 DNA ligase and incubated for 60 min on ice. 2 µl of this or the

pMBP-Parallel2 ligation mixture was added to 50 µl of XL1 blue cells which were placed on ice for 5 min. cells were heat shocked at 42 °C for 1 min, cooled on ice for 2 min and added to 250 µl of SOC medium (0.5 % Yeast extract, 2.0 % tryptone, 10 mM NaCl, 2.5 mM KCl, 10 mM $MgCl_2$, 20 mM $MgSO_4$, 20 mM glucose) with 35 µl of 2 % 5-bromo-4-chloro-3-indolyl-b-D-galactopyranoside (X-gal) and 20 µl of 100 nm Isopropyl-ß-D-thiogalactopyranoside (IPTG). These two reagents allow colonies containing the plasmid with the Spa insert to be easily identified *via* the blue-white screening method because the pMBP-Parallel2 plasmid contains the lacZ operon. When the Spa gene is inserted into the plasmid, the lacZ operon is disrupted inhibiting the transcription of β-galactosidase, a product of the lacZ-α gene. X-gal is a substrate which turns blue when incubated in the presence of β-glactosidase. Therefore, the blue colonies have an intact lacZ operon and do not contain the insert. IPTG binds to the lacZ repressor thus activating the operon and causing expression of the intact gene, if present. The cells were applied to plates containing 10 µg of ampicillin and incubated overnight at 37 °C. White colonies were used to transform 50 ml of LB medium containing 20 µg/ml of ampicillin. The plasmids were harvested as earlier described (section 2.2.5.1).

In the case of pMBP-Spa-His (section 3.5), the insert was
$\frac{100\times0.028\times2}{6.725}=0.833\,ng$.

100 ng of the digested pMBP-Spa plasmid was mixed with 0.833 ng of the Poly-His insert and 1.5 µl of T4 ligase buffer. This was heated at 65 °C for 5 min and cooled down to room temperature before the addition of 1.5 µl of T4 ligase, 1.5 µl of Promega buffer E, 1.5 µl of BSA, 1 µl of *Xba*I and 0.6 µl of H_2O. As a control, 0.833 ng of the Poly-His insert was replaced with H_2O of the same volume. This mixture was incubated at 37 °C for 2 h and then transfected to TB1 competent cells. The transfected cells were grown

overnight in selective LB-Agar (1 % (w/v) Bacto™ Tryptone, 0.5 % (w/v) Bacto™ Yeast Extract, 0.5 % NaCl, 1.5 % (w/v) Agar, pH 7.5, autoclaved) plate and single colony was cultured in a 10 ml mini-culture overnight. The plasmid was extracted with a mini-prep kit (Promega).

6) DNA analysis

DNA products were run on 0.6 % (w/v) agarose Tris-acetate EDTA (TAE) (40 mM Tris-acetate, pH 8, 1 mM EDTA) gels containing 0.1 % (v/v) SYBR Safe™ DNA gel stain (New England Biolabs) at 160 Volts for 20 - 40 min. The DNA bands were visualized by SYBR staining under UV transillumination.

DNA sequencing was carried out using service by MWG Biotech.

7) Preparation of competent cells

A glycerol stock of *E. Coli* bacterial cells (Rosetta (DE3) pLysS; Novagen) was scraped with a sterile pipette tip and inoculated to 200 µl LB and incubated at 37 °C for 30 min. This culture was plated onto a pre-warmed LB plate containing 34 µg/ml of chloramphenicol and was left overnight at 37 °C. The next day, a single colony from the LB plate was inoculated into a 2.5 ml LB medium and then incubated overnight at 37 °C with shaking (approximately 225 rpm). The next day, the entire overnight culture was used to inoculate 250 ml of LB medium containing 20 mM $MgSO_4$ in a 1 L flask. The culture was let grow at 37 °C with shaking until the OD_{600} reached 0.4 - 0.6. The cells were pelleted by centrifugation at 4,500 *g* for 5 min (Beckman Avanti J-25) at 4 °C. The cell pellets were then gently resuspended in 0.4 volume (based on the original culture volume, for a 250 ml culture, 100 ml was used) of ice-cold TFB1 medium (30 mM potassium acetate, 10 mM $CaCl_2$, 50 mM $MnCl_2$, 100 mM RbCl, 15 % (v/v) glycerol, pH

5.8 with 1 M acetic acid, 0.2 µm filter-sterilized). The resuspended cells were maintained on ice for 5 min and then pelleted again at 4,500 *g* for 5 min at 4 °C. The pellet was gently resuspended in 1/25 of the original culture volume (for a 250 ml culture, 10 ml was used) of ice-cold TFB2 medium (10 mM MOPS, 75 mM $CaCl_2$, 10 mM RbCl, 15 % (v/v) glycerol, pH 6.5 with 1 M KOH, 0.2 µm filter-sterilized). The cells were maintained on ice for 15 - 60 min and then aliquoted to 100 µl per tube, snap frozen in liquid nitrogen and stored at -70 °C.

8) Transformation of cDNA constructs to competent cells

An aliquot of competent cells was thawed on ice. 0.5 µl of mini-prep of the desired construct was then added to the competent cells and mixed by gently swirling. The sample was then incubated on ice for 30 min. The tube was heated at 42 °C for 45 - 60 sec then placed on ice to cool for 30 min. 200 µl LB medium was added to the tube which was then left in 37 °C incubator for 45 min. The mixture was plated onto the selection plate (LB supplemented with 20 g/L Agar + selective antibiotics) which was kept (up-side-down) in a 37 °C incubator for overnight culture.

9) Protein expression

A single colony of the transformation was inoculated into 10 ml of LB containing selective antibiotics (200 µg/ml ampicillin for MBP-Spa and MBP-Spa-His; 200 µg/ml ampicillin and 34 µg/ml chloramphenicol for recombinant SNARE proteins). This culture was incubated overnight in a shaking incubator at a speed of 200 rpm at 37 °C. The following morning, 5 ml of the overnight culture was transferred to a 2 L conical flask containing 1 L LB supplemented with selective antibiotics. This was incubated at 37 °C with shaking at 200 rpm until the UV absorbance at 600 nm reached 0.5 - 0.6 (approximately 3 h). IPTG at 0.5 mM final concentration was added to

the culture to induce recombinant protein expression. Then the culture was incubated for a further 3 h. The cells were harvested by centrifugation for 5 min at 5000 *g* (Beckman Avanti J-25) in 250 ml bottles. The supernatant was discarded and the cell pellet was stored at -80 °C.

10) Protein extraction

- MBP-Spa and MBP-Spa-His extraction

The cell pellet from section 2.2.5.9 was resuspended in 50 ml of column buffer containing AEBSF and 1 mM EDTA. Cells were frozen overnight at -20 °C and defrosted on ice. To release the protein, the cell suspension was sonicated for 2 min on ice with a tip sonicator. The suspension was sonicated at amplitude of 15 microns for 8 times 15 sec with intervals of 45 - 60 sec on ice. Then the suspension was centrifuged at 9,000 *g* for 30 min at 4 °C in 50 ml tubes. The supernatant containing MBP-Spa or MBP-Spa-His was collected, aliquoted in 500 µl, snap frozen in liquid N_2 and stored at -80 °C.

- MBP-Spa-His purification

Ni-NTA His-Bind Resin (Novagen) was used for purification of MBP-Spa-His protein. 1 ml of the 50 % Ni-NTA His-Bind slurry was loaded on to a gravity column, washed 3 times with column buffer containing 10 mM imidazole and AEBSF, before 4 ml of cleared MBP-Spa-His lysate was added to the resin. The mixture was rotated at 4 °C for 60 min. The flow through was collected for analysis. The resin was washed with 10 ml Ni-NTA wash buffer (300 mM NaCl, 50 mM sodium phosphate buffer, 20 mM imidazole, pH 8.0). The protein was eluted with 4 times 0.5 ml Ni-NTA Elution Buffer (300 mM NaCl, 50 mM sodium phosphate buffer, 250 mM imidazole, pH 8.0). The fractions were collected and put in a dialysis tubing with a molecular weight cut off of

12 - 14 kDa (Medicell International Ltd) to dialyse against 4 L of column buffer at 4 °C overnight. The next day, the dialysate was collected and the protein concentration was determined and then AEBSF was added to the solution.

- t-SNARE purification

The cell pellet from section 2.2.5.9 was thawed on ice and then fully resuspended in a total of 50 ml ice-cold IB wash buffer (50 mM Tris HCl pH 7.5, 1 mM EDTA, and 1 % (w/v) octyl-β-D-glucoside) and then decanted into a 50 ml tube. The tube was put into a beaker of wet ice and the bacterial cells were sheared by tip sonicating at amplitude of 24 microns with 2 pulses of 45 sec and a pause of 45 sec in between each pulse). The sonicated suspension was transferred to two 30 ml centrifuge tubes and centrifuged at 16,000 *g* for 10 min. The pellets were resuspended in a total of 50 ml IB wash buffer and centrifuged at 16,000 *g* for a further 10 min. The wash was repeated twice. Then the purified inclusion bodies were resuspended in a 2 ml solubilisation buffer (6 M guanidine HCl, 10 mM DTT, 1 % (w/v) octyl-β-D-glucoside). This solution was incubated at room temperature for 20 min. The insoluble material was spun down at 20,000 *g* for 30 min. The solubilised material was buffer exchanged with reconstitution buffer (25 mM HEPES pH 7.4, 100 mM NaCl, 1 mM DTT, 1 % (w/v) octyl-glucoside) using Bio-Spin 6 (Bio-Rad) columns for a total of 400 µl of the solubilised protein. The proteins, in reconstitution buffer, were incubated at room temperature with rotation for 1 h prior to the reconstitution into vesicles.

- V-SNARE purification

The cell pellet from v-SNARE expression (from section 2.2.5.9) was taken out from -80 °C and thawed on ice, and then resuspended in 25 ml of 50 mM sodium phosphate buffer pH 7.9. This sample was then maintained on ice

for 15 min to allow the nuclease to digest the DNA. 15 ml of 5 M NaCl containing 0.5 g octyl-glucoside (to have a final concentration of 1 % (w/v)) was added and the volume was made up to 50 ml. This mixture was rotated at 4 °C for 1 h and then centrifuged at 20,000 *g* for 30 min to remove insoluble material. The supernatant was transferred to a 50 ml tube containing 0.75 ml of His-Bind resin (Novagen). This sample was rotated at 4 °C for 2 h or overnight. The resin was then spun down and resuspended twice at 500 *g* for 2 min and washed with at least 20 ml reconstitution buffer. The resin was then resuspended in the reconstitution buffer and transferred to a 2 ml microfuge tube and allowed to settle. The buffer was removed until the amount remaining was just sufficient to keep the resin in suspension (about 1.2 ml in total). 20 units of thrombin were added to the resin suspension which was incubated at room temperature overnight with end-to-end rotation. The next day, the resin was transferred to a gravity column to recover the digested protein. The column was then placed carefully in a universal tube, transferred to a bench top centrifuge (Beckman Allegra X-22) and then spun at 500 *g* for 1 min to recover the VAMP2 protein.

2.2.6 Preparation of liposomes

1) Plasma membrane protein – reconstituted liposomes

Basal and insulin stimulated plasma membranes were prepared (Simpson et al., 1983) (section 2.2.1.3) and reconstituted in phospholipid liposomes using an adaptation of previously described methods (Kono, 1983; Schurmann et al., 1989). 270 µg of purified plasma membrane was solubilised in 1.25 % (w/v) n-octyl glucoside and applied to Sephadex G50 column. 200 µl aliquots of solubilised eluted plasma membrane protein (300 µg/ml) were gently vortex mixed with 40 µl of 150 mg/ml Soya bean

phosphatidylcholine (Type IV-S Sigma) in 20 mM HEPES pH 7.4. A Biotin-Europium(TMT) ligand (section 4.2 for molecule structure) was added at 55 nM final concentration and the mixture was sonicated for 15 sec in Decon FS100 Frequency Sweep water bath sonicator (Decon Ultrasonics Ltd) and frozen to -70 °C for at least 2 h. The samples were then thawed, resonicated and purified on flotation Histodenz gradients (Weber et al., 1998). Briefly the liposomes were mixed 1:1 with 80 % Histodenz in reconstitution buffer (25 mM HEPES pH 7.4, 100 mM KCl, 1 mM DTT) containing 10 % glycerol. This was overlayed with 30 % Histodenz in reconstitution buffer with glycerol, and then with buffer only. After an 11 h 40 min spin at 151,263 *g* (35,000 rpm in a SW41Ti rotor), liposomes were collected at the 0 - 30 % Histodenz interface. The amount of encapsulated Biotin-Eu(TMT) was monitored by measuring the fluorescence against a standard curve. Typically 1 to 2 nM of Biotin-Eu(TMT) was encapsulated.

2) Recombinant SNARE protein – reconstituted liposomes

A 150 µl mixture of 13 mM PC:PE:PS (102:30:18 volumn ratio) in chloroform was made up. The chloroform was evaporated under a gentle stream of nitrogen. The complete removal of chloroform was ensured by drying under vacuum for 30 min. The dry lipids were resuspended in 400 µl of reconstitution buffer (25 mM HEPES pH 7.4, 100 mM NaCl, 1 mM DTT, 1 % (w/v) octyl-glucoside) containing t/v-SNAREs. For protein-free/plain vesicles, reconstitution buffer without the SNAREs was used. These samples were incubated together for 30 min at room temperature on a rocking platform (with frequent gentle shaking by hand). The vial containing the mixture was vigorously vortexed with 800 µl of liposome buffer. For t-SNARE liposomes, the liposome buffer contains 25 mM HEPES pH 7.4, 100 mM NaCl, 15 mM $EuCl_3$, 150 mM citrate, 1 mM DTT. For v-SNARE liposomes, the liposome buffer contains 25 mM HEPES pH 7.4, 100 mM

NaCl, 150 mM 2,6-pyridinedicaroxylic acid (dipicolinic acid, DPA). The samples were quickly mixed in the vial with vortexing for a further 30 sec. These samples were dialysed against 4 L of dialysis buffer containing 4 g Biobeads SM2 beads (Bio-Rad) at 4 °C overnight. The next morning, an Optiprep gradient was made up in dialysis buffer (25 mM HEPES pH 7.4, 100 mM NaCl, 1 mM DTT): 40 % of Optiprep in liposome dialysate followed on top with 30 % Optiprep in dialysis buffer, 20 % Optiprep in dialysis buffer and dialysis buffer alone. The gradient was spun at 200,620 *g* (50,000 rpm with MLS-50 rotor) for 5.5 h at 4 °C in the Beckman Optima Ultracentrifuge. The liposomes were visible as a white band near the top of the gradient. The liposomes were harvested in a volume of 1 ml.

2.2.7 Fusion assay

1) Plasma membrane protein – reconstituted liposomes and GLUT4 vesicles fusion assay

Fusion assays were performed in duplicate or triplicate. 50 µl of GLUT4 vesicles, liposomes and cytosol were mixed with 25 µl of IC buffer containing 1 µM biocytin on ice. Fusion was initiated by adding 50 µl of ATP regenerating system (final concentration: 1 mM ATP, 5 mM $MgCl_2$, 8 mM phosphocreatine, and 31 U/ml creatine phosphokinase Type 1) at 37 °C. In some cases GLUT4 vesicles and PM liposomes were mixed with the ATP regenerating system on ice and the reaction was initiated by adding cytosol. Fusion was stopped by returning the samples on ice and addition of 1 % TritonX-100 containing excess biocytin. The extent to which fusion had occurred prior to this endpoint was detected by TR-FRET between Europium(TMT) and DyLight647 in a FARCyte microplate reader (Tecan). The TR-FRET signal was calculated from the ratio of the emission at 670 nm / 612 nm with excitation at 340 nm. The zero time point was used as a

measure of the background and was subtracted from each value. Generally the extent of fusion at 5 min was compared with the maximal fusion obtained by incubation at 37 °C for 30 min. Both the 670 nm and the 612 nm emissions were with a lag time of 50 µsec, an integration time of 400 µsec and with 30 flashes. All attempts to monitor fusion activity in real time were unsuccessful.

2) Recombinant SNARE protein-reconstituted liposomes fusion assay

Standard assays were performed in white 96-well LIA-plate (flat-bottomed, medium binding; Greiner Bio-one). Typically 50 µl v-SNARE DPA encapsulated vesicles (VD) were mixed with 50 µl t-SNARE Europium (Eu) encapsulated vesicles (TE) in the presence of 25 µl of 2.3 mg/ml cytoplasm. The plates were then placed in the FARCyte fluorescence plate reader (Tecan). The FARCyte was equilibrated to 37 °C. Fluorescence was followed with filters set at 340 nm (excitation) and 612 nm (emission). The fluorescence was monitored at either 0.5 or 2 min intervals with a lag time of 50 µsec, an integration time of 400 µsec and with 30 flashes.

3) Treatments

- Trypsin treatment

50 µl of VD vesicles were mixed with freshly dissolved TPCK trypsin (final concentration 1 mg/ml) and left in a 37 °C incubator for 30 min.

- Botulinum Neurotoxin B light chain (BoLC/B, BoNT/B) treatment

Recombinant Botulinum neurotoxin B light chain (BoNT/B, BoLC/B) was purchased from the Centre for Applied Microbiology and Research (Porton Down). BoNT/B stock (5 µM) was first diluted in ddH_2O to 500 nM, and then incubated in a 37 °C incubator for 1 h to activate. Inactivated toxin was

generated by heating at 95 - 100 °C in a heating block for 30 min. When the toxin samples were ready, they were added to either v-SNARE DPA encapsulated liposomes or GLUT4 vesicles to the desired final concentrations and incubated in 37 °C for a further 1 h. Then the samples were ready for either a western blot analysis or for the fusion assay.

2.2.8 Data analysis

Densitometric analysis of western blots and DNA gels was performed using Labworks version 4 (UVP). Graphical analysis was performed using GraphPad PRISM version 4.0 (Graphpad Software, Inc). Statistical analysis was carried out using the PRISM programme with unpaired and paired two-tailed t tests as indicated in the figure legends.

Chapter 3 Cloning and characterization of Maltose-Binding Protein-Protein A and Maltose-Binding Protein-Protein A-Poly His fusion proteins for the isolation of GLUT4 vesicles

3.1 Introduction

The isolation of GLUT4 vesicles is important in understanding their biological properties. In most of the work in this thesis, it is essential to keep GLUT4 vesicles intact with preserved biological activity in order to carry out further experiments. Microsomal vesicles are normally obtained from tissues by a process of enzyme digestion, homogenization and the differential centrifugation (Chapter 2, section 2.2.1). The resulting supernatant contains a variety of vesicles and other cellular components of a similar density. A common method of isolating GLUT4 vesicles from this supernatant is by immunoprecipitation with a specific antibody to the GLUT4 molecule (Slot et al., 1991). The constant region (Fc) of the antibody can be bound by *Staphylococcal* protein A (Spa), which is derived from the cell surface of a common bacterial pathogen, *Staphylococcus aureus*. Spa has extraordinary affinity for immunoglobulin G (IgG) from a number of mammalian species such as human, mouse, rabbit, pig and dog (Ey et al., 1978; Goding, 1978; Langone, 1982; Lindmark et al., 1983). This interesting and very useful property has been widely exploited as an immunological tool. However, using this tool to achieve GLUT4 vesicle isolation requires two more conditions: 1) to isolate GLUT4 vesicle from the supernatant, the Spa is required to attach to a solid matrix; 2) to keep the biological activities of the

GLUT4 vesicles for further experiments, the eluting condition needs to be mild and have a minimal effect on intact GLUT4 vesicles.

To fulfill the first condition covalent bonding of Spa to a solid matrix is a frequently used technique, for example, protein A sepharose beads (Miller and Stone, 1978). However, it does not satisfy the latter requirement as the only way to elute the vesicles from these beads is by using a detergent or low pH conditions. Another approach that could be used is to prepare a bi-functional protein using genetic engineering. The structural genes of two proteins are fused in frame, and the resulting protein carries the active site of each protein. The most frequently used gene fusion affinity tags include glutathione S-transferase (GST), maltose binding protein (MBP), and the His_6 peptide (Sheffield et al., 1999). Comparing within these three, MBP has the mildest eluting condition and the easiest operation procedure.

MBP is a periplasmic protein of *E. Coli.* The 40-kDa protein is encoded by the *malE* gene of *E. coli* K12 TB1 cells (Duplay et al., 1988). It has high affinity for maltose but will also bind other sugars (e.g. amylose) less strongly. Since 1988, MBP fusion plasmid has been shown to facilitate the expression and purification of foreign peptides in *E. coli* (Di Guan et al., 1988). The fused proteins can be purified by one-step affinity chromatography on cross-linked amylose matrix. Bound fusion proteins can be eluted with 10 mM maltose in physiological buffer and maltose does not affect the native conformation of most proteins. The absence of detergent in the process would be expected to keep vesicles intact. In addition, MBP fusion protein can make the protein of interest considerably more soluble, preventing the formation of protein aggregates within the cells (Kapust and Waugh, 1999). Therefore, without chemical coupling, the fusion protein between MBP and Spa would be expected to be able to bind amylose resin at one end, and the GLUT4 antibody and then GLUT4 vesicles at the other

end. The complex could be eluted from the amylose resin in maltose-containing buffer. Thus the eluted GLUT4 vesicles would be intact and biologically active (Fig 3.1).

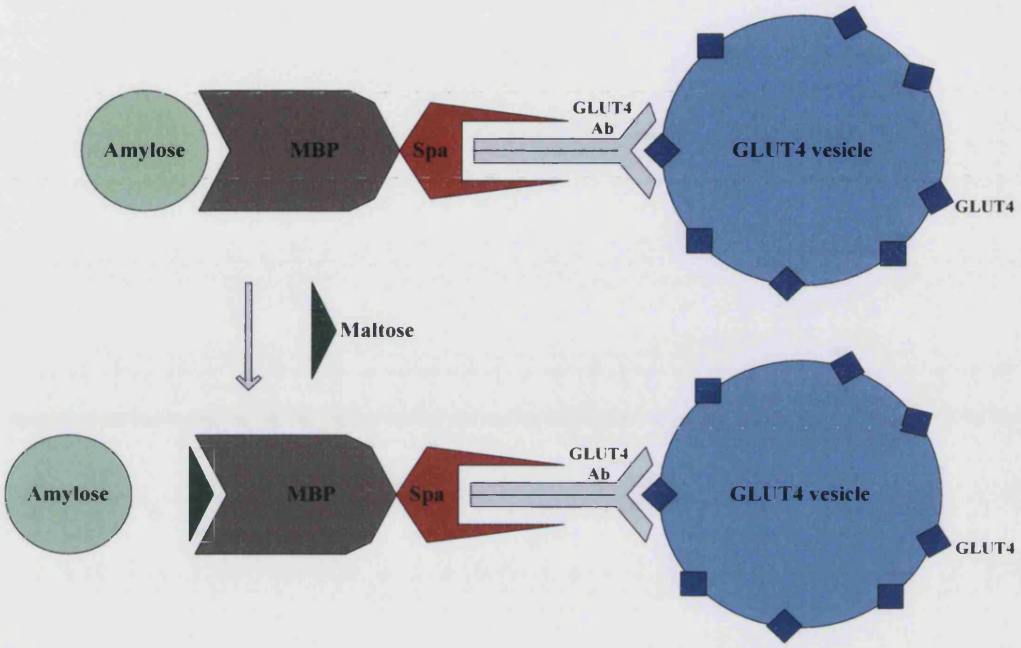

Fig 3.1 Schematic representation of the proposed mechanism to isolate intact GLUT4 vesicles from post high-density microsome supernatant. A specific antibody binds to the GLUT4 molecules on the surface of the vesicle. The protein A component of the fusion protein binds to the constant region (Fc) of the antibody and the maltose-binding component (MBP) binds to the amylose resin. The complex can be eluted from the resin using excess maltose.

In 1995, Kobatake *et al.* produced a MBP-Spa fusion protein to immobilize antibodies for enzyme immunoassays (Kobatake et al., 1995). The Spa gene was excised from a plasmid using restriction enzymes and inserted into pMAL-C2 plasmid (New England Biolabs) which was designed for expression of an MBP fusion protein. The resulting fusion protein had a molecular weight of 65 kDa and demonstrated both efficient IgG binding activity and amylose binding activity. Protein A is a 58 kDa protein (Uhlen et al., 1984). Its gene sequence from N-terminus to C-terminus contains a signal sequence S, five highly homologous IgG-binding regions E, D, A, B

and C, each binding to IgGs independently (Moks et al., 1986), and a C-terminal cell-wall-covalent-binding region X (Lindmark et al., 1977; Uhlen et al., 1984). Kobatake *et al.* excised the Spa gene from a plasmid and ensured three IgG binding domains were complete (Kobatake E et al., 1990). They confirmed that the fusion protein had sufficient binding activity to the Fc region of IgG.

3.2 Cloning strategy

The aim of this chapter is to clone a maltose-binding protein-protein A fusion protein (MBP-Spa) using a modified version of the procedure described by Kobatake *et al* (1995). Two and a half IgG binding regions of Spa were cloned into the maltose-binding protein vector and the fusion protein was expressed in *E.Coli*. The differences from Kobatake *et al*'s method are the proportion of the Spa gene used and the use of the pMBP-Parallel2 plasmid instead of pMAL-C2. The fragment of Spa used in the method described in this chapter was PCR-amplified from pAX11, a vector containing two and a half IgG binding regions in sequence (Zueco and Boyd, 1992). The plasmid pMBP-Parallel2 is based on pMAL-C2. They both contain the maltose-binding protein gene *malE* followed downstream by multiple cloning sites (MCS). The gene of interest can be inserted into the multiple cloning sites. Successful insertion inactivates the β-galactosidase activity of the *malE-lacZ*α fusion. This leads to a blue to white color change on Xgal plates when the construction is transformed into an appropriate host. The fused gene is expressed using a strong P_{tac} promoter in the vector (Fig 3.2). In pMBP-Parallel2 there is a "Parallel" polylinker which replaces the original polylinker between *malE* and *lacZ*α in pMAL-C2. This "Parallel" polylinker was mainly used for easy and direct comparisons of different affinity tags (Sheffield et al., 1999). It does not affect the functional property of the original vector.

A.

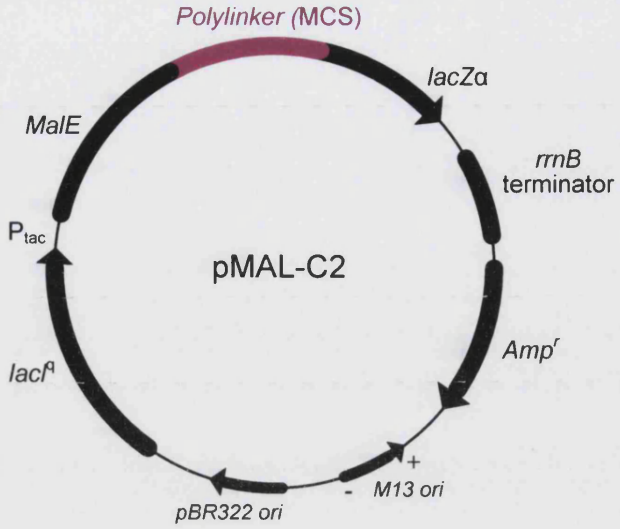

B.

pMBP-Parallel2
(Based on pMal-C2)

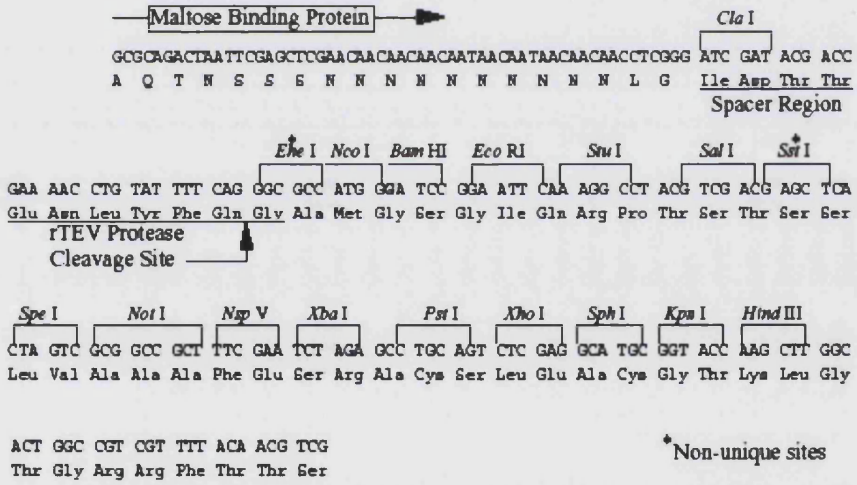

Fig 3.2 Characteristics of pMAL-C2 and pMBP-Parallel2. A: a schematic graph of pMAL-C2 (pMAL Protein Fusion and Purification System Instruction Manual, New England Biolabs). B: Multiple cloning sites of pMBP-Parallel2 (Dr. S. Bagby, University of Bath).

This fusion protein should be able to fulfill the requirements mentioned earlier and provides the foundation for the research carried out in Chapters 4, 5, and 6. This method is a strong tool for intact intracellular vesicle isolation and can be widely used in other studies.

3.3 Results

3.3.1 Cloning of Maltose-Binding Protein-Protein A fusion protein

The preparation of MBP-Spa construct was done by a final year project student Katie Newens (University of Bath). The pAX11 plasmid was sequenced with M13 Uni primer which is located downstream of the Spa gene. The sequencing result confirmed the presence of two and half IgG binding regions by sequence alignment with the entire *Staphylococcal* protein A (Spa) gene obtained from the on-line EMBL nucleotide sequence database (http://www.ebi.ac.uk/embl/). To allow cloning of the Spa fragment into the MBP vector, the gene coding for a fragment of Spa was amplified from pAX11 (Fig 3.3). *BamH*I and *Spe*I were chosen as the restriction sites for insertion into pMBP-Parallel2. pAX11 did contain a *Spe*I site in the MCS downstream of the Spa gene, but did not have a *BamH*I site upstream. Consequently the forward primer was designed to encompass the start of the Spa fragment together with a *BamH*I site and reverse primer was M13 Uni. The designed primer was:

```
5' - GGG GGA TCC CCA AGC TTA AAA GAT GAC CC - 3'
         BamHI      Start of Spa (pAX11)
```

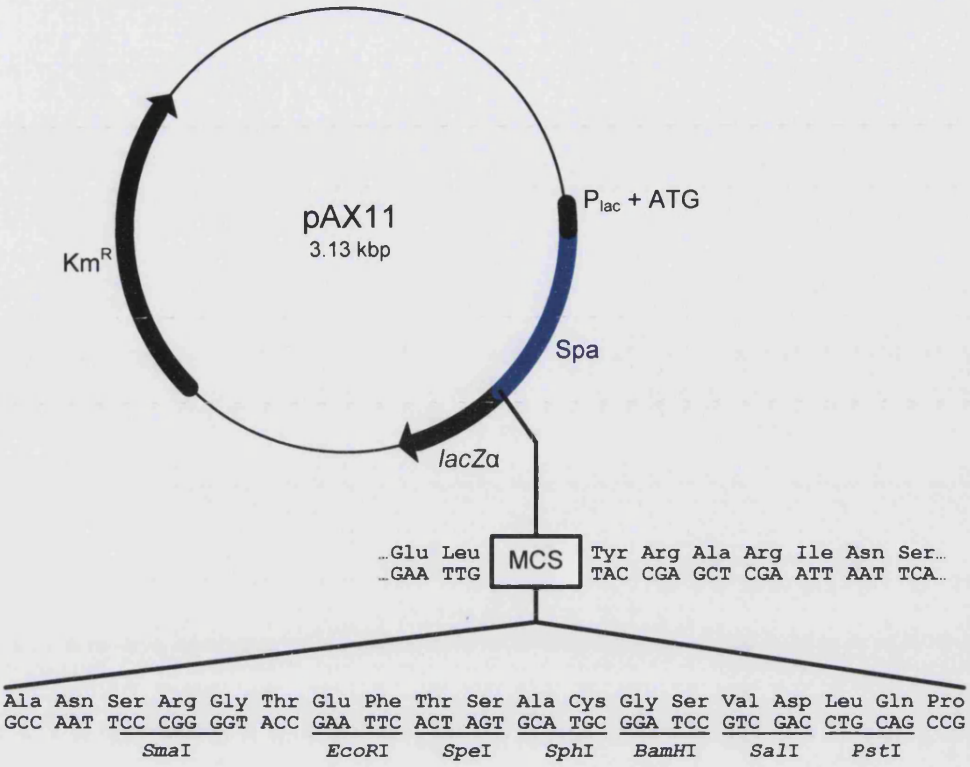

Fig 3.3 Structure of the pAX11 vector. The MCS is downstream of Spa gene. *Spe*I restriction site is in the MCS (Zueco and Boyd, 1992).

*BamH*I and *Spe*I were the chosen restriction enzymes for insertion of the fragment into pMBP-Parallel2 so that cohesive ends would be produced facilitating ligation. This choice of enzymes also allowed the Spa fragment to be kept in frame, and generated a stop codon shortly downstream of pMBP-Parallel2 by frame shift, ensuring that the transcription ceased soon after the fusion protein.

The *Spe*I site in pMBP-Parallel2 is located downstream of maltose binding protein in the multiple cloning sites and cuts the DNA between two codons, thus maintaining the reading frame (Fig 3.4). However, the *Spe*I site of pAX11 induced the enzyme to cut the DNA within a threonine codon, therefore when the Spa fragment is ligated into pMBP-Parallel2 it results in a

frame shift mutation downstream of the *Spe*I site in pMBP-Parallel2. This leads to the formation of stop codon shortly downstream (TAG) (Fig 3.4).

pAX11 multiple cloning sites:

5'- AAT TCC CGG GGT ACC GAA TTC A|CT AGT GCA TGC GGA TCC GTC GAC CTG
Asn Ser Arg Gly Thr Glu Phe Thr ser Ala Cys Gly Ser Val Asp Leu
SmaI *KpnI* *EcoRI* *SpeI* *SphI* *BamHI* *SalI*

CAG CCG
Gln Pro
PstI

pMBP-Paralle2:

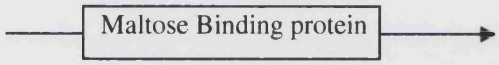

5'-ACT AAT TCG AGC TCG AAC AAC AAC AAC AAT AAC AAT AAC AAC AAC CTC
T N S S S N N N N N N N N N N L

GGG ATC GAT ACG ACC GAA AAC CTG TAT TTT CAG GGC GCC ATG GGA TCC GGA
Gly Ile Asp Thr Thr Glu Asn Leu Tyr Phe Gln Gly Ala Met Gly Ser Gly
Spacer Region *EheI* *NcoI* *BamHI* *EcoRI*

ATT CAA AGG CCT ACG TCG ACG AGC TCA| CTA GTC GCG GCC GCT TTC GAA TCT
Ile Gln Arg Pro Thr Ser Thr Ser Ser Leu Val Ala Ala Ala Phe Glu Ser
StuI *SalI* *SstI* *SpeI* *NotI* *NspV* *XbaI*

AGA GCC TGC AGT CTC GAG GCA TGC GGT ACC AAG CTT GGC ACT GGC CGT CGT
Arg Ala Cys Ser Leu Glu Ala Cys Gly Thr Lys Leu Gly Thr Gly Arg Arg
PstI *XhoI* *SphI* *KpnI* *HindIII*

TTT ACA ACG TCG -3'
Phe Thr Thr Ser

Frame shift in pMBP-Paralle2:

5'-ACT AGT CGC GGC CGC TTT CGA ATC TAG AGC CTG CAG TCT CGA GGC ATG CGG
Thr Ser Arg Gly Arg Phe Arg Ile Stop
SpeI *NotI* *NspV* *XbaI* *PstI* *XhoI* *SphI* *KpnI*

TAC CAA GCT TGG CAC TGG CCG TCG TTT TAC AAC GTC G -3'

Fig 3.4 Sequence detail showing the cutting of pAX11 and pMBP-Parallel2 MCS and the resulting frame shift in pMBP-parallel2 after the Spa fragment insertion. Restriction sites are shown in blue and pink. The restriction sites for Spa insertion in pMBP-parallel2 are highlighted with yellow. Red line shows the cutting of *Spe*I which caused frame shift. The DNA sequence of pMBP-Parallel2 after the frame shift is shown separately and the stop codon highlighted with red.

*Hind*III

The Spa gene fragment was amplified using the designed primer and the forward universal M13 primer and the resulting fragment was purified on an agarose gel (Chapter 2, section 2.2.5.3). The purified gene fragment and the pMBP-Parallel2 plasmid were digested with *BamH*I and *Spe*I and appropriate bands purified from an agarose gel (Fig 3.5).

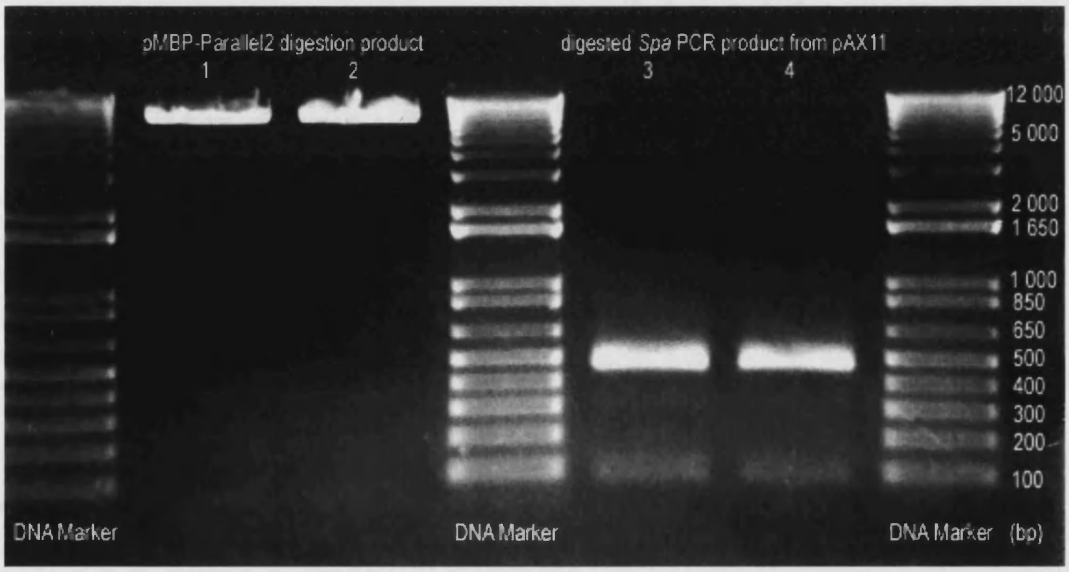

Fig 3.5 DNA gel showing the pMBP-Parallel2 double digestion product (lanes 1, 2) and double digested Spa PCR product from pAX11 (lanes 3, 4).

The digestion products of pMBP-Parallel2 and the Spa fragment were ligated to form a recombinant plasmid. As both the vector and insert were

digested with the same restriction endonucleases, the cohesive ends were joined with DNA ligase. As a back up the Spa fragment was also inserted into the blunt vector pT7 blue, this was ligated using T4 DNA ligase in a blunt ended cloning protocol (Novagen 70183). Both the recombinant plasmids were used to transform XL1 blue cells. White colonies were picked and the plasmid isolated with a mini-prep kit. Test digests of these plasmids with *BamH*I and *Spe*I were performed to confirm the insertion of the Spa gene. These were run on an agarose gel. If the plasmids contained the insert, excision with these enzymes should yield the insert and show a fragment of 0.47 kbp (Fig 3.6).

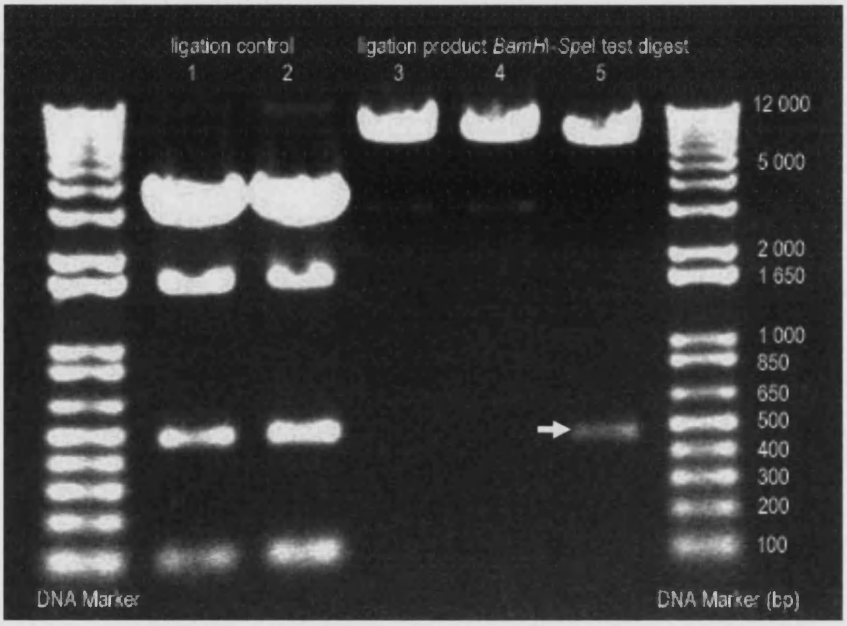

Fig 3.6 DNA gel showing insertion of Spa into pMBP-Parallel2 and pT7 blue vector. Plasmids were test digested with *BamH*I-*Spe*I to check the insertion of Spa (arrow), if present. Lane 1 and 2 – test digests of pT7 blue plasmids, Lanes 3-5 – test digests of pMBP-Parallel2 plasmids. Lane 5 showed a successful ligation of pMBP-Parallel2 and Spa gene.

By comparing the band size of the digested MBP plasmid with the control, a plasmid containing the insert was identified. This was sequenced to confirm that the fragment contained the protein A gene (Fig 3.7).

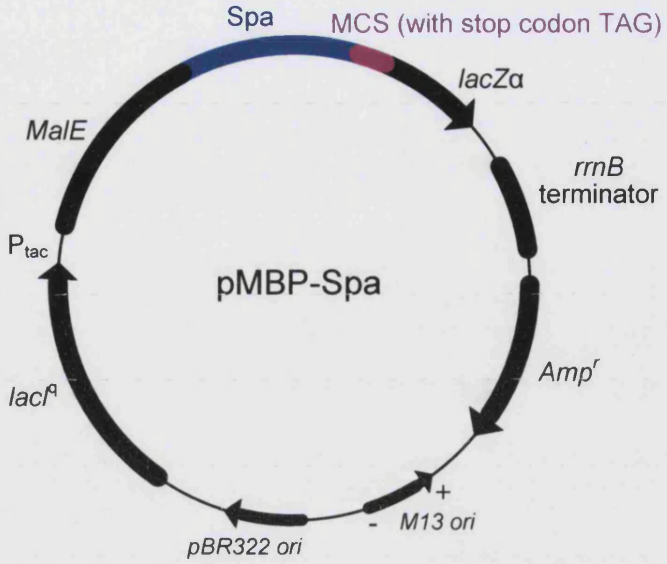

5′-CAGGGCGCCATGGATCCCCAAGCTTAAAAGATGACCCAAGCCAAAGTGCTAACCTATTGTCAGA
AGCTAAAAAGTTAAATGAATCTCAAGCACCGAAAGCGGATAACAAATTCAA

IgG binding region A (half)

CAAAGAACAACAAAATGCTTTCTATGAAATCTTACATTTACCTAACTTAAACGAAGAACAACGCAAT
GGTTTCATCCAAAGCCTAAAAGATGACCCAAGCCAAAGCGCTAACCTTTTAGCAGAAGCTAAAAAGC
TAAATGATGCTCAAGCACCAAAAGCTGACAACAAATTCAA

IgG binding region B (complete)

CAAAGAACAACAAAATGCTTTCTATGAAATTTTACATTTACCTAACTTAACTGAAGAACAACGTAAC
GGCTTCATCCAAAGCCTTAAAGACGATCCTTCAGTGAGCAAAGAAATTTTAGCAGAAGCTAAAAAGC
TAAACGATGCTCAAGCACCAAAAGATGACGATAAAG

IgG binding region C (complete)

AATTGGCCAAT TCC CGG GGT ACC GAA TTC ACT AGT CGC GGC CGC TTT CGA A

Start of MCS *SmaI*[1] *KpnI*[1] *EcoRI*[1] *SpeI*[1,2] *NotI*[2] *NspV*[2]

(frame shift mutation)

TC TAG AGC CTG CAG TCT CGA GGC ATG CGG TAC CAA GCT T

XbaI[2] *PstI*[2] *XhoI*[2] *SphI*[2] *KpnI*[2] *HindIII*[2]

GGCACTGGCCGTCGTTT - 3′

Fig 3.7 Map of pMBP-Spa and sequence detail of Spa gene. Sequencing shows a successful insertion of Spa gene in the MCS downstream of MBP gene *MalE.* A half of IgG binding region and two complete regions are seen, identified as A, B and C. Multiple cloning sites (MCS) downstream of Spa gene are shown in black and pink. Frame shift mutation is labeled and stop codon highlighted with red. Restriction sites [1] were from pAX11 and [2] from pMBP-Parallel2.

The above figure shows the presence of two and half IgG binding domains. These binding regions were identified as A, B and C, the last two and half IgG binding regions of the natural Spa gene. The molecular weight of the fusion protein was calculated by using the Spa fragment sequence shown in Fig 3.7 and the sequence of *MalE* in pMAL-C2 (New England Biolabs website: www.neb.com). The molecular weight was calculated to be 61.07 kDa.

3.3.2 Expression of Maltose-Binding Protein-Protein A and tests on GLUT4 vesicle isolation

E. Coli K12 TB1 cells were transformed with the plasmid pMBP-Spa and the fusion protein expressed by induction with IPTG (Chapter 2, section 2.2.5.9). During growth of the cells, glucose in the growth medium was necessary to repress the maltose genes on the chromosome of the *E. Coli* host. The cells were sonicated to release the protein. To show that protein expression was induced with the IPTG, samples of culture were collected during this process and western blotted with rabbit IgG - peroxidase conjugate (Fig 3.8 A). The IgG detection of bands in appropriate position (62 kDa) proved that the Spa portion of the fusion protein was functional. The band before IPTG induction was barely visible but after IPTG induction was very strong, showing the proper expression of MBP-Spa. In the cell lysate, most of the MBP-Spa appeared in the supernatant after centrifugation at 9000 *g* for 30 min (Chapter 2, section 2.2.5.10), indicating the fusion protein had good cellular solubility. The supernatant of the bacterial lysate was used

as such for various immuno-precipitation procedures. The initial tests showed that after binding the MBP-Spa product to amylose resin, 20 mM maltose successfully eluted over 80 % of the total MBP-Spa protein bound on the amylose resin in the first 3 fractions (E1-E3). Less than 15 % of MBP-Spa was left on the beads (Fig 3.8 B). The bacterial lysate supernatant was routinely kept for 6 months stored in aliquots in -80 °C without a drop in the binding capacity of the protein.

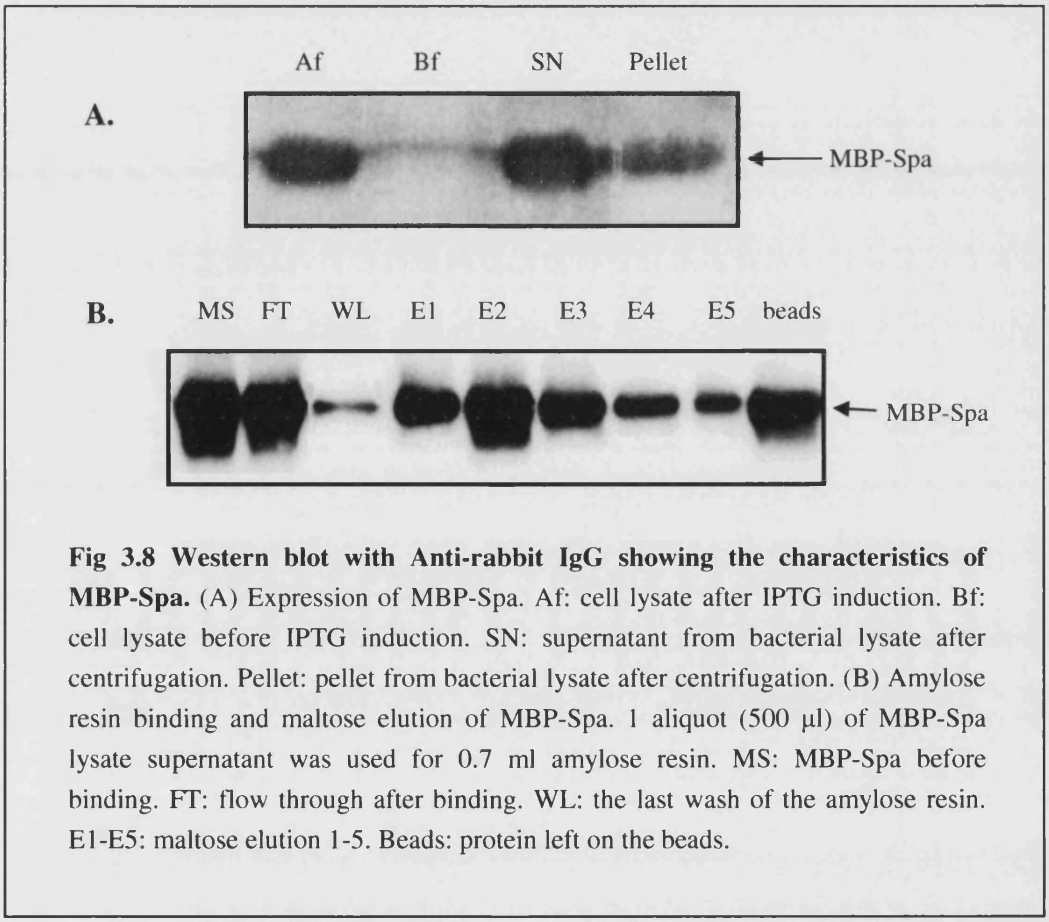

Fig 3.8 Western blot with Anti-rabbit IgG showing the characteristics of MBP-Spa. (A) Expression of MBP-Spa. Af: cell lysate after IPTG induction. Bf: cell lysate before IPTG induction. SN: supernatant from bacterial lysate after centrifugation. Pellet: pellet from bacterial lysate after centrifugation. (B) Amylose resin binding and maltose elution of MBP-Spa. 1 aliquot (500 µl) of MBP-Spa lysate supernatant was used for 0.7 ml amylose resin. MS: MBP-Spa before binding. FT: flow through after binding. WL: the last wash of the amylose resin. E1-E5: maltose elution 1-5. Beads: protein left on the beads.

The initial test on GLUT4 vesicle isolation was done using 500 µl MBP-Spa, 0.7 ml amylose resin, and 100 µg anti GLUT4 Ab to immuno-precipitate the GLUT4 vesicles from the post density microsome supernatant (pHDM SN) from 2 ml of 40 % basal adipocytes (Fig 3.9). MBP-Spa was first bound to amylose resin overnight, then incubated for an additional 2 hours with the anti GLUT4 Ab. The amylose resin - (MBP-Spa) - anti GLUT4 complex was

then incubated with pHDM SN. The MBP-Spa-(anti GLUT4 Ab)-GLUT4 vesicle complexes were then eluted with 20 mM maltose under gravity. It was found that 70 % of GLUT4 from pHDM SN bound to amylose resin, of which 60 - 70 % was eluted by maltose. Noticeably the eluted MBP-Spa was 70 % too. The GLUT4 was mostly concentrated in elution fractions 1 and 2, but in some tests it was fractions 2 and 3 that obtained the bulk of the GLUT4 vesicles. In the most concentrated fraction (E2 in Fig 3.9), the v-SNARE VAMP2 could be detected, which indicated that intact GLUT4 vesicles were precipitated and these vesicles kept their functional protein for membrane fusion. In addition, because VAMP2 is a feature protein for GLUT4 storage vesicles (GSV) (Larance et al., 2005), it meant that these vesicles belonged to GSV, a population of the intracellular GLUT4 compartment that is most ready for insulin-stimulated translocation.

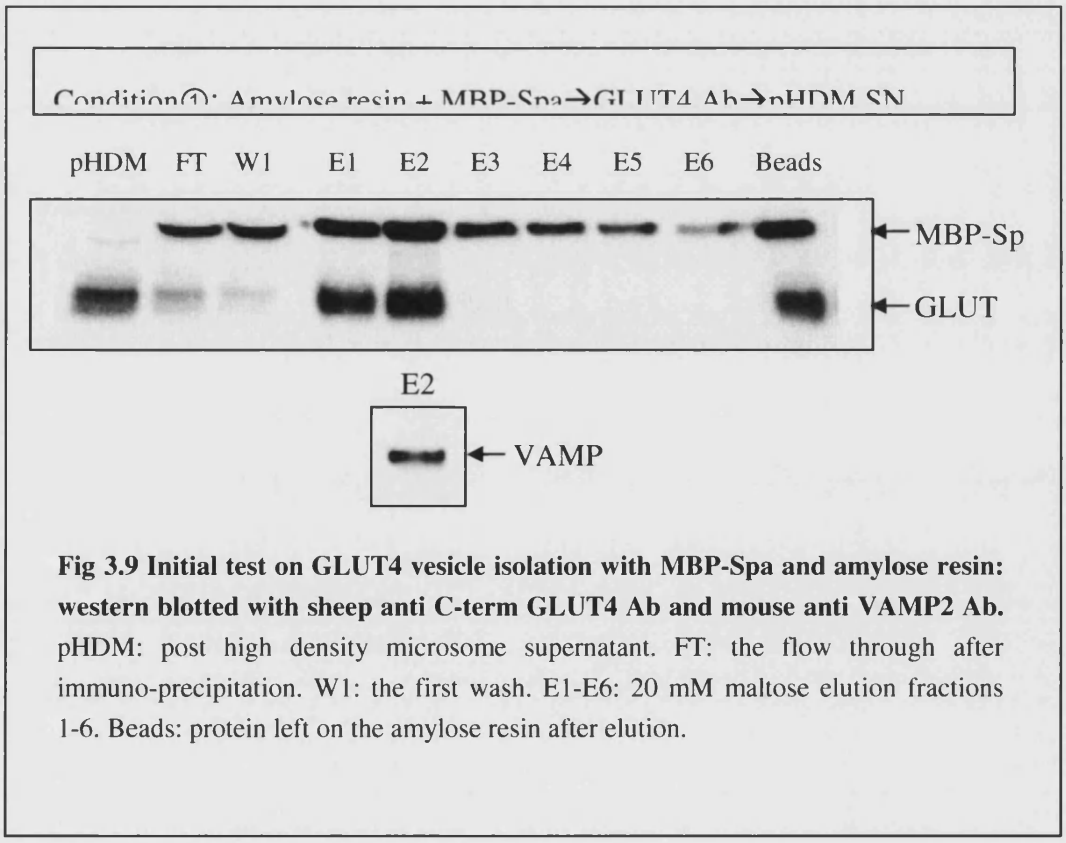

Fig 3.9 Initial test on GLUT4 vesicle isolation with MBP-Spa and amylose resin: western blotted with sheep anti C-term GLUT4 Ab and mouse anti VAMP2 Ab. pHDM: post high density microsome supernatant. FT: the flow through after immuno-precipitation. W1: the first wash. E1-E6: 20 mM maltose elution fractions 1-6. Beads: protein left on the amylose resin after elution.

Although intact GLUT4 vesicles were purified in the above test, the efficiency was not satisfying. As high as 30 % of the total bound GLUT4 was left on the beads after elution. To increase the eluting efficiency, the influencing factors were analysed and a few approaches were tried.

As the MBP-Spa used was in cell lysate, which contained a lot of other bacterial soluble proteins, those proteins might affect the bindings and bring in non-specific interactions. To get rid of some of the impurities, high salt was included when MBP-Spa lysate was incubated with amylose resin. 0.5 M NaCl was added to the protein-resin mixture and after incubation the resin was washed with 1 M NaCl. To maximize the elution, maltose concentrations were doubled to 40 mM and the resin was incubated with the elution buffer for 10 min before collecting the elution fractions. The amylase expressed in *E. Coli* host which stayed in the lysate could degrade the amylose on the affinity resin (Riggs, 2000). Degradation of the MBP-Spa protein was observed during the isolation procedure too (Fig 3.9 samples "FT", "W1"). To prevent amylose degradation 120 U of α-Amylase inhibitor from *Triticum aestivum* (wheat seed) was added in the procedure. All together these optimizations were marked as condition② (Fig 3.10). It showed that about 80 - 85 % of the total bound GLUT4 was eluted in the 1^{st} and 2^{nd} fractions.

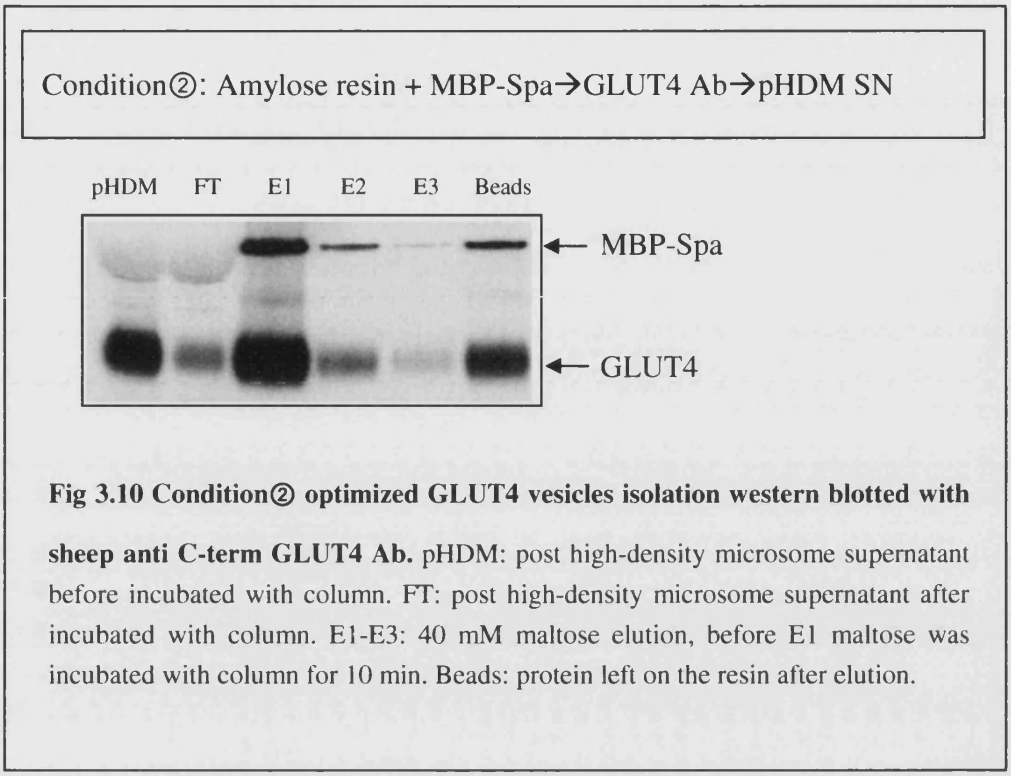

Fig 3.10 Condition② optimized GLUT4 vesicles isolation western blotted with sheep anti C-term GLUT4 Ab. pHDM: post high-density microsome supernatant before incubated with column. FT: post high-density microsome supernatant after incubated with column. E1-E3: 40 mM maltose elution, before E1 maltose was incubated with column for 10 min. Beads: protein left on the resin after elution.

In the multi-step immuno-precipitations there are different options for the precipitation order. These options sometimes result in different precipitation efficiencies. To maximize the precipitation, different orders were tried in this assay. As the MBP-Spa was not purified in this assay, there was only 1 other option to change the precipitation order: react GLUT4 vesicles with anti GLUT4 antibody first, then precipitate with MBP-Spa pre-bound to amylose resin (condition③). Post HDM supernatant was incubated with anti GLUT4 Ab for more than 2 h and then precipitated with MBP-Spa prebound amylose resin. The whole complex was eluted with 40 mM maltose (Fig 3.11). There was above 80 % of the total bound GLUT4 eluted in the first and second fractions.

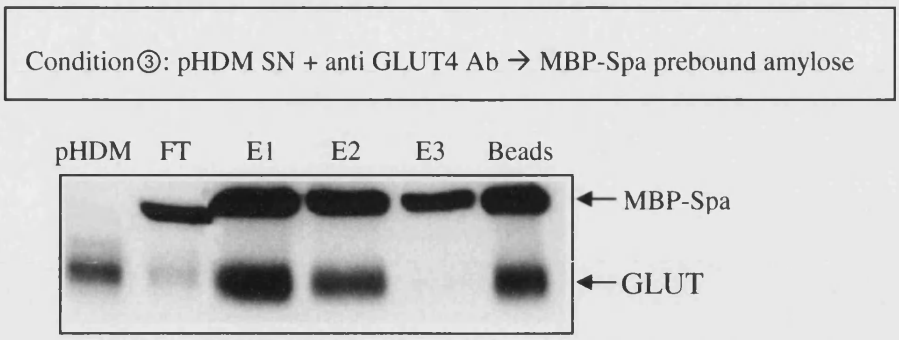

Fig 3.11 Condition③ optimized GLUT4 vesicles isolation western blotted with sheep anti C-term GLUT4 Ab. pHDM: post high-density microsome supernatant before incubated with column. FT: post high-density microsome supernatant after incubated with column. E1-E3: 40 mM maltose elution, before E1 maltose was incubated with column for 10 min. Beads: protein left on the resin after elution

3.3.3 Cloning of Maltose-Binding Protein-Protein A-Poly His fusion protein

An MBP-Spa-His construct was made to be able to further purify the maltose-binding protein. This was mainly aimed to try the different precipitation orders, quantify the MBP-Spa, and to find out the optimal procedure for GLUT4 vesicle isolation.

The construct was made by tagging the existing MBP-Spa fusion protein with a Poly-His tag. It was convenient to clone a Poly-His sequence between two restriction enzyme sites in the multiple cloning sites downstream of Spa (Fig 3.4). *Not*I and *Xho*I were selected as cloning sites and the Poly-His sequence was designed as an oligonuleotide. As in the original sequence between *Not*I and *Xho*I there was a stop codon which would be eliminated due to the cloning, it was necessary to include a stop codon at the end of the insert. A pair of oligonucleotides was originally designed to include poly-His sequence followed by a stop codon and *Not*I-*Xho*I restrictions sites as sticky ends but this was found to be not successful in the cloning. The 2nd

approach for the oligonucleotide construct was still to keep the sequence, but instead the *Xho*I site was destroyed by changing the starting "C" to "G" (Fig 3.12). The 2nd oligonucleotide would still directly replace the sequence in between the *Not*I-*Xho*I in the original plasmid, but after ligation there would not be an *Xho*I site. The designed oligonucleotides are shown in Fig 3.12.

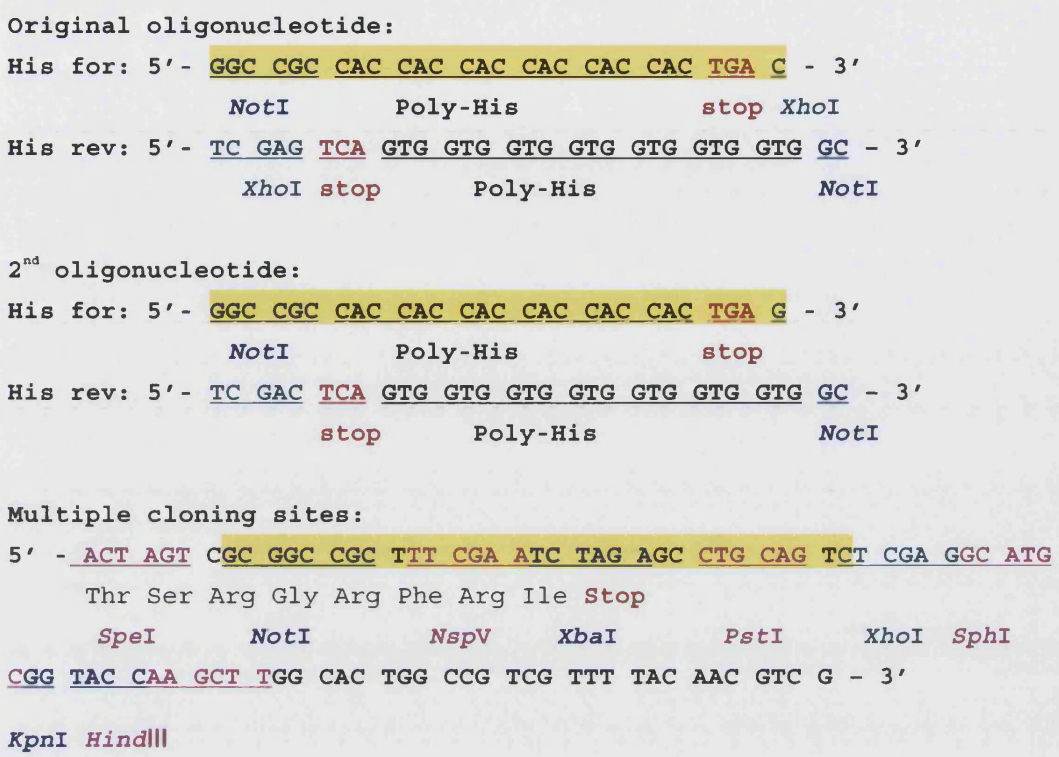

Fig 3.12 Sequence detail of the designed His-tag oligonucleotides and the multiple cloning sites. Restriction sites *Not*I and *Xho*I in designed oligonuleotides and multiple cloning sites were shown in blue and green. The corresponding sequence in the multiple cloning sites which would be substituted by the oligonucleotide was highlighted with yellow. Stop codons in both oligonucleotides and multiple cloning sites were labelled in red. The 2nd oligonuleotide destroyed the *Xho*I site.

Firstly the attempt of doing *Xho*I-*Not*I double digestion of pMBP-Spa was tried but it was not successful (data not shown). Then the double digestion was realized through two sequential single digestions. The pMBP-Spa plasmid was digested with *Xho*I and the linearized DNA was purified on an agarose gel. The extracted DNA was then digested with *Not*I and purified to obtain a double digestion product, which exposed the *Not*I and *Xho*I sticky ends (Fig 3.13 A, B). The His forward and His reverse oligonuleotides were paired to form an insert ready for ligation. The digestion product of pMBP-Spa and the insert fragment were ligated in the presence of *Xba*I restriction endonuclease. The *Xba*I site was between *Not*I and *Xho*I in the original vector, so the *Xba*I enzyme prevented the religation of any

contaminating insert, if any was present. As a control, the insert was replaced by nuclease-free H_2O. The ligation products were transformed into XL1 blue or TB1 cells and plasmids were purified with mini-prep kit. Test digests on these plasmids were carried out with an *Xba*I single digest and a *BamH*1-*Spe*1 double digest (Fig 3.13 C). *Xba*I was used to confirm the successful insertion of the Poly-His insert. The *BamH*I-*Spe*I double digest was to make sure the 0.47 kbp Spa fragment was not affected. The plasmids which showed both negative *Xba*I cleavage and positive *BamH*I-*Spe*I cleavage were sent for sequencing.

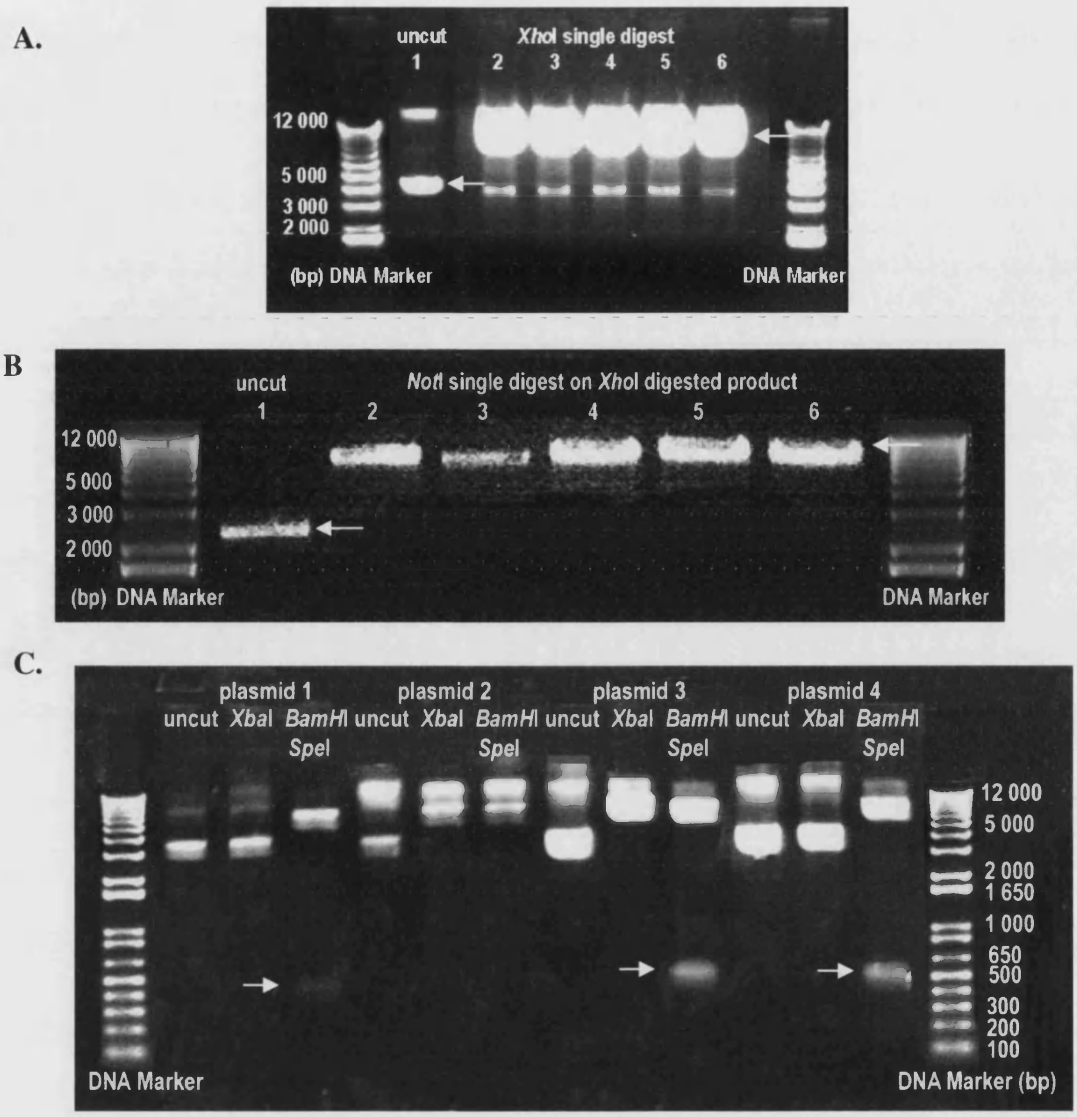

Fig 3.13 DNA gel showing the cloning of pMBP-Spa-His. (A): pMBP-Spa single digested with *Xho*I. Uncut plasmid showed that intact plasmid formed a supercoil (low arrow). *Xho*I single digestion showed linearized plasmid which had a bigger secondary structure (high arrow). (B): *Xho*I single digestion product digested with *Not*I, to realize the double digestion. 1 showed the uncut plasmid was intact and formed a supercoil (low arrow). 2-6 showed the double digestion product was linearized and had a bigger secondary structure (high arrow). (C): mini-prep-purified plasmids tested with *Xba*I single digest and *BamH*I-*Spe*I double digest. Plasmids 1, 3, 4 showed positive *BamH*I-*Spe*I double digest, resulting a 0.47 kbp Spa fragment (arrow). Plasmids 1, 4 showed a negative *Xba*I single digest.

The sequencing result clearly showed a successful cloning of Poly-His followed by a stop codon downstream of Spa (Fig 3.14). There were 6 "CAC"s followed by the stop code "TGA". After "TGA" there was a "G" as designed in the oligonuleotide rather than "C" in the original plasmid. This single nucleotide destroyed the *Xho*I site but did not affect the expression of MBP-Spa-His. The molecular weight of the protein did not change.

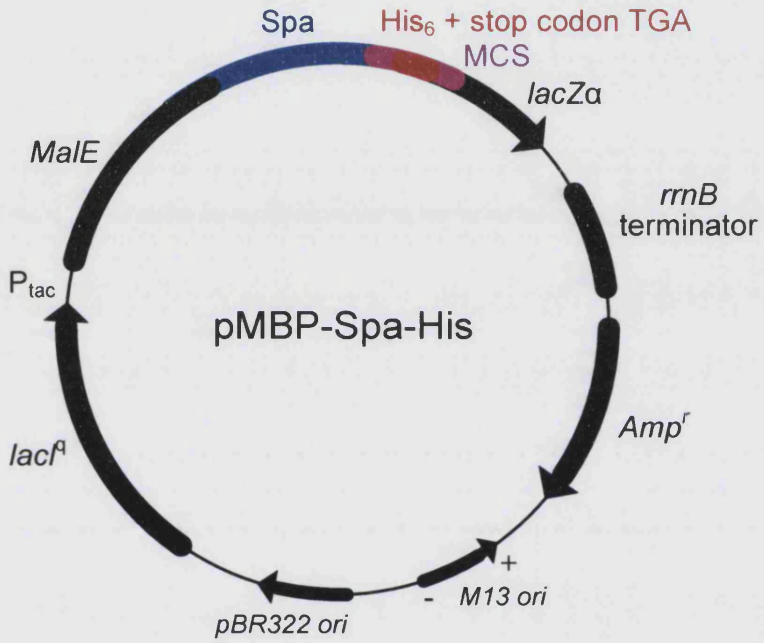


```
                    5'-ATTGGCCAAT TCC CGG GGT ACC GAA TTC
                     Start of MCS   SmaI    KpnI   EcoRI
ACT AGT CGC GGC CGC CAC CAC CAC CAC CAC CAC TGA GTC GAG GCA -3'
 SpeI       NotI        Poly-His              stop
```

Fig 3.14 Map and Sequence detail to show the successful cloning of pMBP-Spa-His. Poly-His was downstream of Spa gene, starting from *Not*I restriction site in MCS. Stop codon was highlight with red. The nucleotide 'G' designed in the oligonuleotide was highlighted with yellow, and it destroyed the *Xho*I site after the stop codon. The sequencing primers used were *MalE*.

3.3.4 Expression of Maltose-Binding Protein-Protein A-Poly His fusion protein (MBP-Spa-His) and Purification by Ni-NTA His-Bind Resin

The Maltose-Binding Protein-Protein A-Poly His fusion protein construct (MBP-Spa-His) was transformed and expressed in the same way as MBP-Spa (Chapter 2, section 2.2.5.9). The cell lysate supernatant was further purified with Ni-NTA His-Bind Resin (Novagen) (Chapter 2, section 2.2.5.10). The MBP-Spa was used in parallel as a control (Fig 3.15). Comparing the bacterial lysate supernatant and pellet from MBP-Spa-His with the ones from MBP-Spa, the expression was confirmed to be normal. The lysate supernatants were then incubated with Ni-NTA His-Bind Resin. To find out the binding capacity of the resin, 50 or 100 µl of 50 µg/ml MBP-Spa-His were incubated with constant amount of resin (30 µl) (Fig 3.15). The Coomassie blue stained gel result confirmed that at least 100 µl MBP-Spa-His could bind to 30 µl of beads. As expected, MBP-Spa did not bind to the resin at all. This purification was scaled up to produce larger amount of protein. The elution was collected and dialysed against column buffer to remove the imidazole. The purified protein was concentrated down to 1.8 mg/ml and was then ready for further tests.

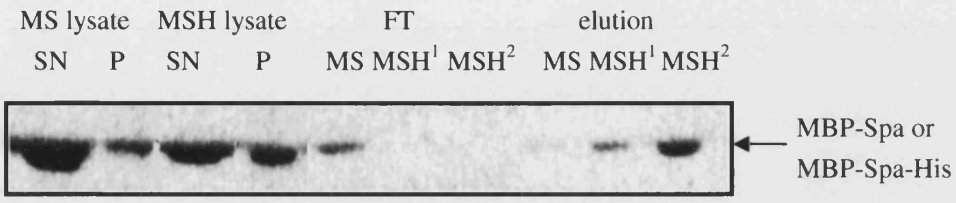

Fig 3.15 Protein gel stained with Coomassie blue stain showing the purification of MBP-Spa-His with Ni-NTA His-Bind Resin. Both MBP-Spa (MS) and MBP-Spa-His (MSH) expression was checked in lysate supernatant (SN) and pellet (P). Supernatant was incubated with Ni-NTA His-Bind Resin for 1 h. Flow through (FT) was checked for protein left after the binding to the resin. Protein bound on the resin was eluted with 250 mM imidazole. 30 µl of resin, 50 µl of MS supernatant, 50 µl (MSH^1) or 100 µl (MSH^2) of MSH supernatant were used for the purification.

3.3.5 Optimization of the GLUT4 vesicle isolation by MBP-Spa-His

As the un-purified MBP-Spa had to be bound to amylose to purify it this limited the attempts to optimise the GLUT4 isolation procedure. The purified MBP-Spa-His enabled the quantification of the protein and provided more options for carrying out the procedure.

To keep it simple, the initial tests were on MBP-Spa-His, anti GLUT4 antibody only and amylose resin, but GLUT4 isolation was not involved. First the purified MBP-Spa-His was pre-mixed with GLUT4 antibody to form a complex, and then the complex was incubated with amylose resin. It was found that if amylose resin was kept at 0.7 ml and the antibody amount at 100 µg (667 pmols), then 48 µg MBP-Spa-His (800 pmols) was enough to bind all the antibody molecules. The binding capacity of amylose resin provided by the manufacturer (New England Biolabs) was 3.0 mg MBP/ml bed volume. According to the binding capacity, 0.7 ml resin was in large

excess over the 48 μg of MBP-Spa-His. To find the optimal amount of amylose resin, a range of the resin amounts were tested. In the tests antibody was scaled down to 37 μg and MBP-Spa-His to 18 μg, for the purpose of saving antibody. 10 μl, 35 μl, 100 μl and 200 μl of amylose resin were tried to bind with MBP-Spa-His-(anti GLUT4 Ab) complex, and the complex was eluted with 40 mM maltose (condition④, Fig 3.16). This test showed that 10 μl of amylose resin was able to bind all the complexes. However, little was found in the elution. In addition, the small amount of resin was hard to manipulate in the experiment procedure. From the sample using 35 μl of resin, 55 % of the total bound protein was eluted in the first elution and from the samples of 100 and 200 μl resin 80 % was eluted. This 80 % eluting efficiency was consistent with the MBP-Spa results (section 3.3.2). When this approach, using 200 μl resin and MBP-Spa-His-GLUT4 Ab complex, was used to isolate GLUT4 vesicles from pHDM supernatant (condition⑤ Fig 3.17), 74 % of the total bound GLUT4 was eluted in the first and second elution fractions. It was slightly better than condition① but not as good as condition②.

From the above result and the results from section 3.3.2, it was noticeable that after elution, there were always some proteins left on the resin, which could not be eluted. In other words, these proteins bound to the resin irreversibly. In theory, if the eluted proteins rebound to the resin, these proteins should be 100 % elutable. So, an idea of purifying the MBP-Spa on an amylose resin for a first time and then rebinding the eluted proteins to a new resin sample was tried. To rebind protein to new amylose resin, the maltose used in the first elution must be removed. Dialysis did not work to remove maltose from maltose-binding protein. This is a general phenomenon of protein/ligand interactions: after the free ligand is gone, ligand that is released from the binding site usually finds another binding site

before it encounters the dialysis membrane (Silhavy et al., 1975). Maltose could be removed by extensive washes. To do the extensive washes the protein needs to be bound to a solid matrix. MBP-Spa-His was first bound to amylose resin and eluted with maltose. Eluted MBP-Spa-His was rebound to Ni-NTA His Bind Resin and extensively washed to remove maltose. The protein was eluted from His-Bind Resin with imidazole, dialyzed to get rid of the imidazole and rebound to a new lot of amylose resin. The protein did not show proper rebinding to the amylose resin (data not shown). It might be because the washing was not good enough to remove the maltose. Maltose was still bound to MBP-Spa-His to some extent and it interfered with the second round of binding.

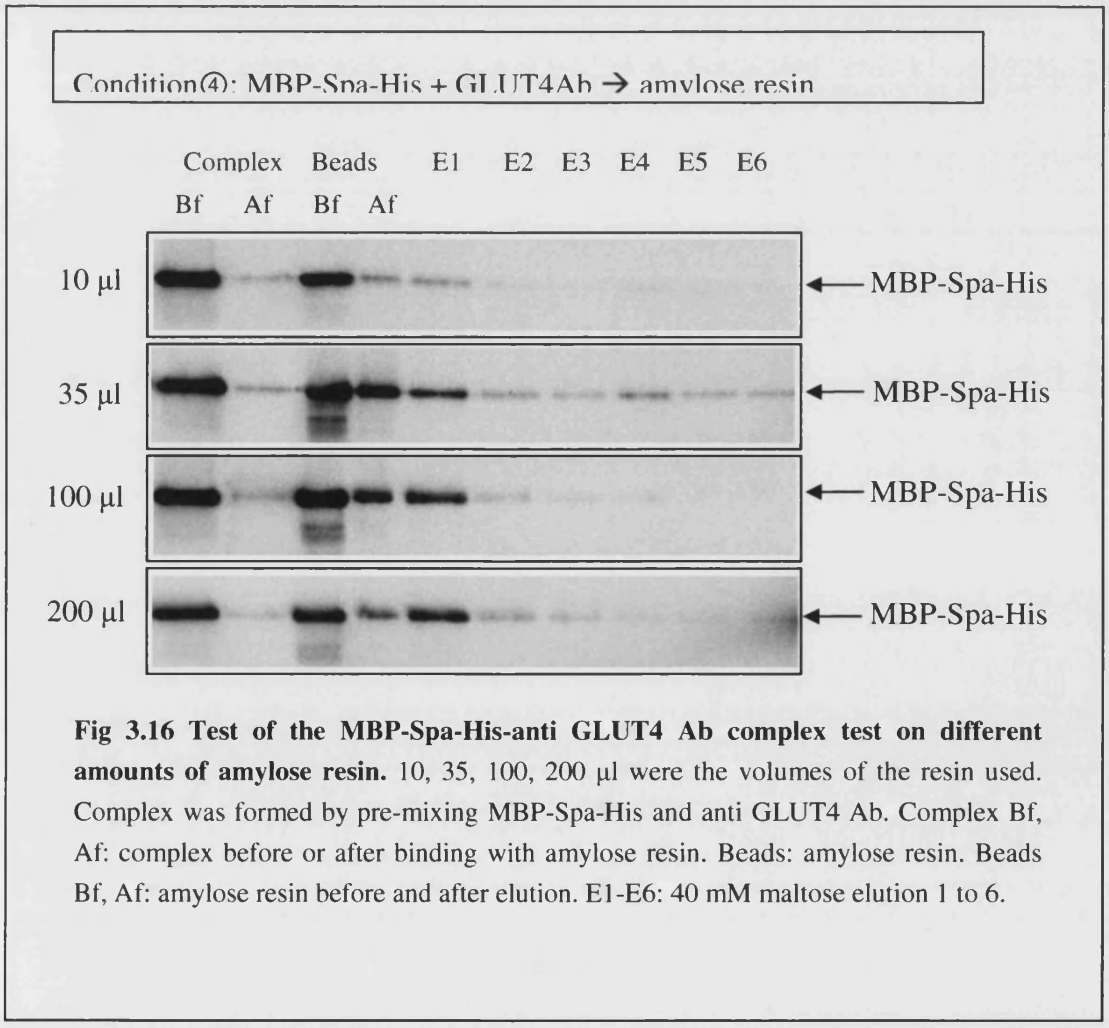

Fig 3.16 Test of the MBP-Spa-His-anti GLUT4 Ab complex test on different amounts of amylose resin. 10, 35, 100, 200 µl were the volumes of the resin used. Complex was formed by pre-mixing MBP-Spa-His and anti GLUT4 Ab. Complex Bf, Af: complex before or after binding with amylose resin. Beads: amylose resin. Beads Bf, Af: amylose resin before and after elution. E1-E6: 40 mM maltose elution 1 to 6.

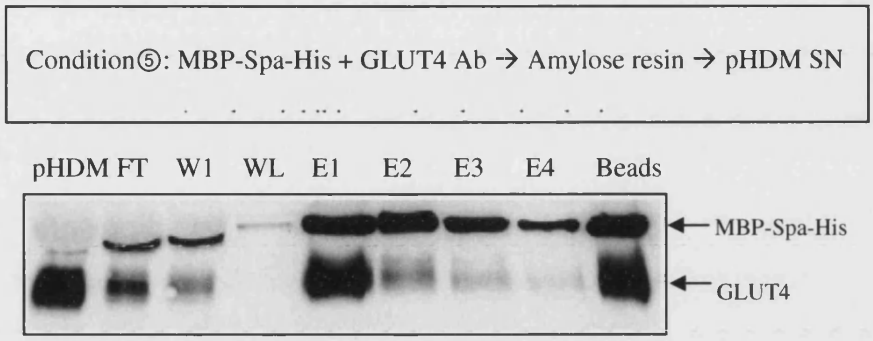

Fig 3.17 GLUT4 vesicle isolation with MBP-Spa-His-anti GLUT4 Ab complex and amylose resin. pHDM: post high-density microsome supernatant before incubated with column. FT: post high-density microsome supernatant after incubated with column. W1: the first wash. WL: the last wash. E1-E4: 40 mM maltose elution, before E1 maltose was incubated with column for 10 min. Beads: protein left on the resin after elution.

3.3.6 GLUT4 vesicles intactness and biological activity

The purified GLUT4 vesicles were expected to be intact and biologically active.

To test the intactness and biological activity of the GLUT4 vesicles, an acridine orange uptake assay (Warnock et al., 1982) was used but did not show successful results. However, the bioactivity was proved in the experiments in Chapter 4.

3.4 Discussion and Conclusion

This chapter showed a successful method to immuno-isolate intact intracellular vesicles. It was the first time maltose binding protein-protein A fusion protein and antibody were used to specifically purify a certain type of vesicles from cell fractions. The purified vesicles were proved to be intact.

GLUT4 vesicles were isolated from other microsomal vesicles with GLUT4 antibody and maltose-binding protein-protein A fusion protein (MBP-Spa or MBP-Spa-His). The 61 kDa fusion protein could be easily expressed in *E. Coli* using a recombinant plasmid containing the maltose-binding protein gene *MalE,* directly followed by two and half IgG binding region of Spa, with or without a tag of Poly-His. The expressed protein had good cellular solubility. MBP-Spa-His could be easily purified by Ni-NTA His Bind Resin.

MBP tag provides advantages over other tags such as GST, poly-His: 1) It does not require additional manipulation such as dialysis of the elution product. 2) It does not involve the use of detergents or other denaturing agents. These advantages keep the purification procedure easy and mild, providing a basis for further experiments carried out on the elution product.

To maximize the GLUT4 vesicle purification efficacy, both MBP-Spa and MBP-Spa-His were tested in different conditions. The consensus of the best condition was: incubate MBP-Spa with amylose resin in the presence of amylase inhibitor and 0.5 M NaCl → wash the resin with 1 M NaCl then normal wash → incubate GLUT4 Ab with amylose resin → wash → incubate pHDM supernatant with resin in the presence of amylase inhibitor → wash → incubate resin with 40 mM maltose for 10 min → collect the first fraction, then elute the following fractions by gravity (condition②, Chapter 2, section 2.2.1.5). This procedure was a combination of reduction in non-specific binding, inhibition of amylase, and maximization of the elution

MBP's affinity for amylose resin and maltose depends on hydrogen bonds, which in turn are positioned by the three-dimensional structure of the protein. The addition of Spa or Spa-His to MBP might have in some way changed the fusion protein's configuration and consequently affected its binding property, which may explain the irreversible binding that happened

in the isolation procedure. Another possibility is that the material that remains bound is non-vesicular and more easily trapped in the column matrix. Unfortunately the purified MBP-Spa-His did not dramatically improve the GLUT4 isolation efficiency, but the construct can be used in the future if any experiments need purified MBP-Spa-His particularly.

To conclude, the intact and active GLUT4 vesicles provided by this procedure would be useful for studies elucidating the various proteins and interactions involved in GLUT4 translocation. This procedure could also be flexibly employed in studies about other important intracellular vesicles.

Chapter 4 Fusion using plasma membrane protein-reconstituted liposomes and immuno-isolated GLUT4 vesicles

4.1 Introduction

Insulin action on peripheral tissues including fat, heart and skeletal muscle leads to increased translocation of GLUT4-storage vesicles (GSV) from an intracellular reservoir compartment to the plasma membrane, which ultimately results in exposure of the GLUT4 at the cell surface where it facilitates glucose transport. There are two aspects to clarify in this event: 1) how is insulin signalling acting on GSV movement towards the plasma membrane; 2) how are GSVs fusing with the plasma membrane.

Although the early steps in insulin signalling have been identified and it is now well accepted that PI 3-kinase and Akt are involved in this process (Bae et al., 2003; Czech and Corvera, 1999; Holman and Kasuga, 1997; Jiang et al., 2003), the downstream mediators leading to GLUT4 trafficking have been difficult to identify. There are some candidates for insulin regulated Akt substrates such as AS160, PIKfyve and synip (section 1.3.3.A) (Berwick et al., 2004; Goncharova et al., 2004; Gridley et al., 2005; Sano et al., 2003), but studies on how they function on GSV and eventually GSV translocation are incomplete. So far, the site of insulin action along the exocytic pathway is unknown. Potentially it could involve increased release or budding of vesicles from tubulo-vesicular structures (Karylowski et al., 2004; Watson et al., 2004a), increased movements of vesicles along microtubules (Bose et al., 2002; Semiz et al., 2003), increased transit through cortical actin near the cell surface (Chunqiu and Pessin, 2003; Tong et al., 2001) or an increased fusion of the vesicles with the plasma membrane.

Like the various fusion events in organisms, GSV fusion with plasma membrane could be a complicated process. It was found that insulin increased docking and then fusion of vesicles at the plasma membrane (Bose et al., 2004; Bryant et al., 2002; Satoh et al., 1993). But how insulin stimulation incorporates other determining factors is under investigation.

Cell free reconstitution of vesicle fusion reactions have many advantages for studying cell biology processes, as the separate components on the fusion reaction can be separately manipulated and combined. This approach has been very powerfully pioneered and applied to the study of intracellular vesicles homotypic and heterotypic membrane fusion (Beckers et al., 1989; Rothman and Sollner, 1997) but the application to the fusion of intracellular vesicles with the limiting plasma membrane has been more difficult to achieve (Avery et al., 1999). To further the resolution of the key insulin regulated step, an *in vitro* fusion reaction has been developed in which GLUT4 vesicles are immuno-isolated and fused with reconstituted plasma membrane in the presence of cell cytoplasm. This delicate system was developed by Dr. Francoise Koumanov (University of Bath) and the results described in this chapter were in collaboration with her. This assay allowed direct analysis of the parameters which functioned in the insulin-stimulated fusion.

4.2 *In vitro* fusion assay design and description

Although membrane fusion can be studied by the lipid mixing approach, it is best studied in assays in which vesicle content mixing occurs (Schuette et al., 2004; Weber et al., 1998). This is because lipid mixing can occur between docked and hemi-fused lipid. Only full fusion results in content mixing. To detect content mixing in the fusion reaction, biotin-streptavidin

technology was employed and TR-FRET was used to detect a fusion complex between a FRET pair that was formed in the fusion reaction (Fig 4.1). Therefore it was necessary to introduce the FRET pair into separate vesicles during their preparation. The FRET pair was consisted of Biotin-Europium(TMT) (donor) and DyLight647-streptavidin (acceptor) (Fig 4.1 A). When Biotin-Europium(TMT) was excited at 340 nm wavelength, the energy transfer from Biotin-Europium(TMT) (donor) to DyLight647-streptavidin (acceptor) caused an emission at 670 nm. This energy transfer was TR-FRET and it required certain proximity. The interaction of biotin and streptavidin provided a proper proximity to allow this reaction to proceed. The procedure involved the separate preparation of GLUT4 vesicles containing DyLight647-streptavidin, plasma membrane liposomes encapsulating Biotin-Europium(TMT), and also cell cytosol from rat adipocytes that were either in the basal state or in an insulin-stimulated state.

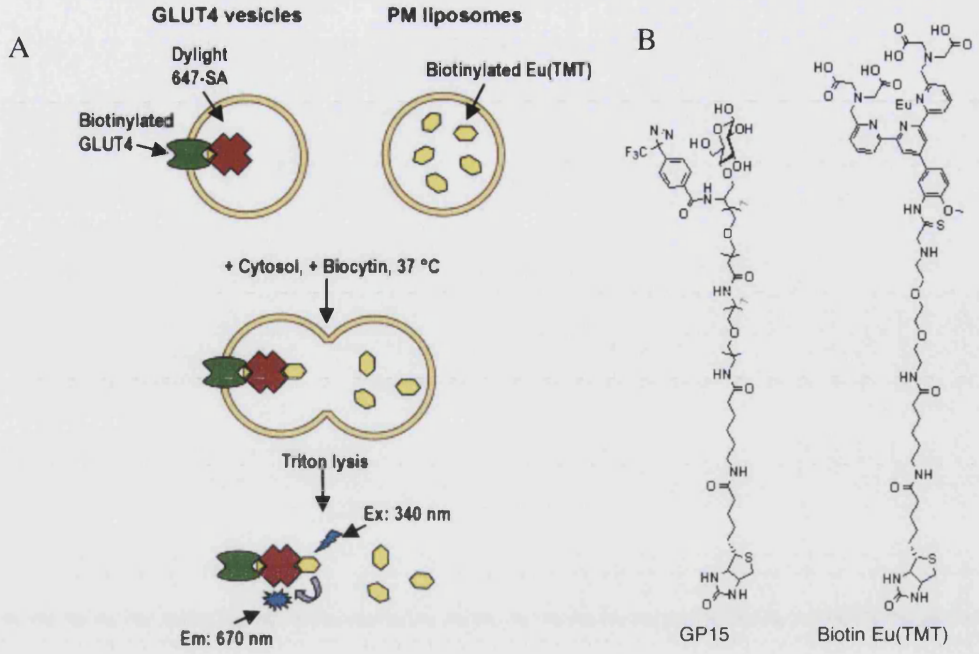

Fig 4.1 *In vitro* fusion of GLUT4 vesicles with reconstituted plasma membrane. A, In the fusion assay GLUT4 vesicles containing DyLight streptavidin-tagged GLUT4 were mixed with PM liposomes containing biotinylated Eu(TMT) in the presence of cytosol. The transmembrane GLUT4 is shown as the green symbol; the tetrameric streptavidin is shown as the multisite red symbol; the Biotin-Eu(TMT) is shown as the yellow symbol. To terminate the fusion reaction, TritonX-100 was added. The solubilised samples were then analysed for the presence of a GLUT4-streptavidin-DyLight647-Biotin-Eu-TMT complex by TR-FRET (with excitation at 340 nm and emission at 670 nm). No FRET occurs from the unreacted Biotin-Eu(TMT). **B,** Structures of the GP15 used to biotin tag GLUT4 and the Biotin-Eu(TMT) complex that was incorporated into the PM liposomes.

In order to isolate and then harvest GLUT4 vesicles in a functional state, Maltose-Binding-Protein/Protein A (MBP-Spa) was expressed and utilised in an immuno-precipitation assay (Chapter 3). The maltose elution of vesicles would keep the vesicles intact and not damage the vesicle content. To encapsulate the DyLight647-streptavidin molecules, GLUT4 was initially tagged at the cell surface with the biotin photoaffinity label GP15 (Fig 4.1 B) (section 2.2.2) and DyLight647-streptavidin, and then internalized. Post HDM supernatant from homogenised cells was then applied directly to an amylose resin column to which a MBP-Spa recombinant protein and an

anti-GLUT4 antibody had been prebound. GLUT4 vesicles were then eluted with maltose (Chapter 3 section 3.3.2 and Chapter 2 section 2.2.1.5).

It was found that plasma membrane alone could not be induced to encapsulate ligands. Therefore an approach that involved reconstitution of plasma membrane in phospholipid liposomes was employed (Kono, 1983; Schurmann et al., 1989; Suzuki and Kono, 1980). The Biotin-Europium(TMT) ligand (Fig 4.1) was incorporated into the plasma membrane liposomes at the reconstitution stage (Chapter 2 section 2.2.6.1). Before the fusion assay, the PM liposomes were purified by flotation on Histodenz gradients (Weber et al., 1998).

This novel approach to the study of the heterotypic fusion of intracellular vesicles with reconstituted plasma membrane is also likely to be a generally applicable technique. The cell free approach is particularly powerful in studying insulin regulated fusion as separate mixing of vesicles containing insulin-activated and non-activated components is feasible. With this approach it was attempted to distinguish whether insulin action leads to activation of GLUT4 vesicles, activation of components of the cytoplasm fraction or activation of components of the plasma membrane fraction.

4.3 Results

4.3.1 Characterizations of the different components of the fusion reaction

To check that the prepared PM liposomes and GLUT4 vesicles indeed contained the required proteins that compose those compartments, samples through the preparation steps were run on protein electrophoresis and different western blots were carried out. It was found that 70 % of the GLUT4 from intracellular membrane fractions from rat adipocytes bound to the amylose column in the immuno-precipitation, and of this 80 - 85 % could

be released with maltose using the optimized procedure in Chapter 3 (Fig 3.10). The vesicles were intact and contained specific v-SNARE protein VAMP2 (Fig 3.9). VAMP2 indicated that the population belonged to GSV. To answer the question whether GLUT1 was also present in the population of immuno-isolated GLUT4 vesicles, the same samples were western blotted with anti-GLUT1 antibody but the protein could not be detected in the samples containing the immuno-isolated GLUT4 vesicles (Fig 4.2).

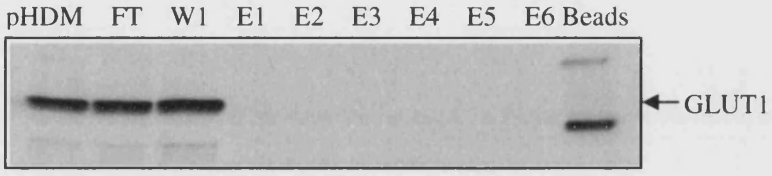

Fig 4.2 Samples from GLUT4 vesicle isolation with MBP-Spa and amylose resin western blotted with mouse anti C-term GLUT1 Ab. pHDM: post high density microsome supernatant. FT: the flow through after immuno-precipitation. W1: the first wash. E1-E6: 40 mM maltose elution fractions 1-6. Beads: protein left on the amylose resin after elution.

From the test on reconstituted liposomes before and after density-gradient spin purification, it was found that 80 % of plasma membrane GLUT4 was recovered in the purified liposomes. The t-SNARE proteins were also detected, respectively 80 % of syntaxin4 and 60 % of SNAP23 were maintained (Fig 4.3). The GLUT4 level in the membranes from insulin treated cells was higher than basal but the levels of recovered syntaxin4 and SNAP23 were not influenced by insulin treatment.

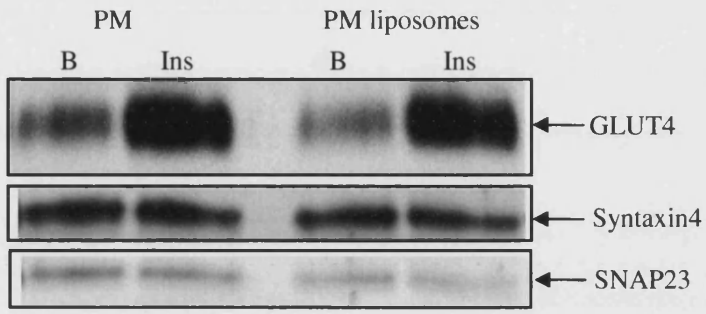

Fig 4.3 Western blots showing important proteins in plasma membranes (PM) and PM liposomes. PM from basal (B) and insulin treated (Ins) adipose cells were reconstituted into phosphatidylcholine liposomes (PM liposomes) and the recoveries of GLUT4, and the t-SNAREs Syntaxin4 and SNAP23 were determined with rabbit anti GLUT4 Ab, rabbit anti Syntaxin 4 Ab, rabbit anti SNAP23 Ab.

4.3.2 Determination of the incorporation extent of the fluorescent probes

For the TR-FRET pair Biotin-Eu(TMT) (donor) and DyLight647-streptavidin (acceptor), the preliminary experiments showed that a donor: acceptor ratio of 10-15:1 gave the best TR-FRET signal/background (not shown). To track and ensure this ratio, the signals for both Biotin-Eu(TMT) (donor) and DyLight647-streptavidin (acceptor) were measured and recorded in the process of GLUT4 vesicles and PM liposomes preparation in every fusion experiment. Tables 4.1 and 4.2 below demonstrate standard measurements for PM liposomes and GLUT4 vesicles in one example of fusion assay.

Table 4.1 PM liposomes biotin-Europium(TMT) signal measurement. The signal measured in the liposomes preparations was compared with a standard curve of 0 to 10 nM free biotin-Eu(TMT). RFU stands for relative fluorescence unit.

sample	10 nM	5 nM	2.5 nM	1 nM	0.5 nM	0.25 nM	0 nM	BasLipo	InsLipo
RFU	44911	28691	20085	15755	12639	11993	10258	17365	17319

Table 4.2 GLUT4 vesicles DyLight647-streptavidin signal measurement. The signal measured in the samples at different stages during the GLUT4 vesicles isolation was compared with a standard curve of 0 to 1 nM free DyLight647-streptavidin

sample	1 nM	0.5 nM	0.25 nM	0.1 nM	0.05 nM	0.025 nM	0 nM	
RFU	46106	19494	13530	8955	6669	5551	4099	
sample	pHDM	FT	W1	W2	W3	W4	W5	W6
RFU	61925	43891	23288	5881	5436	5260	4846	4793
sample	E1	E2	E3	E4	E5	E6		
RFU	11028	10249	8014	4787	4670	4219		

Through curve fit with linear regression, in this particular experiment the donor levels in basal and insulin liposomes were respectively 1.79 nM and 1.78 nM. The acceptor level in maltose elutions E1 and E2 were 0.18 nM and 0.16 nM. Averagely in experiments, the donor levels were 1.5 nM and acceptor levels were 0.1 - 0.15 nM. The donor:acceptor ratio was approximately 10:1, which was in the suitable range. The concentrations of donors in basal and insulin liposomes were similar, which meant the contents of the two liposomes were of similar volume. It helped to directly compare the basal/insulin conditions in fusion assay.

To investigate whether there was any leakage from the liposomes or whether the liposomes were permeable to small molecules, BODIPY-FL-avidin was used because its fluorescence increases strongly on binding of a biotinylated ligand (Emans et al., 1995). For this permeability/leakage test the liposomes were encapsulated with 100 µg/ml BODIPY-FL-Neutravidin instead of Biotin-Eu(TMT). The maximum fluorescence enhancement was determined with 40 nM BODIPY-FL-Neutravidin in the absence of liposomes and using 40 to 200 nM biocytin. 40 nM BODIPY-FL-Neutravidin loaded liposomes were then incubated with 40 to 200 nM biocytin or biotin methyl ester (membrane permeable reagent). The BODIPY-FL fluorescence remained low (< 4 % of maximum) in the presence of biocytin but increased in the presence of biotin

methyl ester (57 % of maximum). Lysing the liposomes with 0.2 % TritonX-100 prior to the biocytin addition also resulted in BODIPY-FL fluorescence enhancement (79 % of maximum). These data confirmed that the liposomes were impermeable to biocytin under the conditions used in the fusion assay.

4.3.3 Kinetic measurements in the fusion assay

Standard fusion assay was carried out as follows. Basal or Insulin liposomes were mixed with basal GLUT4 vesicles in presence of 1 μM biocytin. Biocytin was added to prevent potential leakage of GLUT4 vesicles and block the outside DyLight647-SA, if any was present. ATP regenerating system was mixed and then basal or insulin cytosol was added before or after 30 sec pre-incubation in a 37 °C water bath. The samples were then incubated for 0, 2, 5, 10 and 30 min at 37 °C. A single representative experiment is shown in **Fig 4.4.** Fluorescence excitation and capture parameters were: 30 flashes, a lag time of 50 μsec and an integration signal capture time of 400 μsec. As with all FRET applications there is necessarily overlap of the emissions from the donor into the acceptor capture window. A 670 nm, 10 nm band-width filter was used to capture the acceptor emission and minimise emission from the donor. To measure donor emission alone a 612 nm, 10 nm band-width filter was used. The donor emission in the acceptor window is present at time zero of the time course, is the same in the absence of membranes, and is relatively constant throughout the time course. The averaged time course for fusion (Fig 4.5) was remarkably similar to the time course of insulin stimulated glucose transport in intact cells (Satoh et al., 1993). The first order rate constant was 14-fold faster using plasma membrane liposomes from insulin treated compared with basal cells. The rate constant was increased from 0.015 ± 0.005 to 0.213 ± 0.005 min^{-1} (from 5 separate experiments).

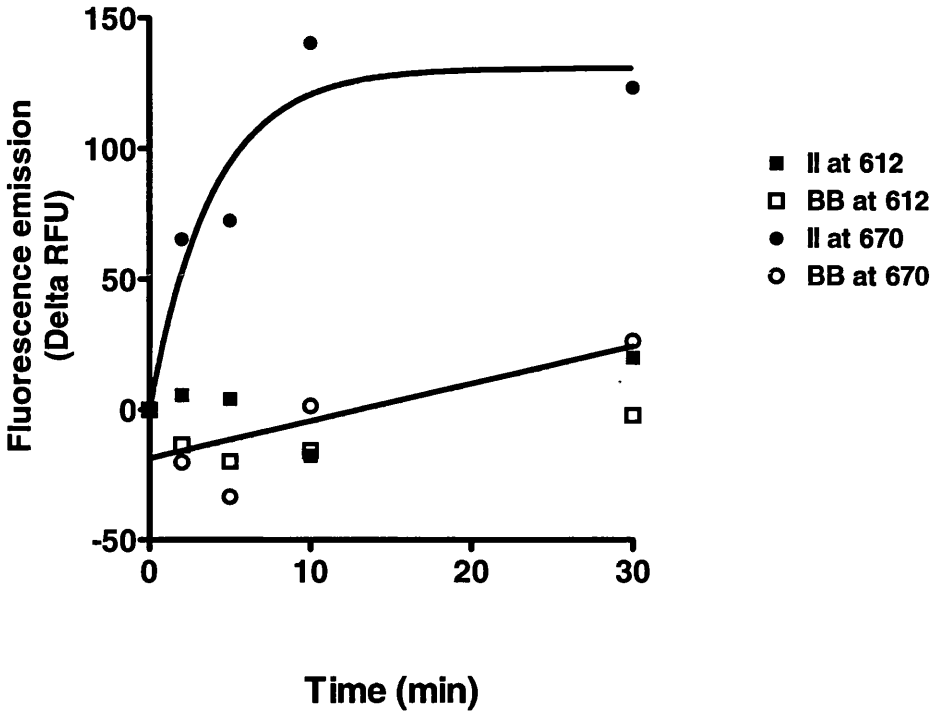

time (min)	II at 612	BB at 612	II at 670	BB at 670
0	444.00	441.85	783.60	773.30

Fig 4.4 Use of time resolved fluorescence energy transfer (TR-FRET) for analysis of GLUT4 vesicle fusion (one representative experiment). Fusion assay components were prepared as described in text. BB and II means conditions in which all components were from basal and insulin treated cells respectively. The subtracted zero time values are tabulated below the graph.

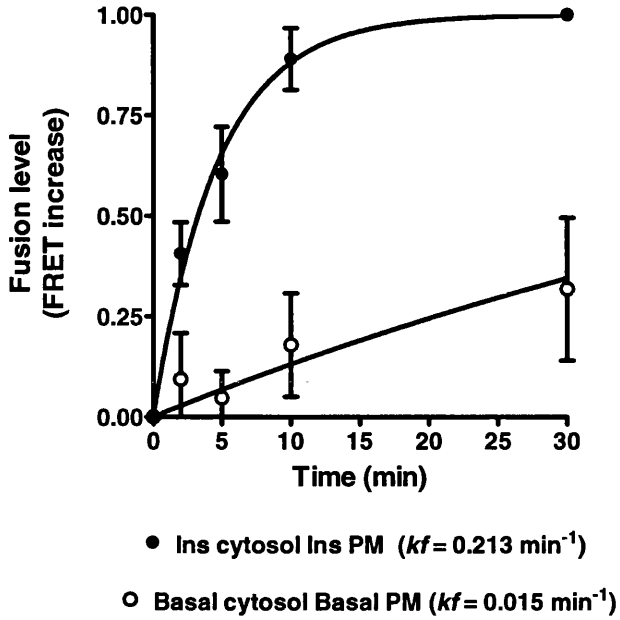

Fig 4.5 Time courses for GLUT4 vesicles and PM liposomes fusion. The time courses were determined using components from either basal (○) or insulin treated (●) cells. The curves were derived from fitting a first order rate constant from which rate constants were obtained. The rate constant were 0.015 ± 0.005 and 0.213 ± 0.014 min^{-1} for basal and insulin samples, respectively. Results are the mean and SEM from 5 experiments.

The extent of fusion was determined by comparing the end points of the time courses with the total amount of complex and FRET signal that was produced when the assay components were treated with detergent in the absence of biocytin. Under these conditions all the DyLight647-streptavidin bound biotinylated Europium(TMT) as there was no competing ligand and no intact membranes to limit their interaction. After 30 min of fusion for the insulin samples, and after 60 min of fusion for the basal samples, the FRET signals were 95 ± 11 % and 77 ± 9 % of the maximum (from 3 separate experiments). These end point values were consistent with the estimated rate constants and suggest that it was the rate rather than the extent of fusion that was stimulated by insulin. Although all the contents of the GLUT4 vesicles used in the assay participate in fusion, it could not eliminate the possibility that the cells contained a population of additional GLUT4 vesicles

that might behave differently. This was because, although fusion was close to 100 % efficient, not all the cell GLUT4 vesicles were recovered using the MBP-Spa affinity isolation technique.

As insulin PM and insulin cytosol induced the full fusion, in the following results, this sample was regarded as positive control for all the other tested conditions. To have convenient and direct comparison, a single 5 min time point was used as an index of fusion for different conditions. This time point may have led to an underestimation of the magnitude of the insulin response as the fusion activity for the insulin treated fractions had reached 60 - 70 % of the maximum within this time. Nevertheless, the use of this single time point assay allowed direct comparisons between assay conditions.

4.3.4 The fusion assay has necessary components

As mentioned earlier, there were mainly four fractions composing the fusion reaction system: basal GLUT4 vesicles, basal/insulin PM liposomes, basal/insulin cytosol, and an ATP regenerating system. Among these four, basal GLUT4 vesicles and basal/insulin PM liposomes were basic constituents to form a fusion assay as they provided the fundamental requirements for membrane fusion - the SNARE proteins. In intact cell studies it has been determined that the v-SNARE protein VAMP2 and the t-SNAREs syntaxin4 and SNAP23 were essential and necessary for GLUT4 vesicles fusion with plasma membrane (Bryant et al., 2002; Cheatham et al., 1996; Foran et al., 1999). To understand whether this *in vitro* system showed an equivalent SNARE dependency, fusion assay was carried out with GLUT4 vesicles containing cleaved VAMP2 cytosolic domain in comparison with normal GLUT4 vesicles. The treatment of the isolated GLUT4 vesicles with Botulinum neurotoxin light chain/B protease (BoLC/B) prior to fusion resulted in cleavage of the GLUT4 vesicle v-SNARE, VAMP2

(Fig 4.6 B), and the fusion with this pre-treated GLUT4 vesicles was completely blocked (Fig 4.6 A). This confirmed that the *in vitro* fusion process was SNARE dependent.

Much accumulated data on GLUT4 trafficking has implicated the involvement of cytoskeletal proteins including microtubules and actin. Therefore it was tested whether the fusion step, a partial step in translocation, was altered by the actin depolymerising drug, latrunculin B. It was found that 250 nM latrunculin B did not inhibit the fusion reaction (Fig 4.6 C), although this concentration is shown to inhibit GLUT4 translocation in cells (Khayat et al., 2000). These data suggest that cytoskeletal components and actin are not involved in facilitating fusion and that the fusion step in translocation can be separated from the steps in translocation that involve the cytoskeleton.

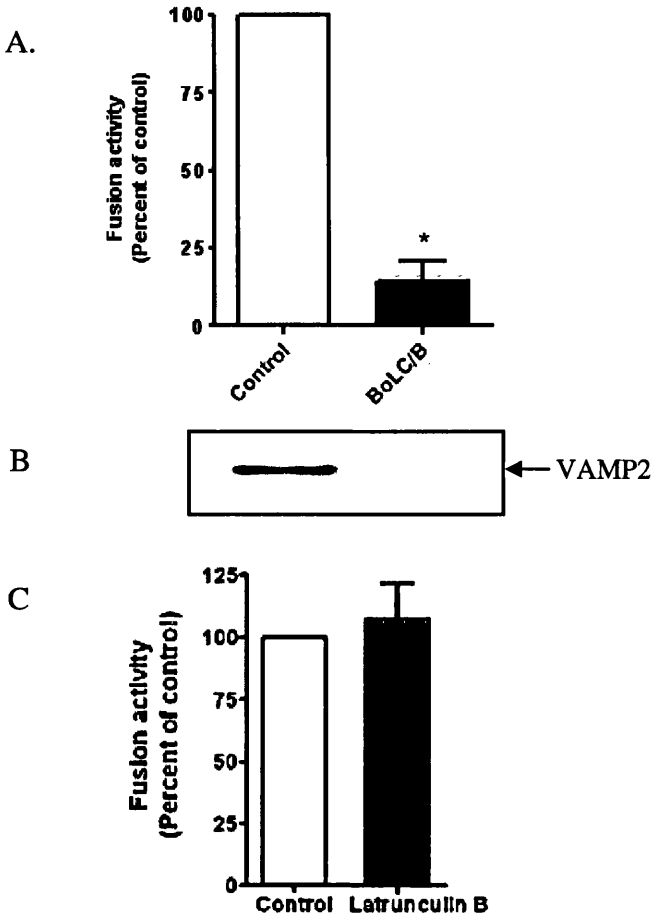

Fig 4.6 GLUT4 vesicle fusion is dependent on SNAREs but not cytoskeleton. A, Fusion activity using GLUT4 vesicles with (BoLC/B) and without (control) protease pre-treatment was determined. VAMP2-cleaved sample showed inhibition. **B,** GLUT4 vesicles were pretreated with 10 nM botulinum light chain/B protease (BoLC/B) for 60 min and cleavage of VAMP 2 was determined by western blotting. The control was without treatment. **C,** Fusion activity with and without 250 nM Latrunculin B was determined. Latrunculin B sample did not show inhibition.

Although this *in vitro* system was confirmed to be SNARE-dependent, unlike the neuronal SNARE fusion assay described by Weber *et al.* (Weber et al., 1998), SNARE complex alone was not sufficient to support the fusion. In other words, basal GLUT4 vesicles and insulin pre-activated PM liposomes could not fuse on their own. It was found that cell cytoplasm from insulin-treated cells supported fusion in a concentration dependent manner. Eventually, if cytoplasm was completely eliminated, fusion would not happen

at all (Fig 4.7). This suggested that factors from cytoplasm were required to facilitate and drive fusion and that pre-activated plasma membrane alone was insufficient.

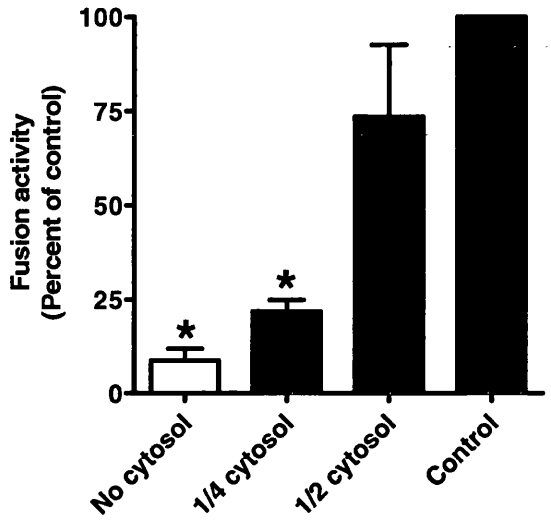

Fig 4.7 GLUT4 vesicle fusion is dependent on cytosol. GLUT4 vesicle fusion activity was determined using PM liposomes from insulin-treated cells. Cytosol was prepared from a concentrated cell suspension (> 70% cytocrit) of insulin treated adipose cells. The concentrated cytoplasm was diluted by a half and a quarter with a corresponding decrease in fusion activity. Data were mean and SEM from 3 experiments in each case, * $p < 0.05$ vs control.

In the comparison between pure basal and pure insulin conditions, mixing insulin-treated cytoplasm and insulin-treated plasma membrane liposomes produced an 8-fold higher rate of fusion than mixing basal cytoplasm and basal liposomes at 5 min at 37 °C. Surprisingly it showed that insulin-treated plasma membrane liposomes were able to support fusion in the presence of basal cytoplasm. By contrast, basal plasma membrane was not able to support rapid fusion even in the presence of cytoplasm from insulin-treated cells (Fig 4.8), although SNARE proteins were present and cytoplasm requirements fulfilled. These data suggested that although factors from

cytoplasm were required they alone did not provide any regulation of fusion. Insulin stimulated plasma membrane components were capable of either activating or recruiting factors from the cytoplasm that led to activation of fusion.

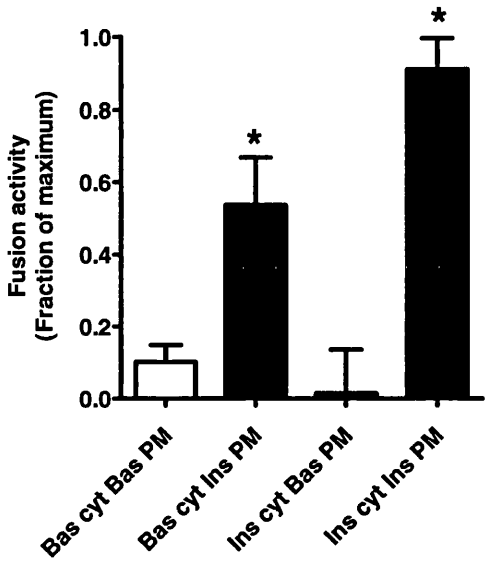

Fig 4.8 Dependence of fusion activity on insulin-treated plasma membrane. GLUT4 vesicle fusion activity was determined using cytosol and PM liposomes from either basal (Bas) or insulin-treated cells (Ins). A 7-9 fold difference in fusion activity was observed when comparing all basal and all insulin components. * $p < 0.05$ vs Bas cyt, Bas PM. Data are mean and SEM from 3 - 10 experiments.

4.3.5 Insulin signalling cascade in regulation of fusion

Because plasma membrane from insulin treated cells played the main role on driving GLUT4 vesicle fusion, it was wondered in which way this component was capable of doing this. The early insulin signalling events that led to stimulated glucose transport were understood so far as activation of PI 3-kinase (Czech and Corvera, 1999; Hara et al., 1994) and then

activation of Akt (Foran et al., 1999; Jiang et al., 2003; Murata et al., 2003; Whiteman et al., 2002) (Chapter 1, section 1.3.3). To test the function of this pathway, blockers for individual steps were used and results were shown as following.

PI 3-kinase

To evaluate the role of PI 3-kinase, wortmannin was used as a PI 3-kinase inhibitor. When all the components of the fusion assay were pre-treated with wortmannin *in vitro*, fusion was blocked completely at 100 nM and by approximately half at 10 nM (Fig 4.9 B). This data was consistent with the data from GLUT4 exocytosis and transport assay by Dr. Jing Yang in our laboratory (University of Bath) (Fig 4.9 A). GLUT4 exocytosis (Yang et al., 2002b) was determined by measuring the extent to which internalized biotin-tagged GLUT4 re-emerged at the cell surface. Transport activity was determined using 3-O-methyl-D-glucose as a tracer (Satoh et al., 1993). The dose responses for wortmannin inhibition of GLUT4 exocytosis and glucose transport both showed an inhibition with an IC_{50} of approximately 10 nM (Fig 4.9). The inhibition was also confirmed by a GLUT4 exocytosis western blot (Fig 4.9 C top panel). This dose response was markedly well matched by the corresponding decrease in phosphoThr308-Akt levels (Fig 4.9 C). The wortmannin inhibition data collectively suggested that the fusion rate had the same PI 3-kinase dependence as the subsequent steps and therefore rate limited these subsequent steps.

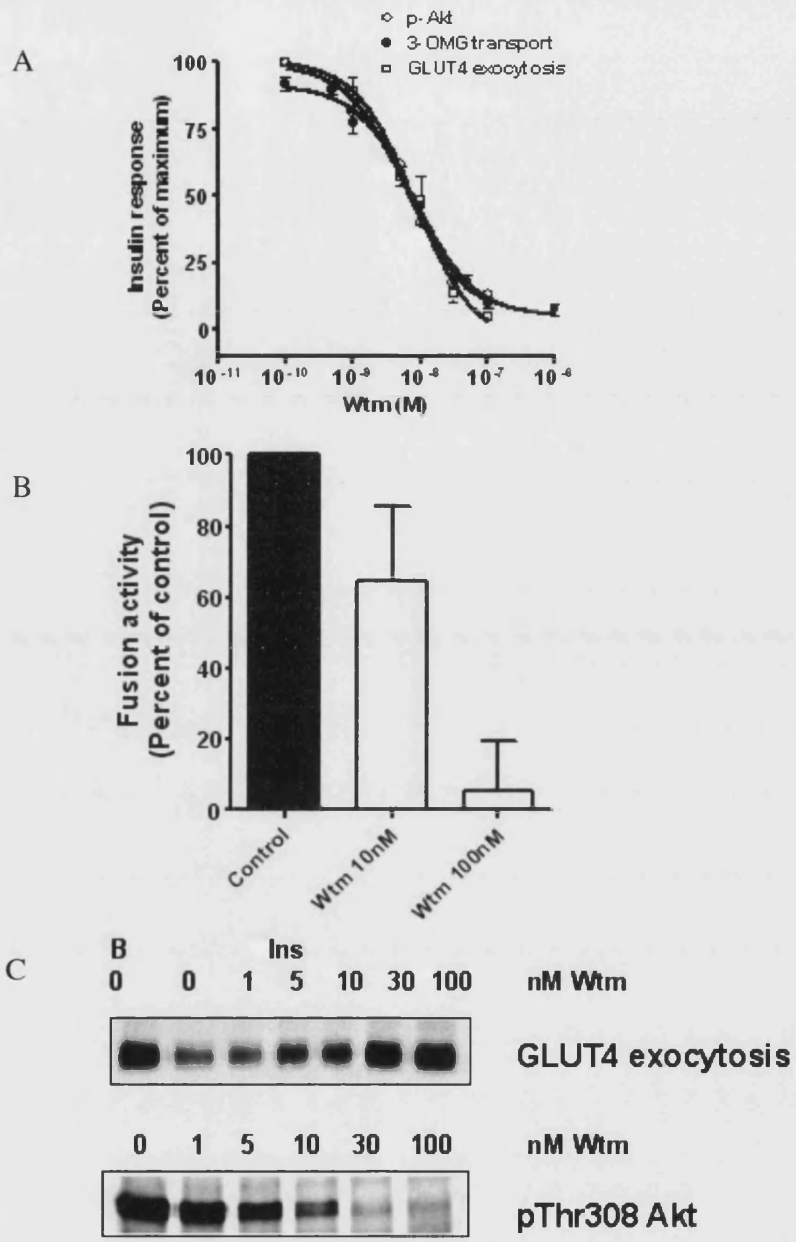

Fig 4.9 PI 3-kinase dependent signalling in regulation of fusion assay and GLUT4 exocytosis. A, Wortmannin (Wtm) at the indicated concentrations was used to inhibit glucose transport activity (●) and GLUT4 exocytosis (□) and phosphorylation of Akt (○). Data were mean and SEM from 3 experiments for transport and exocytosis and mean of two experiments for Akt phosphorylation. **B,** GLUT4 vesicle fusion activity with insulin PM liposomes was inhibited by 10 nM and 100 nM wortmannin added to reaction components for 10 min at 18 °C and present during the fusion reaction. Data were mean and SEM from 3 experiments. **C,** Top panels were from a representative blot of GLUT4 exocytosis in basal cells (B) or insulin-treated cells (Ins) in the presence of the indicated concentrations of wortmannin. In the absence of wortmannin GLUT4 returned to the surface rapidly and was quenched by extracellular avidin (low GLUT4 signal on the blot). At high wortmannin concentrations, GLUT4 returned to the surface slowly at a rate comparable with that of basal cells. The bottom panels were from a representative blot of Akt phosphorylation at threonine308 at the indicated concentrations of wortmannin.

To examine whether the PI 3-kinase activation was carried through the plasma membrane or the cytoplasm or both, the fractions for the fusion assay were prepared from wortmannin-treated insulin-stimulated cells (Fig 4.10). When mixed with normal insulin PM liposome and GLUT4 vesicles, the cytosol from wortmannin-treated cells did not show inhibition to fusion. This might be because the effect of wortmannin was rapidly lost as the reagent was inactivated by water and amines over long incubations. In addition, this insulin-signalling blocked cytosol showed similar result with basal cytosol earlier (Fig 4.8), both of them supported fusion to some extent. On the contrary, the plasma membrane fraction from wortmannin-treated cells was inactive in the fusion assay. Again, this was consistent with earlier observations and interpretations (Fig 4.8), suggesting that the insulin-stimulated plasma membrane was the key fraction to regulate the fusion activity.

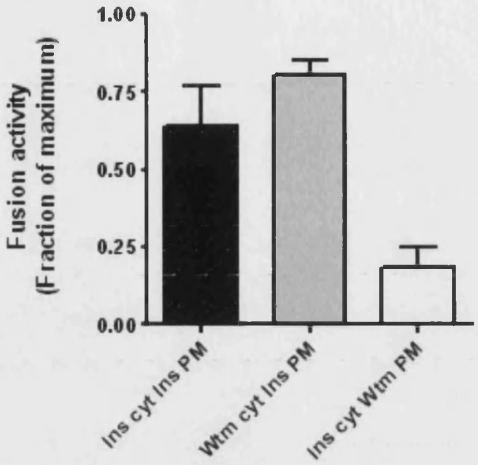

Fig 4.10 Fusion with fractions from wortmannin-treated insulin-stimulated cells. Intact cells were treated with insulin in the absence or presence with 100 nM wortmannin and subsequent isolation of separate plasma membrane (Ins PM, Wtm PM) and cytosol (Ins cyt, Wtm cyt) fractions were used in fusion assay. Then it was determined whether inhibitory activity was retained in either the plasma membrane or the cytosol fraction. Results were the mean and SEM from 3 experiments.

Akt

In the fractions for fusion assay Akt was detectable in cytoplasm but not plasma membrane (Fig 4.11 A, C). Therefore, to establish whether Akt was required for the vesicle fusion reaction Akt was removed from the cytoplasm by immuno-precipitation (Chapter 2, section 2.2.1.5) (Fig 4.11 A). Depletion of Akt1 alone from the cytoplasm fraction reduced fusion activity by approximately 50 % while depletion of both Akt1 and Akt2 reduced the fusion activity by 80 % (Fig 4.11 B). Although the depletion procedures reduced the total amounts of Akt1 and Akt2 to less than 7 % and 3 % of their initial levels respectively, there was still some residual fusion noticeable. This residual fusion activity may have been due to some low level of activated Akt that was already recruited to the plasma membrane, although not detectable in western blot (Fig 4.11 C). Alternatively the residual fusion

activity may have been due to the presence of an Akt isoform that was not removed by the depletion protocol. Or this residual fusion showed a background reaction under insulin stimulation but not through the PI 3-kinase pathway. Overall, This inhibition corresponded closely with data obtained in intact 3T3-L1 adipocytes using siRNA directed against these two Akt isoforms (Jiang et al., 2003).

Knowing that Akt was essential in supporting fusion, it was natural to wonder how it has been activated and how the active form acted on GLUT4 fusion. It was thought that PI 3-kinase increases the concentration of PI(3,4,5)P3 in the membrane and PI(3,4,5)P3 promoted the cell-surface localization of PDK1 and Akt (Watson and Pessin, 2006) (section 1.3.3). Then Akt was phosphorylated on Thr308 and Ser473 and activated. Under the conditions of the fusion reaction (but in the absence of GLUT4 vesicles), the recruitment of both Akt1 and Akt2 from cytosol onto liposomes was investigated (Fig 4.11 C). It was confirmed that Akt1 and 2 can be recruited to the liposomes. The levels of recruitment onto liposomes prepared from the insulin-treated samples were significantly higher than from basal samples. Similarly when cells were pretreated with the PI 3-kinase inhibitor wortmannin before insulin, the levels of Akt subsequently recruited onto isolated liposomes were the same as those recruited from the liposomes from basal cells. This finding is consistent with the one that liposomes prepared from wortmannin and insulin treated cells did not support fusion (Fig 4.10).

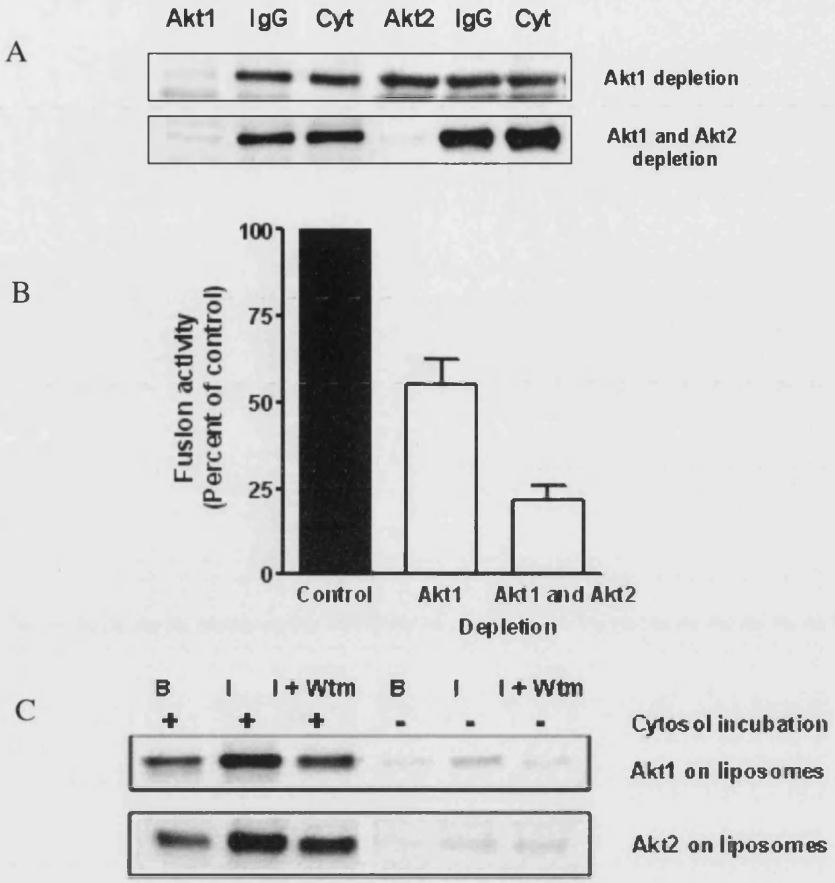

Fig 4.11 Requirement of cytoplasmic Akt for GLUT4 vesicle fusion and recruitment onto lipsomes. A, Akt1 was depleted from cytoplasm of insulin stimulated cells using immobilised Akt1 antibody clone 5G3 (Cell Signaling Technology). No depletion was observed with an irrelevant IgG control. Very little depletion of Akt2 occurred using this antibody. Successive use of anti-Akt1 antibody and anti-Akt2 antibody clone AW114 (Upstate) depleted the cytoplasm of both Akt1 and Akt2. **B,** Fusion activity of GLUT4 vesicles with insulin PM liposomes was determined using cytoplasm from the IgG control and following Akt1 and Akt2 depletion. Data were mean and SEM from 3 experiments. * $p < 0.05$ vs. control. **C,** PM liposomes prepared from basal (B) or insulin-treated cells (Ins) or cells treated with 200 nM wortmannin (Wtm) and then insulin were incubated for 15 min at 37°C in the fusion buffer in the absence (right panels) and presence (left panels) of the respective cytosol but without the GLUT4 vesicles (which interfere with the detection of the Akt). Following the incubations the liposomes were reisolated and separately analyzed for the presence of associated Akt1 and Akt2. Results are representative blots from two very similar experiments.

phospho-Akt

Phosphorylation of Thr308 was only found occurring on the Akt that had been recruited onto insulin liposomes and this phosphorylation was inhibited by *in vitro* wortmannin treatment (Fig 4.12 A, B). However, the *in vitro* wortmannin treatment would not affect the levels of phosphorylated Akt in the plasma membrane liposomes or the cytoplasm individually (Fig 4.12 C). The phospho-Akt on the plasma membrane was undetectable and the phospho-Akt remained high in the insulin-stimulated cytoplasm as it had already been activated. The comparison of with and without *in vitro* wortmannin in the recruitment assay indicated that it was the phosphorylation of recruited Akt that was blocked by wortmannin.

Akt was mainly driven onto insulin-activated plasma membrane liposomes from insulin activated cytoplasm (Fig 4.12 A, Fig 4.11 C). However, it was found that some Akt phosphorylation was still detectable with insulin-treated plasma membrane liposomes and basal cytoplasm (Fig 4.12 A, B). This suggested that *de novo* phosphorylation of Akt was occurring under these conditions as the basal cytoplasm did not contain any activated Akt. This provides an explanation for the *in vitro* wortmannin sensitivity of the fusion reaction (Fig 4.9 B). The Akt was most likely recruited onto the plasma membrane from insulin-treated cells because these membranes contain phosphatidylinositol-(3,4,5)-triphosphate (PIP3). The continuing PI 3-kinase activity would continuously recruit PDK1 which would lead to continuous Akt phosphorylation. This essential *de novo* phosphorylation process may explain the observed fusion using samples from insulin-treated plasma membrane liposomes and basal cytosol (Fig 4.8). By contrast pre-activated and phosphorylated Akt was in abundance in the cytosol from insulin-treated cells (Fig 4.12 C) but this was insufficient to drive fusion of GLUT4 vesicles with basal plasma membrane liposomes (Fig 4.8). These data suggested

that the already-phosphorylated Akt in the cytoplasm alone was insufficient to drive fusion and it was the Akt recruitment to the plasma membrane and the following phosphorylation that facilitated the fusion process.

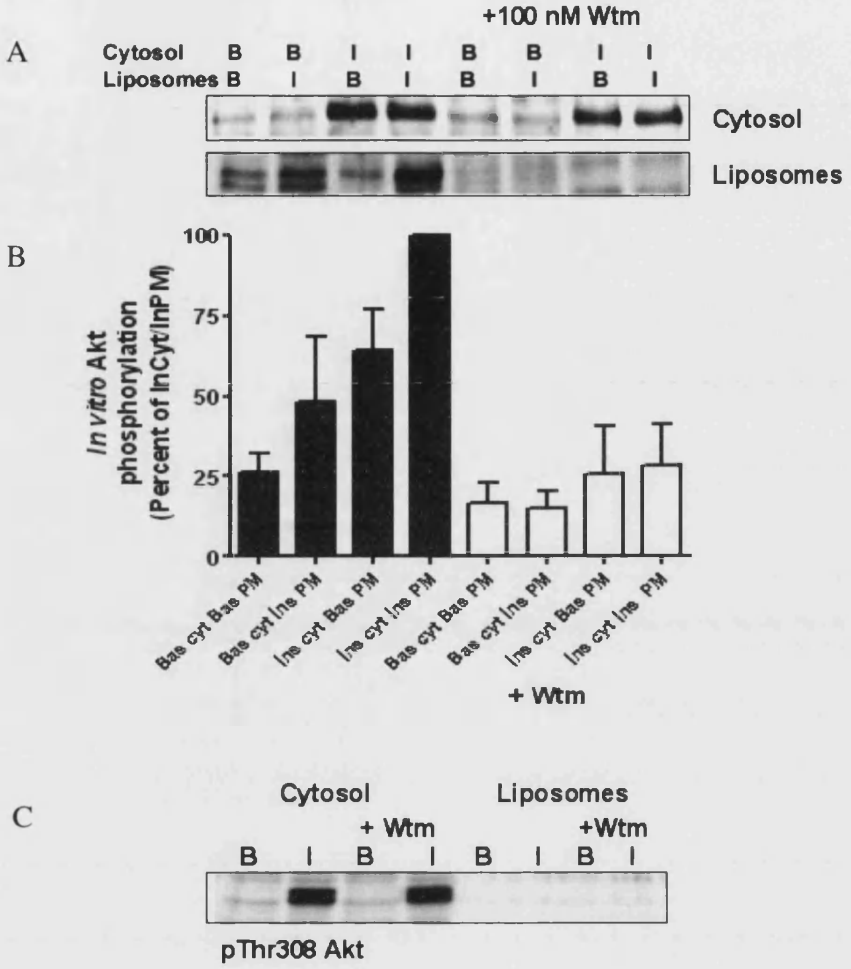

Fig 4.12 *In vitro* wortmannin treatment blocks phosphorylation of Akt recruited onto insulin-stimulated PM liposomes. A, The cytosol and PM liposome components of the fusion reaction were incubated for 15 min at 37 °C in the fusion system but without the GLUT4 vesicles (which interfere with the detection of the Akt). The liposome and cytoplasm were then re-isolated and separately analysed for the presence of threone308-phosphorylated Akt. Phospho-threonine308 Akt was increased in the liposome pellet (comparing the liposome samples from A and B) and this was blocked by the wortmannin treatment. **B,** Quantification of *in vitro* Akt phosphorylation of Akt recruited to PM liposomes in correspondence of the samples from A. Data were the mean and SEM from 4 experiments. **C,** Treatment of separate cytosol and PM liposomes from basal (B) and insulin-treated cells (I) with wortmannin (Wtm) at 100 nM at 37 °C for 10 min did not alter the levels of phospho-threonine 308 Akt.

4.4 Discussion

This novel assay reconstitutes and directly demonstrates insulin-stimulated GLUT4 vesicle fusion with plasma membrane for the first time. The *in vitro* approach provides an excellent evaluation of the roles of different factors in the GLUT4 vesicle fusion process. Remarkably the magnitude and time course for insulin's action on glucose transport are fully recapitulated in the vesicle fusion reaction. On the contrary, from experiments *in vivo* and using gene-silencing or various inhibitors (Bose et al., 2005; Kanda et al., 2005; van Dam et al., 2005) to study the regulation of insulin-stimulated GLUT4 translocation, it is difficult to dissect the fusion step from insulin signalling. The fusion component is hard to interpret because the factors before and after fusion could largely influence the appearance of tagged-GLUT4 at the cell surface. Using low temperature block on 3T3-L1 adipocytes, van Dam *et al.* implicate two insulin-regulated steps in GLUT4 translocation, the Akt-independent redistribution of GLUT4 vesicles towards the cell cortex, and the Akt-dependent docking and fusion of GLUT4 vesicles with the PM (van Dam et al., 2005). The small interfering RNA-based gene silencing used by Bose *et al.* inhibited insulin-stimulated glucose transport (Bose et al., 2005). The gene knock-out technique can also show effectors in this process (Kanda et al., 2005). However, all of these techniques are not able to separate the process of GLUT4 vesicle fusion with the plasma membrane from other translocation steps, nor are they able to study factors involved in this particular process. As an improvement, the use of total internal reflection fluorescence (TIRF) microscopy (TIRFM) (Lizunov et al., 2005) has narrowed down the number of partial reactions involved in the insulin stimulated translocation, but the interpretation of these microscopy images is ambiguous because the net incorporation of GLUT4 into the plasma membrane can be interpreted as indicating an involvement of the cytoskeleton, docking and fusion and endocytosis (Lizunov et al., 2005). The

in vitro assay of the fusion reaction described in this chapter not only allows the fusion event to be studied in isolation from any involvement of the cytoskeleton or the endocytosis steps, but also allows the dissection of the fusion components. Interference protein or inhibitors can be added directly to the assay. Selected proteins can also be immuno-depleted from the fusion reaction. At present the fusion assay has demonstrated that the magnitude and time course of insulin stimulation of fusion is comparable with its stimulatory effect on glucose transport in target cells. Furthermore as the stimulation of fusion has been shown to be dependent on PI 3-kinase and on Akt activities, the study provides a direct identification of the sites of action of these signalling intermediates.

Components for fusion assay

The GLUT4 vesicles used in the fusion reaction are labelled and tagged by GP15 and streptavidin and then internalized in the absence of insulin. Thus, the vesicles obtained in this way represent GLUT4 vesicles in the basal or non-stimulated state. The presence of VAMP2 proves the vesicles belong to the population of GLUT4 storage vesicles (GSV) and the BoLC/B protease cleavage experiments demonstrated that the fusion is SNARE-dependent. The GLUT4 vesicle population isolated from rat adipocyte is more homogeneous than that from 3T3-L1 cells (Lizunov et al., 2005; Malide et al., 1997). In our lab it was found that when using homogenates of rat adipose cells only a single population of GLUT4 vesicles can be resolved on iodixanol gradients (unpublished data). This population does not contain GLUT1 and the levels of GLUT1 in the intracellular compartment of rat adipocytes are less than 10 % of the levels of GLUT4 (Holman et al., 1990a). This situation is different from that found in the 3T3-L1 adipocytes system where the ratio of GLUT1:GLUT4 is 1:1 or greater (Calderhead et al., 1990; Palfreyman et al., 1992).

In primary adipocytes, the disperse cytoplasmic GLUT4 vesicles already make up a majority of the GLUT4-containing compartments (Lee et al., 1999; Malide et al., 2000). But there is thought to be a fraction of peripheral GLUT4 vesicles located near the PM, which are suggested to be an initial source of GLUT4 that fuses with the PM upon insulin stimulation (Fletcher et al., 2000; Semiz et al., 2003). These peripheral vesicles have never been directly demonstrated. The GLUT4 vesicles obtained in this assay should be mainly cytoplasmic but also contain a certain amount of the peripheral vesicles. An attempt to purify the peripheral vesicles was tried by re-homogenizing plasma membrane. But these re-purified vesicles failed to show fusion competency in fusion assay. The re-purified vesicles might be the internalizing vesicles which are still attaching to plasma membrane. As they are in the process of leaving the plasma membrane and heading to the inside of the cell, they are not likely to be fusable with plasma membrane.

The cytosol appears to be necessary and important in providing components that stimulate fusion after their recruitment to the plasma membrane. Using immuno-depletion it was found that Akt is required for fusion. The Akt isoform specificity for the fusion reaction is similar to that revealed using siRNA techniques (Jiang et al., 2003) in that depletion of both Akt1 and Akt2 is necessary for marked inhibition of translocation (as measured in cells) and fusion (as measured *in vitro*). Our data indicate somewhat more dependence on Akt1 as depletion of this isoform alone reduces fusion by 50 %. This is different from Zhou *et al*'s finding that Akt2 is the key intermediate in insulin acted GLUT4 translocation (Zhou et al., 2004).

Insulin-activated cytosol alone is insufficient to facilitate fusion with plasma membrane liposomes prepared under basal conditions. It reveals that the insulin regulated fraction is not the cytosol or the GLUT4 vesicles; instead it

is the plasma membrane. This conclusion is consistent with several additional observations. These observations include that insulin-stimulated plasma membrane liposomes can support fusion using cytoplasm from basal or wortmannin-treated cells, and insulin-stimulated plasma membrane liposomes can recruit and then phosphorylate Akt from the basal, signalling-inactive cytoplasm. This cell-free approach has therefore led to a focus on the plasma membrane fraction for follow-up studies. Further studies will be required to fully identify which components of the plasma membrane are pre-activated by insulin treatment of cells. In principle it is also possible to immuno-deplete selected proteins from the plasma membrane liposomes in the solubilised membrane stage (Chapter 2, section 2.2.6.1).

Insulin signalling coupling to fusion

From the fact that the dose response effects of wortmannin on Akt phosphorylation, glucose transport activity and GP15 labeled GLUT4 exocytosis are in close parallel, it is concluded that there is no activation of GLUT4 after it is exposed at the cell surface. Therefore it suggests that the rate limiting step happens before the exposure of GLUT4 at the surface.

Previous studies have shown that co-sedimentation of GLUT4 vesicles with insulin-stimulated plasma membrane is not wortmannin sensitive (Inoue et al., 1999). This suggests that after the wortmannin treatment the co-sedimented fraction contains docked vesicles and that docking may not be wortmannin sensitive. Studies on 3T3-L1 cells (Hausdorff et al., 1999) have shown that the incorporation of GLUT4 into the plasma membrane as measured in isolated lawns is somewhat less sensitive to PI 3-kinase inhibition than the full incorporation of GLUT4 as detected by measurements of transport activity. As this lawn procedure measures both docked and fused GLUT4 vesicles, one interpretation of these findings is that the

docking step is less dependent on PI 3-kinase. In addition recent studies in 3T3-L1 cells have shown that partial inhibition of signalling, either by inhibition of PI 3-kinase with LY294002 (Bose et al., 2004) or by inhibition of Akt phosphorylation *via* a low temperature block (van Dam et al., 2005) leads to the accumulation of docked vesicles. Collectively these data suggest that the wortmannin sensitive step may lie beyond the docking step. However, future studies addressing this issue in a cell free system are warranted.

Data in this chapter suggests that it is the association of the Akt with the liposomes that is the insulin-sensitive step in signalling that leads to the activation of fusion. The *in vitro* wortmannin effect on Akt phosphorylation suggests a dynamic and continuous PI 3-kinase and phospho-Akt requirement for fusion. An activation of all the fusion components would have already occurred in samples in which all components are from insulin-stimulated cells. Therefore steps beyond the wortmannin-sensitive PI 3-kinase step might be expected to no longer require the continuous activation of PIP3 production. Our observation that wortmannin still inhibits fusion under these conditions suggests that there is turnover of the activated and phosphorylated form of Akt. This leads to the conclusion that Akt phosphorylation does not lead to a triggering mode of activation of fusion but instead a continuous cycling of phosphorylated Akt production is required to drive fusion.

Homotypic membrane fusion processes such as endosome/endosome fusion reactions are known to be dependent on PI 3-kinases and are inhibited by wortmannin. Although somewhat controversial, it seems that the PI 3-kinase dependent step in fusion can be bypassed using constitutively active Rab isoforms (Jones et al., 1998; Lawe et al., 2001). Therefore potential mediators of fusion include the Rab proteins. In this

context, a common theme in insulin action that appears to be emerging is that many Akt substrates are small GTPase GAP proteins (Gridley et al., 2005; Sano et al., 2003). These substrates include AS160, AS250, TSC1/TSC2 etc. In each case phosphorylation *via* Akt reduces GAP activity and therefore leads to activation of the corresponding small G-protein activity. It would be of interest to determine whether a protein containing a GAP activity is a mediator of membrane fusion of GLUT4 vesicles. A link between Rab proteins and fusion may be mediated by Rab effectors that combine with the SNARE fusion apparatus and its associated proteins such as Munc18c (Bryant et al., 2002; Kanda et al., 2005; Nielsen et al., 2000).

To conclude, in this chapter an *in vitro* fusion assay to mimic the insulin-stimulated GLUT4 vesicle fusion with plasma membrane is demonstrated. Crucial factors are studied and this system provides a strong tool to reveal the remaining mysteries in this event.

Chapter 5 Investigation of Ca^{2+} effects on fusion assay

5.1 Introduction

At the neuronal synapse, Ca^{2+} triggers neurotransmitter release by synaptic vesicle exocytosis. This trigger is with a delay of less than 1 msec, possibly less than 100 μsec (Sabatini and Regehr, 1996). The speed of Ca^{2+} action suggests that Ca^{2+} does not induce release by a complex reaction, for example by initiating assembly of new SNARE complexes or causing large conformational changes. Instead, it is likely that the fusion reaction is largely completed before the arrival of trigger Ca^{2+} (Sudhof, 1995).

Ca^{2+} triggers neurotransmitter release by binding to Ca^{2+} sensors that are localized at the site of exocytosis and these sensors bind multiple Ca^{2+} ions. In forebrain synapses the Ca^{2+} sensor is most likely the synaptic vesicle protein synaptotagmin (Brose et al., 1992; Perin et al., 1990). Synaptotagmin acts on a state of synaptic vesicles in which SNARE complexes have fully assembled, suggesting that SNARE complex assembly creates a metastable fusion intermediate, perhaps a stalk-like state. Ca^{2+}-triggered insertion of the synaptotagmin is sufficient to destabilize the intermediate and to trigger fusion pore opening (Jahn et al., 2003).

In the field of glucose transport and GLUT4 translocation, as early as 1987, Draznin *et al.* found that reduction of intracellular Ca^{2+} in rat adipocytes markedly inhibited insulin-stimulated glucose transport (Draznin et al., 1987). They indicated that there must be a minimal concentration of intracellular calcium to promote insulin action, but increased levels of intracellular calcium may provide a critical signal for attenuation of the insulin action too. The optimal effect of insulin was observed at Ca^{2+} levels between 140 and

370 nM. This means Ca^{2+} may play a permissive role in glucose transport, or it may actively drive one or more of the steps involved in insulin-stimulated GLUT4 trafficking. In the former case there may be no change in cytosolic Ca^{2+} with insulin stimulation. In the latter case insulin may increase cytosolic Ca^{2+} by regulating the activity of a Ca^{2+} channel. It has been proved that insulin treatment of adipocytes does not elevate the intracelluar concentration of free Ca^{2+} (Klip and Ramlal, 1987), which indicates that Ca^{2+} plays a permissive role rather than a driving role. In 3T3-L1 cells, Whitehead *el al.* employed the Ca^{2+}-chelating agent 1,2-bis(o-aminophenoxy)ethane-N,N,N',N'-tetraacetic acid tetrakis(acetoxymethyl ester) (BAPTA-AM) and the calmodulin antagonist N-(4-aminobutyl)-5-chloro-2-naphthalenesulfonamide (W13) to investigate the role of Ca^{2+} in insulin-stimulated glucose transport (Whitehead et al., 2001). BAPTA-AM is a membrane permeable Ca^{2+} chelator whose association and dissociation rates are more than 100-fold higher than EGTA. They found BAPTA-AM and calmodulin antagonist W13 reduced insulin-stimulated glucose uptake by 95 and 60 % and Akt phosphorylation by 75 and 70 %, respectively. GLUT4 translocation was inhibited by 50 % as determined by subcellular fractionation analysis and 100 % by antibody binding assay. These indicate that Ca^{2+}/calmodulin is required both for the efficient activation of Akt and at a late post-docking stage in GLUT4 vesicle fusion. Similarly, another group demonstrated a positive role for intracellular Ca^{2+} in distal insulin signalling events, including initiation/maintenance of Akt phosphorylation, insulin-responsive glucose transporter isoform translocation, and glucose transport (Worrall and Olefsky, 2002). Additionally studies about the effect of Ca^{2+} influx on insulin-mediated glucose uptake in skeletal muscle also indicated that Ca^{2+} acts late in the insulin signalling pathway, for instance, in the GLUT4 translocation to the plasma membrane (Lanner et al., 2006).

Recently it was found that calmodulin binds to AS160 which is an Akt substrate protein with a Rab GTPase activating protein domain (Kane and Lienhard, 2005). This association was Ca^{2+} ion dependent. However the point mutant of AS160 which did not bind calmodulin did not interfere with the capacity of AS160 lacking Akt phosphorylation sites to inhibit GLUT4 translocation. Consequently calmodulin binding is probably not required for the participation of AS160 in insulin-stimulated GLUT4 translocation.

The fusion system designed in Chapter 4 allows us to study the steps of GLUT4 vesicle fusion with the plasma membrane. Using this system, it would be much clearer to study Ca^{2+}/calmodulin effects on GLUT4 vesicle fusion.

5.2 Results

5.2.1 BAPTA-AM inhibition

As described in Chapter 4, a successful fusion assay was set up using insulin PM liposomes and basal GLUT4 vesicles in the presence of insulin cytosol and ATP regenerating system. To investigate the involvement of Ca^{2+} in the process of GLUT4 vesicle fusion with plasma membrane, cytosol was first pre-incubated with the membrane impermeable Ca^{2+} chelator 1,2-bis(o-aminophenoxy)ethane-N,N,N',N'-tetraacetic acid, sodium (BAPTA) but no effect was observed. Ca^{2+} in the cytosol was also chelated by 1 mM EGTA but this slow chelator did not interfere or inhibit fusion (Fig 5.1). This observation was consistent with the report by Whitehead *et al.*, in which the slow chelator EGTA did not show inhibition on glucose uptake (Whitehead et al., 2001). Then cytosol and GLUT4 vesicles were pre-incubated with the membrane permeable Ca^{2+} chelator BAPTA-AM before the fusion assay to chelate all the free Ca^{2+} in the system. 20, 100, 200 μM of BAPTA-AM was mixed with cytosol and GLUT4 vesicles respectively and incubated on ice

for 15 min. The results from the fusion reaction showed that BAPTA-AM inhibited fusion activity in a concentration dependent manner (Fig 5.2). In this experiment, BAPTA-AM chelated the Ca^{2+} both outside and inside of GLUT4 vesicles. Adding back free Ca^{2+} to fusion system to compensate the BAPTA-AM inhibition was not possible because in the presence of BATPA-AM, large amounts of Ca^{2+} were needed to reach the desired concentration (nanomolar range). This level of calcium was found to interfere with the fluorescence signal.

To determine if the observed inhibition was due to chelating of calcium in the cytosol or in the intra-lumenal space of GLUT4 vesicles, only the GLUT4 vesicles were incubated with BAPTA-AM. Using these pre-treated GLUT4 vesicles it was observed that fusion was inhibited (Fig 5.3), which suggested a role of intra-lumenal vesicular Ca^{2+} in the fusion process.

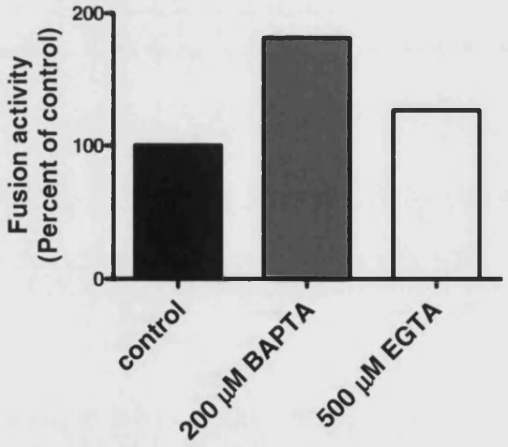

Fig 5.1 BAPTA and EGTA do not inhibit fusion activity. BAPTA and EGTA at the indicated concentration was added to cytosol. GLUT4 vesicle fusion activity was determined using cytosol and PM liposomes from insulin-treated cells. No inhibition was observed when comparing control with 200 μM BAPTA or EGTA pre-treated sample. Data are mean from two very similar experiments.

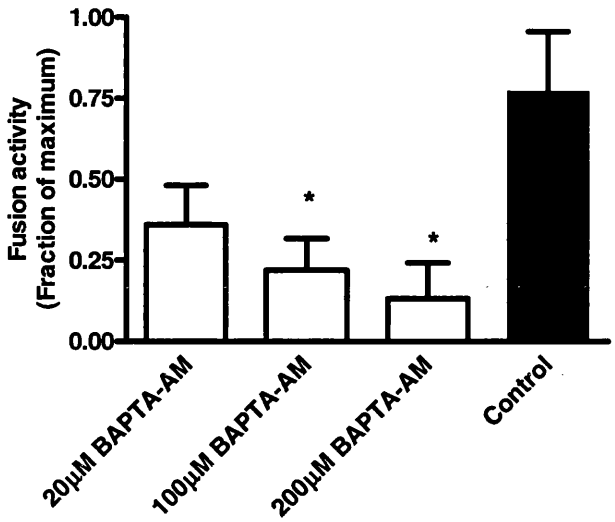

Fig 5.2 BAPTA-AM inhibited fusion activity in a concentration dependent manner. BAPTA-AM at the indicated concentration was added to GLUT4 vesicle and cytosol respectively. GLUT4 vesicle fusion activity was determined using cytosol and PM liposomes from insulin-treated cells. A 3.5-fold difference in fusion activity was observed when comparing control with 100 μM BAPTA-AM pre-treated sample; a 6-fold difference was observed when comparing with 200 μM BAPTA-AM pre-treated sample. Data are mean and SEM from 5 experiments. Comparison control *vs* different BAPTA-AM concentrations * $p < 0.05$.

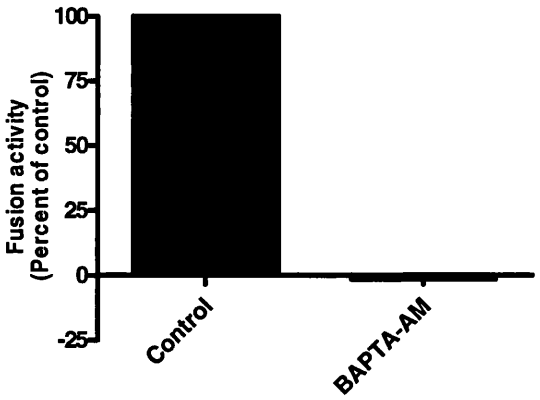

Fig 5.3 BAPTA-AM inhibited fusion activity when treated with GLUT4 vesicles only. GLUT4 vesicles were treated with 200 μM BATPA-AM. GLUT4 vesicle fusion activity was determined using cytosol and PM liposomes from insulin-treated cells. Data are mean from 2 experiments.

5.2.2 Lack of calcium gradient and calmodulin dependence of fusion

To further investigate the effect of Ca^{2+} inside the GLUT4 vesicles on fusion, GLUT4 vesicles were pre-incubated with 1 μM A23187. A23187 is a Ca^{2+} ionophore which should dissipate an existing Ca^{2+} gradient between the inside and the outside of the vesicles. A23187 did not affect the fusion activity (Fig 5.4). This might suggest that the Ca^{2+} inside of GLUT4 vesicles did not act on the fusion but alternative explanations can also be put forward (see discussion).

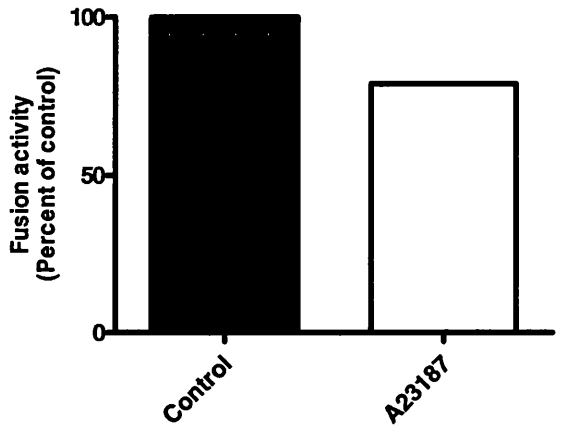

Fig 5.4 A23187 did not affect fusion activity. GLUT4 vesicle fusion activity was determined using cytosol and PM liposomes from insulin-treated cells. Data are mean from 2 very similar experiments.

To investigate the involvement of calmodulin in the fusion process, W13, a calmodulin antagonist, was added to fusion system (Fig 5.5). The result showed that W13 did not inhibit fusion activity, which meant calmodulin was not involved in the fusion process.

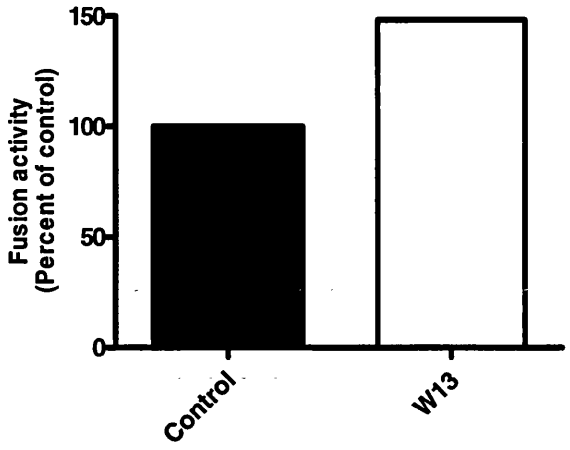

Fig 5.5 W13 did not affect fusion activity. 100 μM of W13 was incubated with cytosol before the fusion assay. GLUT4 vesicle fusion activity was determined using cytosol and PM liposomes from insulin-treated cells. Data are from one experiment.

5.3 Discussion

In the current study the role of Ca^{2+} in GLUT4 vesicle fusion with plasma membrane was investigated by chelating intra-cellular and intra-vesicular Ca^{2+} with a strong chelator BATPA-AM. The results in this chapter showed that BAPTA-AM inhibited GLUT4 vesicle fusion with plasma membrane and that this effect was due to an action on the GLUT4 vesicles content rather than on the cytosol. The inhibition result was consistent with a previous report on 3T3-L1 cells which showed BAPTA-AM inhibition on glucose transport (Whitehead et al., 2001) but whether this inhibition is because of the intra-cellular and intra-vesicular Ca^{2+} chelation by BAPTA-AM needs to be further investigated. This is because BAPTA-AM can also reduce the insulin-stimulated phosphorylation of Akt (Whitehead et al., 2001), the inhibition shown in this chapter could be at least partly explained by the impairment in insulin-signalling.

The sole treatment of BAPTA-AM on GLUT4 vesicles was performed to chelate the intra-vesicular Ca^{2+} inside the GLUT4 vesicles. Although it showed inhibition of the fusion activity the proof was not strong enough to guarantee it was only because of the intra-vesicular Ca^{2+}. It was possible that excess BAPTA-AM could still be able to chelate the intracellular Ca^{2+} in the cytosol as BAPTA-AM was present during the whole fusion reaction. This problem can be resolved if the GLUT4 vesicles are treated with BAPTA-AM before isolation.

Addition of Ca^{2+} ionophore A23187 was another way to study the intra-vesicular Ca^{2+} inside of GLUT4 vesicles. The adjustment of Ca^{2+} concentration between the inside and the outside of GLUT4 vesicles through this ionophore did not inhibit fusion activity. This could indicate that the BAPTA-AM inhibition was only due to the action on Akt phosphorylation. Alternatively, it might also be because the gradient of Ca^{2+} between the inside and the outside of GLUT4 vesicles does not affect the mechanism by which Ca^{2+} triggers fusion. Several studies have shown that Ca^{2+} is released from the lumen of the vesicles during the actual fusion process (Holroyd et al., 1999; Peters and Mayer, 1998; Porat and Elazar, 2000; Pryor et al., 2000), thus promoting fusion. Based on their conclusion, if a burst in the release of intra-lumenal vesicular Ca^{2+} triggers fusion rather than a global increase in intracellular Ca^{2+}, it is reasonable that fusion could not be inhibited by ionophores because ionophores only equilibrate the ion concentration on both sides of a membrane but do not stop the ion movement. The equilibrated Ca^{2+} might still be able to form a burst from one side of the membrane to the other side. Additionally, in skeletal muscle it has been found that insulin application resulted in a significant increase in Ca^{2+} concentration close to the cell membrane. The insulin concentration required for half-maximal increase in this Ca^{2+} concentration was similar to that needed for half-maximal activation of insulin-mediated glucose uptake

(Bruton et al., 2001; Bruton et al., 1999). Although it was demonstrated that the Ca^{2+} influx was from the extracellular buffer, it suggested that the quick movement of Ca^{2+} ions near membranes was playing an important role in insulin-stimulated glucose transport. The near membrane Ca^{2+} concentration can be detected by a membrane-associated Ca^{2+} indicator FFP18 (Bruton et al., 1999; Etter et al., 1994). This indicator could be used in the fusion system in the future to monitor the near membrane Ca^{2+} concentration changes during the fusion event. If any near membrane Ca^{2+} is detected, it should be due to the ion movements between the cytosol and the GLUT4 vesicles. This is because in the fusion system there is no Ca^{2+} in the buffer.

W13 was shown to impair the phosphorylation of Akt and glucose transport (Whitehead et al., 2001), however in my experiments it did not inhibit the fusion activity. It is interesting because both W13 and BAPTA-AM can decrease the phosphorylation of Akt but BAPTA-AM showed inhibition to GLUT4 vesicle fusion with plasma membrane whereas W13 did not. BAPTA-AM can chelate free Ca^{2+} and W13 competes with calmodulin. An explanation could be that Ca^{2+} (but not calmodulin) is required for the continuous Akt phosphorylation after all the fractions have been fully-stimulated, or merely that the postdocking event requires Ca^{2+} but not calmodulin. The lack of effect of the calmodulin antagonist W13 is also in accordance with the studies on AS160 which showed that although an interaction between AS160 and calmodulin is possible this interaction did not have an effect on AS160 function on GLUT4 trafficking (Kane and Lienhard, 2005).

Recently studies in our laboratory demonstrated that the GLUT4 vesicles from insulin-stimulated cells also supported fusion (Koumanov and Holman, unpublished observations). It provides another route to study the

Ca^{2+}/calmodulin relationship with insulin signalling and GLUT4 vesicle fusion. If BAPTA-AM still inhibits fusion with GLUT4 vesicles from insulin-stimulated cells it means Ca^{2+} acts in the postdocking stage, no matter whether it affects insulin signalling or not.

To conclude, an inhibition of the fusion with BAPTA-AM was observed. However, more experiments will be needed to monitor precisely how this effect is exerted.

Chapter 6 Investigation of V-ATPase effects on the fusion assay

6.1 Introduction

The vacuolar H^+ ATPase (V-ATPase) is an ATP-driven enzyme that transforms the energy of ATP hydrolysis to electrochemical potential differences of protons across diverse biological membranes *via* the primary active transport of H^+. First found in association with endosomal membranes, the V-type H^+ ATPase is now also found in increasing examples of plasma membranes where the proton pump energizes transport across cell membranes and entire epithelia. The molecular details reveal up to 14 protein subunits arranged in a cytoplasmic V1 complex, which mediates the hydrolysis of ATP and a membrane-embedded V0 complex, which translocates H^+ across the membrane. It has been shown that the V-ATPase acts as a molecular rotor akin to F-type ATPase (Nishi and Forgac, 2002). The hydrolysis of ATP turns a rotor consisting largely of one copy of subunits D and F of the V1 complex and a ring of six or more copies of subunit c of the V0 complex. The rotation of the ring is thought to deliver H^+ from the cytoplasmic to the endosomal or extracellular side of the membrane, probably *via* channels formed by subunit a from the V0 complex (Fig 6.1). The association/dissociation of V1 and V0 complexes is reversible, which was recognized as one mechanism of its physiological regulation (Beyenbach and Wieczorek, 2006).

Apart from SNARE proteins which are commonly recognized as membrane fusion machinery, V-ATPase has also been studied actively in membrane fusion, independently of its role in vesicle acidification. The V0 complex was first implicated in membrane fusion when its subunit c was found to be the

"mediatophore", a protein that could produce calcium-dependent release of neurotransmitter (Brochier and Morel, 1993). More recently V0 subunit was reported to associate with target membrane SNAREs and play a role in the fusion of yeast vacuoles (Peters et al., 2001), Eventually it has been demonstrated that V0 functions after trans-SNARE pairing and is coupled to the Ca^{2+}-releasing channel (Bayer et al., 2003). Lately Hiesinger *et al.* screened the proteins required for neurotransmission in Drosophila and identified the gene vha100, the 110 kDa subunit of V0 (generally referred to as subunit a) (Hiesinger et al., 2005). Mutations that resulted in truncated vha100 led to a significant decrease in transmission. They also revealed that this subunit binds to t-SNAREs, suggesting a model in which SNARE proteins guide V0 pores in vesicle and acceptor membranes into apposition, thus forming a pore spanning both membranes (Almers, 2001). A possible structure of fusion pore that is formed by V0 dimers are shown in Fig 6.2.

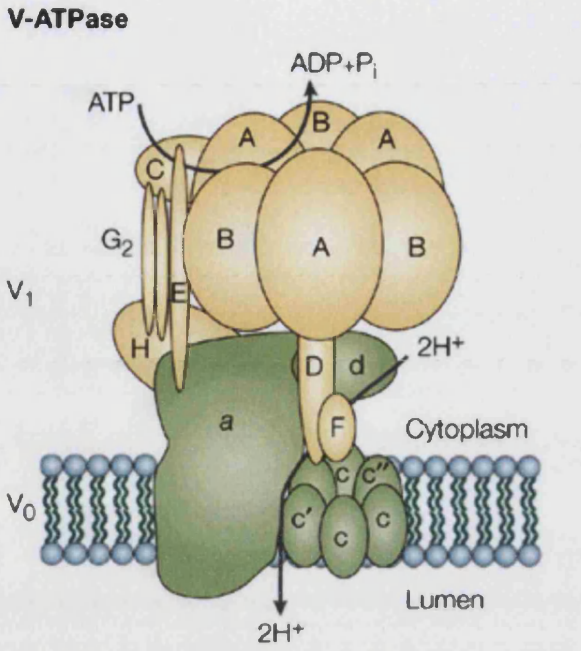

Fig 6.1 Schematic representation of the structure of V-ATPase (Nishi and Forgac, 2002). V-ATPase consists of peripheral complex V1 and integral membrane complex V0. V1 is formed by eight different subunits identified with capital letters A-H. V0 complex consists of at least three different subunits identified with small letter (a,c,d). Hydrolysis of ATP brings about rotation of the V1 central shaft together with the c-ring of the V0 complex. Subunit a hypothetically provides two H^+ from the cytoplasm to the lumen/extracellular fluid. The H^+ moves via an intermediary H^+ binding step to one subunit c (Beyenbach and Wieczorek, 2006).

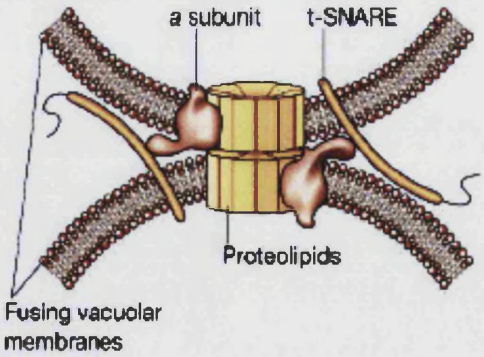

Fig 6.2 Possible structure of the dimer of V0 that may form a fusion pore during vacuole fusion. Two rings of proteolipid, two a subunits and two t-SNARE proteins are shown (Almers, 2001).

It has been found that exposure of cells to insulin causes an increase in intracellular pH in fat (Civelek et al., 1996), 3T3-L1 cells (Klip et al., 1988), muscle (Klip et al., 1986), and liver (Peak et al., 1992). The work on rat adipocytes (Yang et al., 2002b) and cardiomyocytes (Yang et al., 2002a) suggested that insulin-stimulated cytosol alkalinization facilitated the final stages of translocation and incorporation of fully functional GLUT4 at the surface-limiting membrane. It has been showed the alkalinization effect of insulin was blocked by treatment of V-ATPase inhibitor bafilomycin A1 (Yang et al., 2002a). These studies on a GLUT4-occluded intermediate in exocytosis added to the growing evidence for regulation of membrane fusion intermediates by electrochemical gradient for H^+ ($\Delta\mu H^+$) (Peters et al., 2001; Ungermann et al., 1999).

Using Mass Spectrometry Larance *et al.* identified proteins present on GLUT4 vesicles from 3T3-L1 adipocytes (Larance et al., 2005). Among these proteins there is V-ATPase subunit a (110 kDa) from complex V0. Based on this fact, an attempt was made towards elucidating the role of V-ATPase from GLUT4 vesicles in their fusion with the plasma membrane, using the fusion system described in Chapter 4.

6.2 Results

6.2.1 Concanamycin A inhibition

To confirm the presence of V-ATPase on GLUT4 vesicles, concentrated GLUT4 vesicle proteins were resolved by SDS-PAGE and western blotted with anti goat V-ATPase subunit a antibody. Rat brain lysate and low density microsomes were run in parallel as an indication for the exact position of the protein band (Fig 6.3). An immunoreactive band at 110 kDa was detected in GLUT4 vesicles. In parallel with other controls, it confirmed the presence of V-ATPase on GLUT4 vesicles.

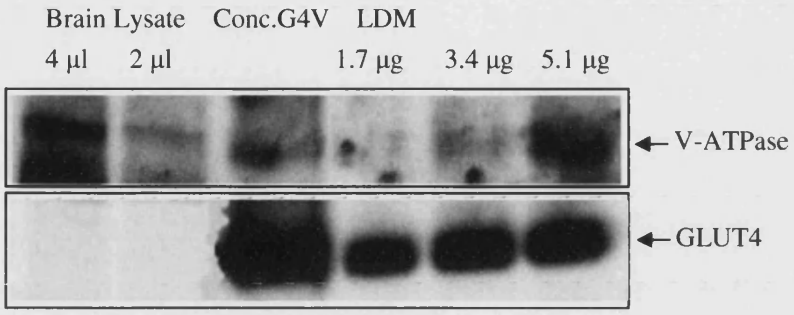

Fig 6.3 Western blots showing V-ATPase subunit a on GLUT4 vesicles. GLUT4 vesicles immuno-isolated with MBP-Spa and anti-GLUT4 abtibody method (Chapter 3) from 2 rats were concentrated to 50 µl by using a VIVASpin column. LDM were from rat adipocytes subfractiation. V-ATPase subunit a was detected with goat anti-V-ATPase subunit a antibody.

To reveal the role of V-ATPase in GLUT4 vesicle fusion with plasma membranes, 200 nM concanamycin A was incubated with GLUT4 vesicles before the fusion reaction (Fig 6.4). Concanamycin A is an antibiotic which binds to the subunit c of the V0 complex in V-ATPase (Beyenbach and Wieczorek, 2006; Bowman et al., 2004). The concanamycin A pre-treated GLUT4 vesicles had a significantly inhibited fusion activity, indicating that the V-ATPase is playing a role in the process of fusion.

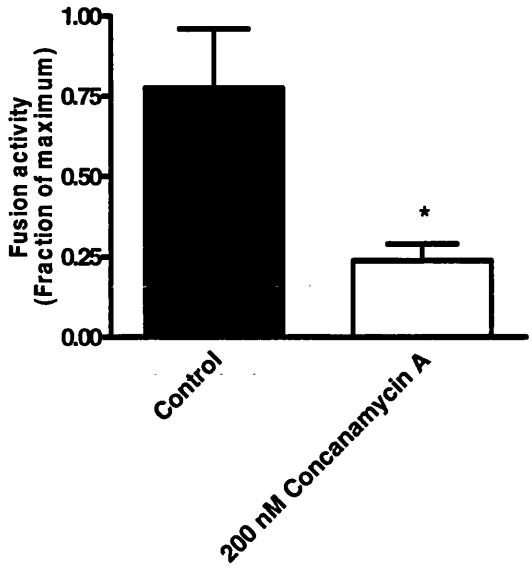

Fig 6.4 Concanamycin A inhibits the fusion activity of GLUT4 vesicles. GLUT4 vesicles were treated with 200 nM concanamycin A . GLUT4 vesicle fusion activity was determined using cytosol and PM liposomes from insulin-treated cells. A 3.24-fold difference in fusion activity was observed when comparing control with 200 nM concanamycin A pre-treated sample. Data are mean and SEM from 4 experiments. * $p < 0.05$ vs Ins cyt, Ins PM.

6.2.2 Investigation of whether the V-ATPase acts on a pH gradient or as fusion pore

There are two hypotheses as to how the V-ATPase may act on GLUT4 vesicle fusion with plasma membrane: 1) the V-ATPase creates the H^+ gradient between the inside and the outside of GLUT4 vesicles and this H^+ gradient affects fusion, 2) V0 complex of V-ATPase acts as a fusion pore independent of vesicle acidification. If the V-ATPase acidifies the lumen of GLUT4 vesicles, the environment outside GLUT4 vesicles would be relatively basic. The environment in a normal fusion reaction was pH 7.4. If the environment was modified to pH 6.5, the H^+ gradient would be reduced. When performing the fusion reactions in an environment at pH 6.5, the fusion activity was reduced down to 1/3 of the control at pH 7.4 (Fig 6.5).

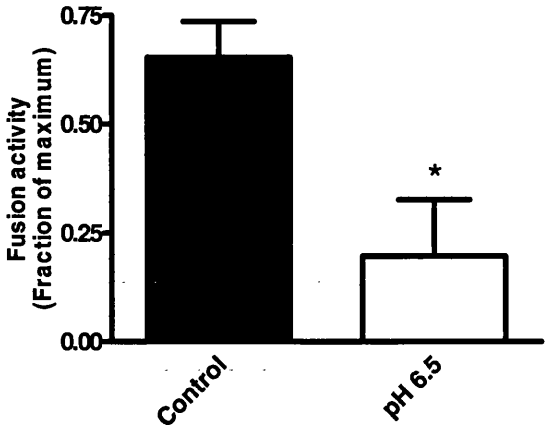

Fig 6.5 Low pH (pH 6.5) inhibited fusion activity. GLUT4 vesicle fusion activity was determined using cytosol and PM liposomes from insulin-treated cells in the environment of pH 6.5 or pH 7.4 (control). A 3.3-fold difference in fusion activity was observed when comparing control with pH 6.5 sample. Data are mean and SEM from 3 experiments. * $p < 0.05$ vs Ins cyt, Ins PM.

6.3 Discussion

In this chapter the effect of V-ATPase on GLUT4 vesicle fusion with the plasma membrane was studied in two ways: by 1) V-ATPase inhibitor concanamycin A treatment of GLUT4 vesicles in order to stop the H^+ pump activity of V-ATPase, and by 2) perturbation of H^+ gradient between inside and outside of GLUT4 vesicles.

Concanamycin A treatment showed inhibition of fusion activity and suggested a role of V-ATPase in this fusion event. Although concanamycin A inhibited GLUT4 vesicle acidification, the mechanism by which the V-ATPase was inhibiting the fusion was still not clear. Perturbation of the pH gradient by carrying out fusion reaction in a pH 6.5 environment is one way to reveal the role of H^+ gradient. Fusion activity was blocked in pH 6.5 medium. An additional useful test would be to study fusion activity in a

medium buffered at pH 8.0. If fusion activity is stimulated in pH 8.0 compared with pH 7.4, then this would mean that a H^+ gradient is important in the fusion reaction. If no stimulation is found when comparing pH 8.0 with pH 7.4 then this may mean that the fusion reaction requires an optimal pH environment and that a low pH (for example at pH 6.5) is sub-optimal. However, even if the fusion was stimulated at pH 8.0, this would not exclude the possibility that the V0 complex of the V-ATPase might work as a fusion pore in the fusion reaction.

A H^+ gradient has been suggested to facilitate the translocation of GLUT4 to the cell surface and fusion with the plasma membrane (Yang et al., 2002b). Several studies suggested the involvement of endosome acidification in receptor tail recognition and in control of recycling *via* interactions with internalization motifs (Basu et al., 1981; Reaves and Banting, 1994). In the analysis of TfR recycling (Johnson et al., 1993; Presley et al., 1997), it has been revealed that reduced endosome acidification results in a reduced rate of exit of TfRs from the recycling compartment to the plasma membrane. In addition, the distribution of ADP ribosylation factor (ARF) to the cytoplasmic face of the trans-Golgi network, where it is required for vesicle coating and budding of secretory vesicles, is a pH-dependent process (Zeuzem et al., 1992). GLUT4 contains targeting motifs at both the N- and C-terminal domains. These domains include acidic motifs that may act to fine-tune the recognition by adaptor complexes of motifs based on hydrophobic residues, phenylalanine at the N-terminus and di-leucine at the C-terminus (Holman and Sandoval, 2001; Martinez-Arca et al., 2000; Sandoval et al., 2000; Shewan et al., 2000). It seems likely that these acidic domains may be recognized by vesicle-coating proteins (Holman and Sandoval, 2001). It is hypothesized that the recognition of these domains maybe dependent on pH around the GLUT4 vesicles and tubulo-vesicular structures and may influence vesicle coating, budding and release steps.

A more important site for pH regulation of GLUT4 trafficking appears to be at the vesicle fusion step at the plasma membrane. Perturbation at this step could account for the low transport activity and reduced exposure of GLUT4 to the impermeant photolabeling reagent but retention of high levels of GLUT4 immunocytochemically localized in the vicinity of the plasma membrane (Yang et al., 2002b). Analysis of the kinetics of exocytosis has revealed that there is an initial rapid burst of exposure of GLUT4 at the cell surface, which is then followed by a slower phase. These burst kinetics in GLUT4 exocytosis are similar to those reported for other vesicle secretory systems (Jahn and Sudhof, 1999; Xu et al., 1999), which indicates that there are two vesicle fusion intermediates present in sequence, possibly SNARE interaction and another trigger (which could be Ca^{2+} or a pH gradient for example).

Recently more and more studies have revealed the V-ATPase's role as a fusion pore component which is independent of a role in acidification (Bayer et al., 2003; Hiesinger et al., 2005; Poea-Guyon et al., 2006). The fact that V0 binds to t-SNAREs is consistent with other reports suggesting t-SNARE syntaxin is a component of the fusion pore (Han et al., 2004; Han et al., 2005). The links of the V-ATPase with Ca^{2+}-releasing channel (Bayer et al., 2003) and with calmodulin (Peters et al., 2001) make its relation to fusion even more interesting.

As mentioned earlier, fusion assays in pH 6.5 and pH 8.0 can be considered to reveal the pH gradient mechanism. Various proton ionophores, such as nigericin, FCCP, can also be implemented to break the pH gradient. In addition, if the fusion pore hypothesis is true, it is crucial to prove that the loss of V0 complex halts fusion. The failure of V0 complex can be realized by immuno-depletion, recombinant protein or antibody interference, and other techniques.

So far there have not been reports on the intra-vesicular pH inside of GLUT4 vesicles. Using a method similar to that described by Bai *et al.* (Bai et al., 2006), VAMP2 could be fused with a pH sensitive marker and this recombinant VAMP2 could be transfected into insulin sensitive cells containing GLUT4 vesicles. Using microscopy to visualize the pH sensitive marker, it should be possible to show a series of changes in the process of insulin-stimulated GLUT4 translocation.

In summary in this chapter it has shown that the V-ATPase V0 subunit a is present in the GLUT4 vesicles and that the use of an inhibitor of the V-ATPase decrease significantly the amount of fusion. The change of the pH of the incubation medium leads also to a reduction in the fusion process, pointing towards an effect of the pH gradient on GLUT4 vesicle fusion with the plasma membranes.

Chapter 7 Liposome fusion using recombinant SNAREs

7.1 Introduction

As discussed in earlier chapters, the incorporation of GLUT4 into the plasma membrane of muscle and fat cells is an important biological phenomenon involving vesicle-membrane fusion. Insulin signalling results in the movement of GLUT4 vesicles towards the plasma membrane and fusion of GLUT4 storage vesicles with the plasma membrane. This appears to fail in the insulin resistance state, which accompanies several forms of diabetes.

The functional proteins in vesicle/membrane fusion are soluble *N*-ethylmaleimide sensitive factor attachment protein receptor (SNARE) proteins (section 1.4.2). As mentioned earlier, the fusion of transport vesicles into acceptor membranes is mediated by a complex of proteins known as t-SNAREs and v-SNAREs. T-SNAREs are found on target/acceptor membranes and are composed of the syntaxin (Stx) and SNAP (soluble *N*-ethylmaleimide-sensitive fusion factor attachment protein) family of proteins. V-SNAREs are members of the VAMP (vesicle-associated membrane protein)/synaptobrevin family and are found on vesicle/donor membranes (Bonifacino and Glick, 2004; Hong, 2005) (section 1.4.2). The mechanism underlying membrane bilayer fusion requires the formation of high-affinity, parallel, four-α-helix bundles containing one coiled-coil Stx domain, two coiled-coil SNAP domains, and a coiled-coil VAMP domain (Antonin et al., 2002; Sutton et al., 1998). Because of the physiological importance of insulin-dependent GLUT4 translocation to the cell surface, attempts have been made to characterize the final GLUT4 vesicle fusion step, drawing from lessons learned from neural synaptic transmission, which has been well studied (Table 7.1).

Table 7.1 Functional SNARE proteins in neuronal transmission and GLUT4 storage vesicles (GSV) fusion with the plasma membrane.

	Neuronal Transmission	GSV Fusion
v-SNARE	VAMP2	VAMP2
t-SNARE	Syntaxin1	Syntaxin4
	SNAP25	SNAP23

As Table 7.1 shows, the functional SNAREs in neuronal transmission are VAMP2 (v-SNARE), syntaxin1 (t-SNARE) and SNAP25 (t-SNARE) (Leabu, 2006; Schuette et al., 2004) (section 1.4.3). For the GLUT4 storage vesicles (GSV) which fuse with the plasma membrane, the counterparts are VAMP2 (v-SNARE), syntaxin4 (t-SNARE) and SNAP23 (t-SNARE) (Foster and Klip, 2000). They have been shown to bind pair-wise *in vitro* with affinities similar to those of the neuronal homologs (Foster et al., 1998). They also form a ternary complex *in vitro* (Rea et al., 1998; Widberg et al., 2003) and are present together in 20S SNARE complexes in adipose cells (St-Denis et al., 1999). Their function and detailed mechanism of action in the fusion is still elusive. Generally, it is believed that their interaction occurs as illustrated in Fig 7.1. VAMP2 is present in GLUT4 vesicles and participates in the formation of a fusion complex with the plasma membrane t-SNAREs, syntaxin4 and SNAP23. In this crucial step of fusion, other proteins have been reported to play active roles in the fusion complex formation. For example, the availability of syntaxin4 might be controlled by Munc18c, which has a negative "clamping" effect on syntaxin4 or may induce a conformational change in syntaxin4 that renders it available for SNARE pairing (Foster and Klip, 2000). Proteins of the Rab family can interact with Rab effectors. In neuronal cells, Rab effector such as Rabenosyn5 binds to Rab5 and to the syntaxin interacting protein Munc18. The latter interaction then regulates the SNARE pairing (Schimmoller et al., 1998). In

insulin-sensitive tissues, Rab4 has been implicated in GLUT4 vesicles trafficking and has also been shown to interact with syntaxin4 (Foster and Klip, 2000).

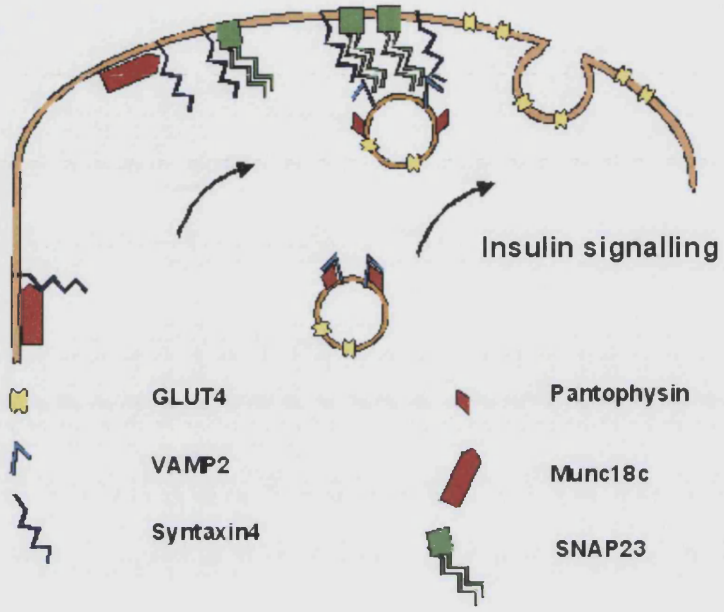

Fig 7.1 SNARE protein interaction in regulation of GLUT4 vesicle fusion with the plasma membrane.

7.2 Principle and the design of the SNARE-dependent fusion assay

The idea of the work described in this chapter is inspired by the milestone work in the field of membrane fusion by Weber *et al* (Weber et al., 1998). They expressed the recombinant v- and t-SNAREs, reconstituted the SNARE proteins into artificial liposomes, and allowed these liposomes to fuse with assistance of SNARE proteins in an absolutely cell-free environment. The success of this system provides evidence that SNARE proteins constitute the minimal machinery for membrane fusion. The basis of this assay is lipid mixing with fluorescence dequenching (Struck et al., 1981): when liposomes fuse, the distance between fluorescence quenching pairs increases, the quenching decreases and fluorescence signal

increases. As mentioned in Chapter 1 (section 1.4.4), lipid mixing could produce a pseudo signal at a hemi-fusion stage. To avoid this, the assay described in this chapter is instead a content mixing assay and based on the formation of the fluorescent $Eu(DPA)_3^{3-}$ chelation complex. Eu^{3+} and dipicolinic acid (DPA) are encapsulated in two sets of liposomes of interest, namely t-SNARE and v-SNARE liposomes. When these liposomes fuse under certain conditions, Eu^{3+} and DPA form $Eu(DPA)_3^{3-}$ chelation complex. The fluorescence intensity of Eu on its own is very low, but when the complex is excited at a wavelength close to the absorption maximum of DPA, the fluorescence is enhanced 10^4-fold because of an internal energy transfer from the ligand to the metal ion. Fusion of the liposomes would then register as an increase of the fluorescence intensity due to the formation of the $Eu(DPA)_3^{3-}$ complex (Fig 7.2).

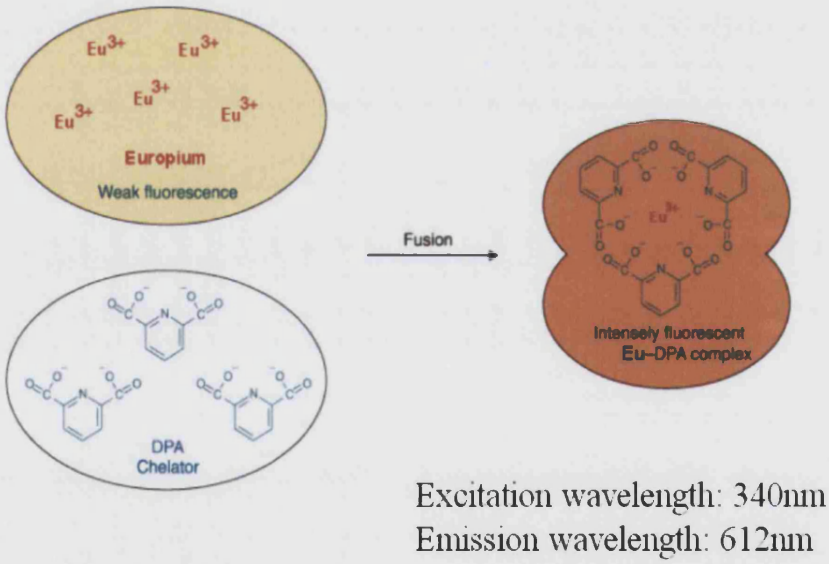

Fig 7.2 Content mixing with Eu/DPA probes. See text for details.

For practical applicability of this assay, several conditions have to be met. First, both $EuCl_3$ and DPA have to be able to be encapsulated within phospholipid vesicles without affecting the structure of the bilayer; their rates

of leakage from the vesicles should be low. Second, the formation of the Eu/DPA complex should be fast enough to permit kinetic analysis of vesicle fusion. Third, in order to eliminate the possibility that mere leakage of vesicle contents would result in fluorescence development, the composition of the external medium has to be such that formation of the complex outside the vesicles is effectively prevented.

7.3 Results

7.3.1 Fusion of plain liposomes induced by PEG

To determine if DPA and Eu^{3+} are a good pair to measure the extent of liposome fusion, experiments were first performed with plain liposomes containing either DPA or Eu^{3+}, namely PD and PE liposomes. To induce the fusion of the plain liposomes, the fusogenic reagent polyethelene glycol (PEG) was used at concentrations of 1 to 4 % (w/v). As shown in Fig 7.3, 4 % PEG induced a quicker increase in the detected fluorescent signal. The relative fluorescent unit was normalized relative to the maximum signal obtained after detergent addition which was set as 100 % fluorescence. This result demonstrated that the content mixing method is occurring and allows real-time monitoring of liposome fusion.

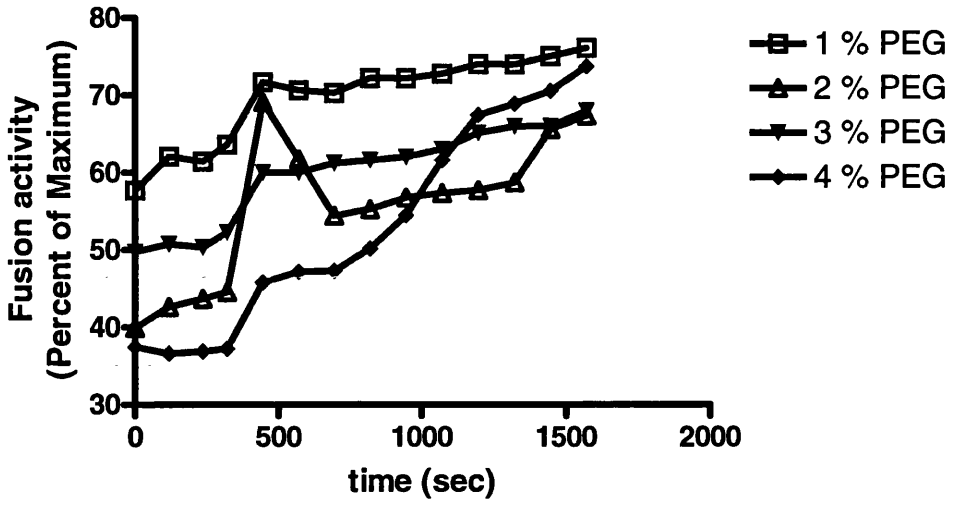

Fig 7.3 PEG induced plain liposomes fusion. 5 µl of Eu encapsulated plain liposomes (PE) were mixed with 5 µl of DPA encapsulated plain liposomes (PD), in the presence purified PEG. Fluorescence was expressed as a percentage of the signal obtained after addition of 0.1 % TritonX-100 (considered as 100 %). PEG was added at 0 sec.

7.3.2 Reconstitution of t- and v-SNAREs into liposomes

Recombinant t- and v-SNAREs were expressed, purified and reconstituted into liposomes (sections 2.2.5, 2.2.6). The last step in the reconstitution of the SNARE proteins into the liposomes is the separation of the liposomes from the crude material on an Optiprep gradient (Chapter 2, section 2.2.6.2). After the end of the centrifugation, different layers were collected from the top to the bottom of the tube (Fig 7.4). Sample of these layers were analysed by western blotting to detect the SNARE protein distribution across the gradient. The t-SNAREs syntaxin4, SNAP23 and v-SNARE VAMP2 were mainly present in the top layers (labelled 1 and 2 in Fig 7.5). In all the subsequent experiments, Eu^{3+} encapsulated t-SNARE liposomes (TE) and DPA encapsulated v-SNARE liposomes (VD) were harvested from layers 1 and 2 (1 ml in total). There was also a tiny amount of sytaxin4 present in the layer 3 (Fig 7.5).

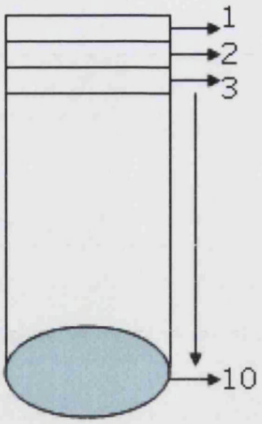

Fig 7.4 Representation of the layers distribution in an Optiprep gradient. 10 fractions were collected from the top to the bottom of the gradient (0.5 ml from each layer)

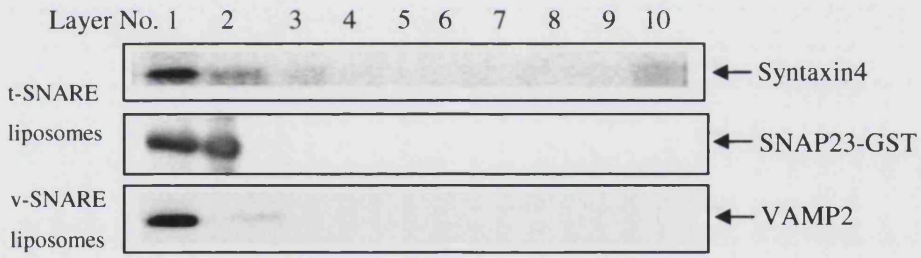

Fig 7.5 Reconstitution of t- and v-SNAREs into liposomes and their analysis by western blotting. Rabbit anti Syntaxin4 antibody showed a syntaxin 4 band at 34 kDa. Rabbit anti GST antibody showed a SNAP23-GST band at 50 kDa. Rabbit anti VAMP2 antibody showed a VAMP2 band at 13 kDa.

7.3.3 Orientation of t- and v-SNAREs in liposomes

To test the SNARE orientation when incorporated in the liposomes, t-SNARE or v-SNARE liposomes were treated with trypsin in the absence or

presence of detergent (Fig 7.6). The t-SNAREs (syntaxin4, SNAP23) in TE liposomes were completely digested by 1 mg/ml trypsin with or without detergent. The complete digestion was most likely due to the trypsin amount being present in large excess. The v-SNARE (VAMP2) in VD liposomes was digested incompletely in the absence of detergent but completely with detergent. For VAMP2, Botulinum neurotoxin light chain/B protease (BoLC/B) cleavage experiments were carried out to test whether VAMP2 were inserted properly in VD liposomes (Fig 7.7).

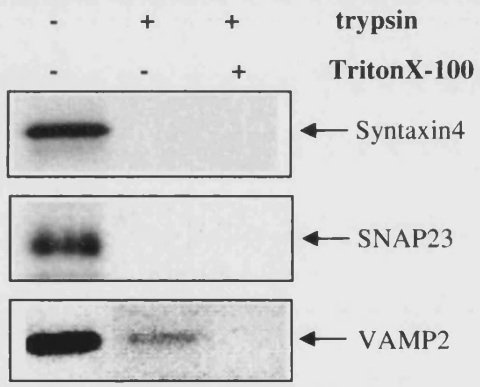

Fig 7.6 A test of the orientation of t- and v-SNAREs in liposomes by trypsin digestion. All liposomes were incubated at 37 °C for 30 min. Trypsin was present at 1 mg/ml and TritonX-100 was present at 0.2 % (w/v) as final concentrations.

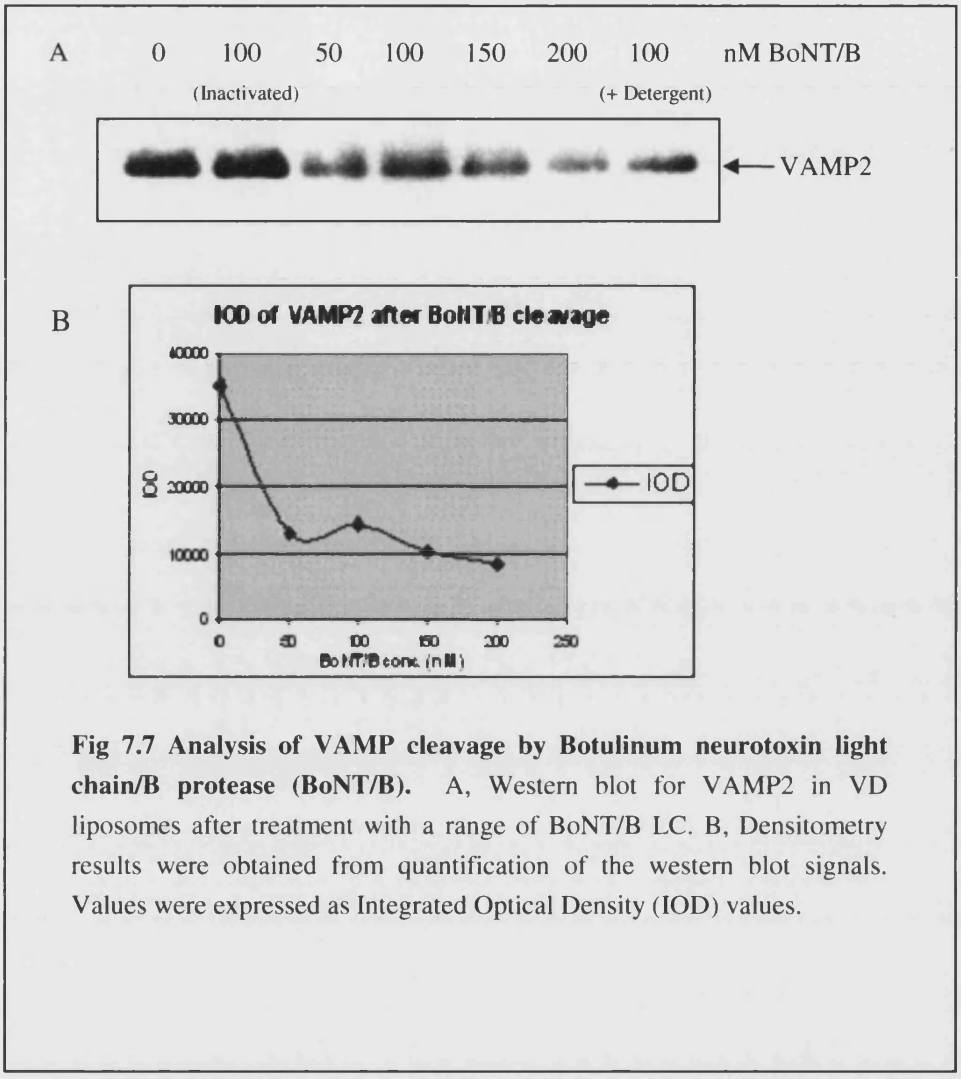

Fig 7.7 Analysis of VAMP cleavage by Botulinum neurotoxin light chain/B protease (BoNT/B). A, Western blot for VAMP2 in VD liposomes after treatment with a range of BoNT/B LC. B, Densitometry results were obtained from quantification of the western blot signals. Values were expressed as Integrated Optical Density (IOD) values.

Increasing amounts of the v-SNARE VAMP2 present in VD vesicles were cleaved by BoNT/B LC as the enzyme concentration was increased. The band intensities were quantified as IOD values. These reached a plateau of digestion at 100 nM enzyme treatment (Fig 7.7 B). Even in presence of detergent some of the VAMP2 protein remained uncleaved. The quantification result indicates that 65.7 % of the VAMP2 is inserted in the right orientation in the liposomes (cytoplasmic-side out). However, the quantification of trypsin digestion of VAMP2 (Fig 7.6) showed that 92 % was digested. This higher percentage may be due to the over digestion of some internally orientated VAMP2 by trypsin at high concentration (1 mg/ml).

7.3.4 Quantifications of t- and v-SNAREs in liposomes

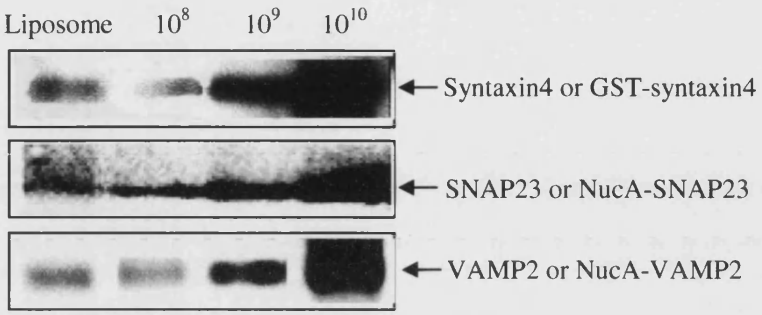

Fig 7.8 Quantification of t- and v-SNAREs in liposomes. The indicated liposome samples were 10 µl each. The amounts of recombinant protein standard sample were 10^8, 10^9, 10^{10} molecules/µl, with 10 µl of each added to the gel. Standards: GST-syntaxin4 (56 kDa), NucA-SNAP23 (43 kDa), NucA-VAMP (33 kDa). This result shown was from two very similar experiments.

To estimate the amount of each one of the SNARE protein in the liposomes, a sample of TE or VD liposomes was analysed by western blot alongside known amount of the respective recombinant protein (Fig 7.8). The amount of t-SNARE syntaxin4 reconstituted was approximately 10^8 molecules/µl TE liposomes; SNAP23 reconstituted was approximately 10^8 molecules/µl TE liposomes. The amount of v-SNARE VAMP2 reconstituted was 10^8 - 10^9 molecules/µl VD liposomes.

7.3.5 SNARE-reconstituted liposome fusion is induced by Ca^{2+} and cytoplasm

When normalization of the fluorescence signal was carried out for the experiments in which PEG-induced fusion was studied, 0.1 % TritonX-100 (w/v) was used to gain the maximum 100 % fluorescence value. In the

SNARE fusion assay, octyl-glucoside, TritonX-100, Tween20, $C_{12}E_9$, sodium cholate, n-Dodecyl-maltoside were tried in an attempt to obtain a maximum 100 % fluorescence value. However, none of these reagents produced a fluorescence increase. Instead, the fluorescence even decreased in some of the cases. This decrease may occur if, in the presence of the IC buffer and cytoplasm, the Eu^{3+} is quenched by the EGTA in the IC buffer. However, in the presence of surrounding dialysis buffer, the decrease could not be explained in this way. Instead it is suggested that perhaps there is a quenching effect of the detergent more directly on the fluorescence of the probe. Because the SNARE vesicle fusion was mainly carried out in the presence of surrounding IC/cytoplasm which contains EGTA, the highest/plateau fluorescence signal after the Ca^{2+} inducing was set as 100 %.

When TE and VD liposomes or the plain liposomes were mixed in 1:1 ratio in presence of IC buffer only, the fluorescence went slowly down (Fig 7.9), indicating no fusion was induced and a slow leakage of fluorescent material was occurring. The addition of Ca^{2+} to these liposomes did not modify the pattern of fluorescent change.

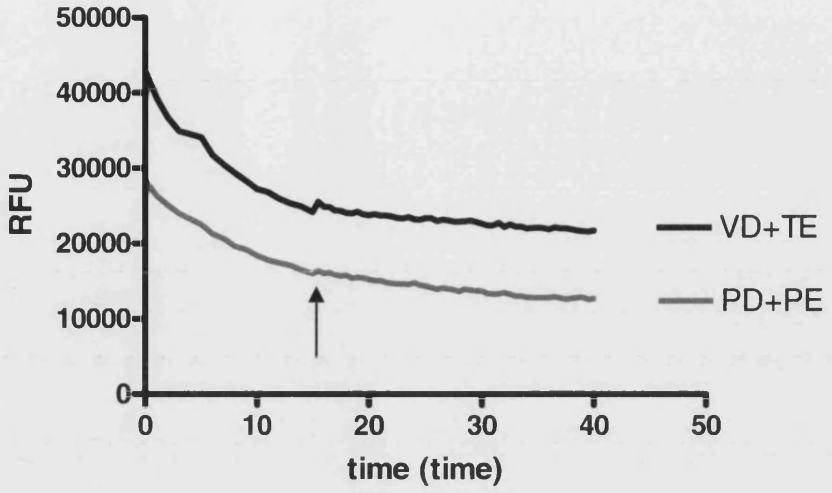

Fig 7.9 Liposome fusion in the presence of IC buffer alone. 50 µl of Eu containing liposomes (PE, TE) were mixed with 50 µl of DPA containing liposomes (PD, VD) in the presence of 25 µl IC buffer. 3.5 µl of 200 mM $CaCl_2$ was added at the indicated 15 min time point to achieve a free Ca^{2+} final concentration of 100 µM for the induction. The fluorescent intensity is expressed as Relative Fluorescent Units (RFU). The result shown was from two very similar experiments.

In the presence of cytoplasm the fluorescence remained constantly flat. Basal and insulin stimulated cytoplasm affected the fluorescent signal in the same way (Fig 7.10).

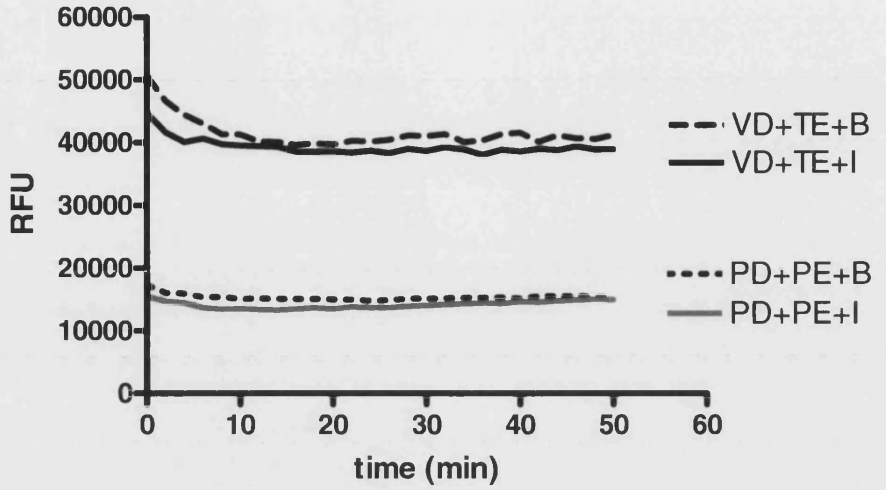

Fig 7.10 Liposome fusion in the presence of cytoplasm. 50 µl of Eu liposomes (PE, TE) were mixed with 50 µl of DPA liposomes (PD, VD) in the presence of 25 µl of cytoplasm from basal (B) or insulin stimulated (I) cells (2.3 mg/ml). The fluorescent intensity is expressed as Relative Fluorescent Units (RFU).

Fig 7.11 shows the time course of the fusion with Eu^{3+} and DPA liposomes after Ca^{2+} was added. A single representative experiment is also shown in Fig 7.12 in Ca^{2+} added samples. After the addition of $CaCl_2$ to the liposome suspension in cytoplasm and from time zero, the Europium fluorescence intensity increased gradually until a maximum was reached. This was followed by a plateau. These results indicate that when Ca^{2+} and cytoplasm are surrounding the liposomes, they induce a mixing of liposome contents. For SNARE liposome fusion in the presence of Ca^{2+}, the $t_{1/2}$ was 15.12 min. For plain liposomes, it was 40.97 min.

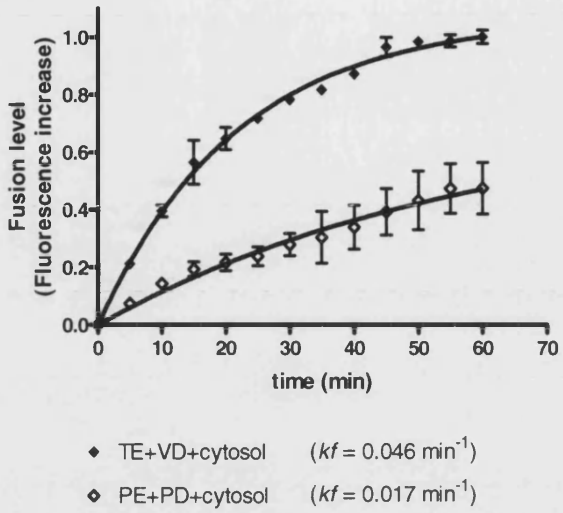

Fig 7.11 Ca^{2+} and cytosol induced fusion. 50 µl of Eu liposomes were mixed with 50 µl of DPA liposomes in the presence of 25 µl of cytosol (2.3 mg/ml) from rat adipocytes. Normalization of fluorescence changes was carried out as follows. Fluorescence was plotted from time point 0 at which Ca^{2+} was added. 3.5 µl of 200 mM Ca^{2+} stock was added to achieve free Ca^{2+} of 100 µM. For SNARE liposomes, the lowest signal before Ca^{2+} was added was F_0. The highest signal after Ca^{2+} was added was F_{100}. The Fluorescence level = $(F-F_0) / (F_{100}-F_0)$. For plain vesicles, the lowest signal before Ca^{2+} was added was F'_0. The Fluorescence level = $(F'-F'_0) / (F_{100}-F_0)$. The results were mean ± SEM (n=3).

7.3.6 The effect of different divalent cations effect on SNARE-reconstituted liposome fusion

To determine whether the Ca^{2+} effect observed was specific, another divalent cation Mg^{2+} at the same concentration was used in parallel and in the same assay. As Fig 7.12 shows, no fusion was induced by Mg^{2+}, indicating the induced fusion was a Ca^{2+}-specific effect.

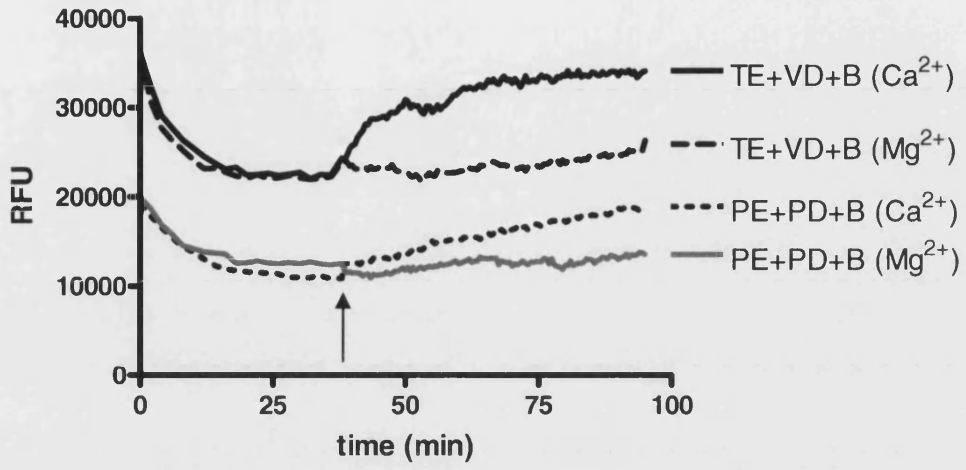

Fig 7.12 The effect of different divalent cations on fusion. 50 µl of Eu liposomes were mixed with 50 µl of DPA liposomes in the presence of 25 µl cytoplasm (2.3 mg/ml) from basal cells (B). The arrow points to the time of Ca^{2+} or Mg^{2+} addition. The fluorescent intensity is expressed as Relative Fluorescent Units (RFU).

7.3.7 Analysis of fusion following BoNT/B cleavage of SNAREs

To study whether the Ca^{2+} and cytoplasm induced fusion is SNARE-dependent, BoNT/B cleaved VD liposomes were compared with the normal VD liposomes. As Figure 7.13 shows that, BoNT/B cleaved liposomes, inactivated BoNT/B liposomes (control), and normal VD liposomes produced the same pattern of fluorescence change in the fusion assay. However, the western blot analysis showed BoNT/B had successfully cleaved the v-SNAREs.

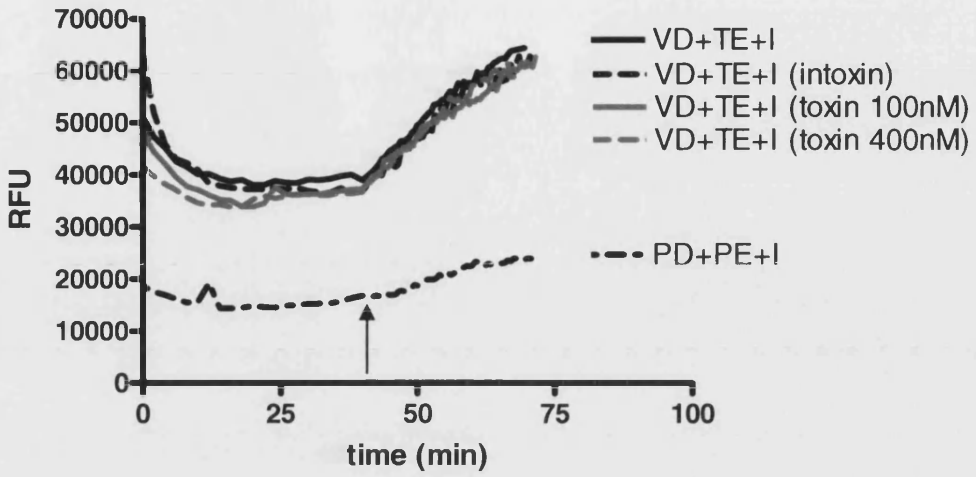

Fig 7.13 Analysis of whether fusion in BoNT/B LC cleaved-liposomes is inhibited. 50 µl of Eu^{3+} liposomes were mixed with 50 µl of DPA liposomes (preincubated with 100 nM (labeled as "toxin 100 nM"), 400 nM BoNT/B ("toxin 400 nM"), inactivated BoNT/B ("intoxin") at 37°C for 1 h) in the presence of 25 µl of cytoplasm from insulin stimulated cells (I) (2.3 mg/ml). The arrow points to the time of Ca^{2+} addition. The fluorescent intensity is expressed as Relative Fluorescent Units (RFU).

7.4 Discussion

The main objective of the work in this chapter was to set up an *in vitro* system to study the fusion that is solely dependent on the SNARE proteins that are present in the system that mediates fusion of GLUT4-containing vesicles with plasma membranes from insulin responsive tissue.

Previous work by Weber *et al* (Weber et al., 1998) has described the successful reconstitution of the neuronal SNAREs in liposomes and their use in an *in vitro* system based on the detection of lipid mixing. The fluorescent probe pair they used was NBD and Rhodamine. The probes were inserted in the phospholipid bilayers. When the two fluorescent probes were in close proximity and in the same liposome, the fluorescence was quenched and no signal was detected. When the fusion occurred, the distance between the two probes was increased and a fluorescent

dequenching occurred, which was detected as the signal of fusion. As described earlier, the drawback of this method is in the hemi-fusion step, in which the probe can go through the "bridge" between liposomes (section 1.4.4). In this case, the distance of the two probes can be enhanced, but fusion is not complete and the content of the two liposomes do not mix. Recently, Vicogne et al set up a very similar system using SNARE protein pairs involved in insulin-stimulated GLUT4 vesicles fusion with plasma membrane (Vicogne et al., 2006). In their report, they described a method to improve the lipid mixing assay. With sodium dithionite in the environment buffer, the outer membrane half-bilayer signal was reduced and a fluorescent signal from only the inner membrane lipids was recorded. In this way the pseudo signal from the hemi-fusion is eliminated as the inner lipids of the bilayers only mix if a full fusion has occurred.

In comparison, the content mixing method which has been used in this chapter (Fig 7.2) has its advantages. It directly gets rid of the hemi-fusion signal to make the fusion detection more convincing. The Eu^{3+}/DPA fluorescence enhancement is a novel assay compared to Tb^{3+}/DPA assay, which has been used in various investigations previously (Chien et al., 1994; Glaser and Gross, 1994; Wilschut et al., 1980; Wilschut and Papahadjopoulos, 1979).

The phospholipid liposome preparation involved a detergent dialysis method and for the most part it followed the method described by Weber *et al.* (Weber et al., 1998) apart from that the lipid solution was diluted two times for the purpose of forming the liposome and encapsulating the Eu^{3+} or DPA. After this the detergent was dialysed out and liposomes were collected after a gradient spin. The whole preparation was first carried out in sodium phosphate buffer pH 7.4 but it was found that Eu^{3+} precipitated with

phosphate (data not shown). Then the buffer was modified to HEPES/NaCl pH 7.4.

Comparing the Vicogne *et al.* and Weber *et al.*'s systems, another major difference appears to be related to the recombinant t-SNARE protein used.

In their systems, t-SNAREs were co-expressed and tagged with either GST (Weber et al., 1998) or poly-His (Vicogne et al., 2006) to further purify the proteins. In Weber's system the respective plasmids pTW19 for syntaxin1A and pGEX-mSNARE25B for GST-SNAP25 were co-transformed. The cytoplasmic t-SNARE complex was purified through glutathione agarose beads. In Vicogne's system syntaxin4 and SNAP23 cDNAs were cloned into the dual protein expression vector pET-duet. In the vector the syntaxin4 coding sequence was cloned in-frame with the N-terminal 6His-tag of the first multicloning site, and the SNAP23 coding sequence was in-frame with the second multicloning site. The t-SNARE complex was purified with Ni-NTA His-Bind Resin. These purifications used in the above two systems enabled the t-SNARE quantification before reconstitution. The quantification was used to adjust and monitor the amount of protein incorporated in liposomes.

In the method used in this chapter, although SNAP23 was tagged with GST, the attempt to purify the t-SNARE complex through glutathione agarose beads was unsuccessful (Ribe, 2005). In the studies of the former PhD student David Ribe, syntaxin4 was observed to stick to the glutathione agarose beads and could not be eluted together with SNAP23 (Ribe, 2005). The main problems lie in the following two aspects. Firstly, the pGEX vector used in t-SNARE co-expression described in this chapter was not designed for protein dual-expression. The system used may potentially cause problems in protein expression and folding. Secondly, t-SNAREs were sequestered in inclusion bodies, and then the inclusion body proteins were

denatured and buffer-exchanged to remove the denaturing reagent guanidine. Under these conditions the proteins were expected to renature but this may not occur efficiently. All these steps may have affected the biological properties of the protein and resulted to the unsuccessful GST purification. The t-SNARE liposomes were therefore reconstituted from the inclusion body protein solution instead of from purified t-SNARE complex (section 2.2.6.2). Because of the transmembrane characteristics of syntaxin4 and the interaction between syntaxin4 and SNAP23, the t-SNAREs were expected to form a complex and insert properly into the liposome membranes in the liposome reconstitution step. In the following gradient spin step (section 2.2.6.2), the reconstituted liposomes were expected to separate from other contamination proteins that were present in the inclusion body protein solution. Hence, using this method, the amount of t-SNARE protein involved in reconstitution could not be monitored and adjusted, leaving more variability from experiment to experiment. Although from the western blot analysis, the t-SNARE proteins after reconstitution appeared to be largely purified as we expected, the un-ideal conditions involved could affect the liposome quality to variable extents: the denaturing-renaturing step could influence the protein stability; the contaminating proteins could affect the efficiency and quality of reconstitution.

The content mixing experiments described in this chapter showed that the simple mixing of the two sets of liposomes does not induce fusion, which is contrary to what is observed both with the neuronal SNAREs (Weber et al., 1998) and GLUT4 fusion SNAREs (Vicogne et al., 2006). Consistency with the findings in Chapters 4 and 5, results described in this chapter suggest that Ca^{2+} and additional elements contained in the cytoplasm are needed. Although attempts to demonstrate SNARE-specific fusion failed, Ca^{2+} did induce the fusion to different extents depending on whether SNARE

liposomes or plain liposomes were used. This finding somewhat implies that the Ca^{2+} effect was not dependent on lipid alone. Also the difference of Ca^{2+} and Mg^{2+} effects on fusion further confirmed that the fusion induced by Ca^{2+} and cytosol described in this chapter was not simply a non-specific divalent cation effect on lipids. However, in other studies Mg^{2+} could produce positive effects for neuronal SNAREs fusion (Fix et al., 2004).

Vicogne *et al* proposed and proved that fusogenic reagents phosphatidic acid (PA) and phosphatidylinositol-4,5-bisphosphate (PIP2) promoted the formation of membrane layer curvature, so as to form hemi-fusion status and eventually full fusion (Vicogne et al., 2006). Through kinetic studies they proved the hemi-fusion step is the rate-limiting factor for the *in vitro* membrane fusion. This conclusion adds new insights into the properties required for SNARE-mediated membrane fusion. It will also be interesting to test this idea in the fusion system described in Chapter 4.

Chapter 8 Final conclusion and discussion

8.1 Conclusion

This thesis demonstrated two *in vitro* fusion systems and investigated the mechanisms involved in insulin-stimulated GLUT4 translocation in rat adipocytes with these two systems.

The first system is composed of reconstituted rat adipocytes plasma membrane liposomes, immuno-isolated GLUT4 vesicles from rat adipocytes, rat adipocytes cytosol and an ATP-regenerating system. Fractions from basal or insulin pre-treated rat adipocytes enable testing of different conditions of interest. Reagents like inhibitors can be added to the system.

The construct of MBP-Spa described in Chapter 3 enabled the generation of an important fraction in the fusion system - biologically active GLUT4 vesicles. In detail, MBP-Spa bound to amylose resin, then bound to C-terminal GLUT4 antibodies and the antibodies immunologically isolated GLUT4 vesicles from rat adipocytes subfractionation. The formed complex was then eluted by maltose. The presence of VAMP2 confirmed that this population of isolated GLUT4 vesicles should be categorized to GLUT4 storage vesicles, which are the most competent intracellular GLUT4 compartments for insulin-stimulated GLUT4 translocation (Larance et al., 2005).

As described in Chapter 4, the system successfully showed different extents of fusion when comparing between basal and insulin-stimulated conditions. With detailed time course curves for both of the conditions, the kinetics were observed to be markedly similar to those of glucose transport recorded in

real cells. This suggested that fusion is the rate-limiting step in insulin-stimulated glucose uptake. The SNARE protein VAMP2 and cytosol were found to be necessary in the fusion event, while cell skeleton was not necessary. Insulin plasma membrane was demonstrated to be the crucial component in supporting fusion. The effect of the insulin signalling cascade on fusion reaction was studied. Inhibition of PI 3-kinase and Akt activities eliminated fusion. Akt was found to be recruited to the insulin plasma membrane and phosphorylated there. The recruitment and phosphorylation promoted fusion.

Preliminarily the studies of Ca^{2+} and V-ATPase effects and requirements in this fusion system have been described in Chapters 5 and 6. Addition of the membrane-permeable strong Ca^{2+} chelator BAPTA-AM and the V-ATPase inhibitor concanamycin A produced inhibition of fusion. However, the studies were insufficiently complete to show a clear picture on their mechanisms of inhibition.

The second system, which is described in Chapter 7, is liposome fusion using reconstituted SNARE proteins. Components of the SNARE system were reconstituted *in vitro* but experiments on fusion failed to provide evidence for SNARE-specificity. Nevertheless, the requirements for cytosol and Ca^{2+} in this fusion did show consistency with the first system, the fusion of GLUT4 vesicles and PM liposomes.

8.2 Discussion

In this thesis the factors that influence insulin-stimulated GLUT4 vesicle fusion with plasma membrane are studied with *in vitro* fusion systems. These factors ranged from the members of insulin signalling cascade to final membrane fusion facilitators.

Several studies have suggested that under conditions in which insulin action is perturbed, some GLUT4 vesicles are released from the intracellular reserve compartment and accumulate under the plasma membrane but do not fuse with it. These studies include the use of a low temperature block (Satoh et al., 1993; van Dam et al., 2005), the use of insulin counter-regulatory treatments with isoproterenol and cytosol acidification (Vannucci et al., 1992; Yang et al., 2002b; Yang et al., 2002a), and inhibition or loss of function of the SNARE-regulatory protein Munc18c (Kanda et al., 2005; Thurmond and Pessin, 2000). One interpretation of these findings is that insulin action on a separate release or transit step involving the cytoskeleton may account for accumulation of non-fused GLUT4 vesicles (Baumann et al., 2000; Kanda et al., 2005; Thurmond and Pessin, 2000; van Dam et al., 2005). However, cytoskeleton components are not directly involved in fusion as no Latrunculin B effect is found using the system described in Chapter 4.

As the available GLUT4 for glucose transport is directly derived from the fusion step, a low basal rate of fusion will rate limit and determine the overall rate of the GLUT4 translocation process. It has been found that the full cellular insulin response on glucose transport is recapitulated in the magnitude, time course and PI 3-kinase dependence of the fusion step. This leads to the hypothesis that insulin regulation of fusion is not only limiting the appearance of GLUT4 at the surface but is indirectly and consequentially influencing the extent to which the internal reserves are emptied, and the extent to which vesicles are associated with the cytoskeleton. This indirect effect could occur if there is queuing for fusion and transit along microtubules. The extent and location of queuing could then be dependent on the extent of release of GLUT4 at the fusion site. Instead of having a regulating role, the cytoskeletal proteins may have a permissive role in allowing and facilitating access of GLUT4 vesicles to the plasma membrane

fusion apparatus (Bose et al., 2004). Perturbation of cytoskeletal proteins including microtubules and actin may block the insulin response in intact cells since the translocation-facilitating function of these proteins would be blocked. Such a queuing mechanism would be consistent with the observation that low concentrations of insulin lead to partial release of GLUT4 to the cell surface (Govers et al., 2004).

Despite advances in the understanding of GLUT4 intracellular trafficking and strong evidence of PI 3-kinase and Akt being crucial regulators of insulin-induced GLUT4 vesicle fusion with plasma membrane, the specific input of Akt signalling to GLUT4 trafficking is still not known. The Akt substrate AS160, as a Rab GTPase-activating protein (GAP), has been found to be required for basal GLUT4 intracellular retention as well as for insulin-induced GLUT4 redistribution to the PM (Sano et al., 2003; Zeigerer et al., 2004). Knockdown of AS160 has resulted in an increase in basal GLUT4 exocytosis (Eguez et al., 2005). However, the range of Akt substrate involvement in insulin-stimulated GLUT4 translocation is not limited to AS160. It has been shown that inhibition of Akt in AS160-knockdown adipocytes can still impair insulin-stimulated GLUT4 exocytosis by two-fold, suggesting that Akt substrates other than AS160 are involved in insulin regulation of GLUT4 exocytosis (Gonzalez et al., 2006). Moreover, it is suggested that signalling pathways other than Akt contribute to the full effect of insulin on GLUT4 redistribution to the plasma membrane (Gonzalez et al., 2006). The observation that insulin promotes an acceleration of GLUT4 exocytosis in Akt1/2 inhibitor (Akti-1/2)-treated AS160-knockdown adipocytes also provides additional evidence for non-Akt–mediated regulation of GLUT4 exocytosis (Gonzalez et al., 2006).

Although the candidates that bridge the insulin signalling cascade and SNARE mediated GLUT4 vesicle fusion with plasma membrane remain

mysterious, the SNARE mediated membrane fusion has been studied extensively. In terms of the kinetics of fusion, in the artificial fusion assays to mimic the synaptic vesicle fusion event, when VAMP is reconstituted in liposomes and t-SNARE in a planar lipid bilayer, the kinetics are similar to those occurring *in vivo* (Fix et al., 2004). When both sets of SNAREs are in liposomes, the reaction is slower (Parlati et al., 1999). Therefore the geometries of the lipid bilayers affect the kinetics of reconstituted fusion. In the system described in Chapter 4, although the size of the plasma membrane liposomes used was remarkably smaller than living cells (data not shown), the kinetics of the fusion is close to the kinetics of insulin-stimulated glucose uptake *in vivo*. This suggests that the system described in Chapter 4 reconstitutes well the real event in cells. In the fusion assay using recombinant t- and v-SNAREs the kinetics are expected to be slower than the real event.

Some reports questioned the requirement for SNAP25 in SNARE-mediated membrane fusion. Reconstituted VAMP2 liposomes and synaptic vesicles are able to fuse with planar lipid bilayers containing only syntaxin1 (Bowen et al., 2004; Woodbury and Rognlien, 2000). SNAP25-knockdown mice show normal vesicle docking and fusion, with stimulus-dependent neurotransmitter release abolished (Woodbury and Rognlien, 2000). It is suggested that SNAP25 and its homologues are more involved in regulating fusion rather than directly participating in catalyzing fusion. SNAP25 and SNAP23 are shown to control the different conditions of granule release by forming docking complexes at different Ca^{2+} thresholds (Chieregatti et al., 2004).

Connecting with the regulation to SNARE-mediated membrane fusion, the effects and functions of the Ca^{2+} chelation and the V-ATPase inhibition of insulin-stimulated GLUT4 vesicle fusion with plasma membrane have also

been intriguing. Ca^{2+} might work as a trigger to break the balance in a "stalk" stage in hemi-fusion and to assist the completion of the fusion. It may also affect Akt signalling in the first place (Whitehead et al., 2001). H^+ gradient generated by V-ATPase can be another trigger for fusion that may assist the SNARE interaction. V-ATPase itself may also work for the formation of a fusion pore.

The cell biology of insulin-stimulated GLUT4 trafficking is complex. Many issues and controversies have yet to be solved. The identification of fusion as the key regulated step in the overall translocation process should facilitate further focus on this topic. Innovative approaches have identified much of the machinery of membrane fusion (Bryant et al., 2002). Further application of such approaches to the problem of insulin regulation of cell glucose metabolism would be expected to be a fruitful avenue of further research. Hopefully these research projects may lead to the better cures for diabetes mellitus.

Reference List

Al Hasani,H., Kunamneni,R.K., Dawson,K., Hinck,C.S., Muller-Wieland,D., and Cushman,S.W. (2002). Roles of the N- and C-termini of GLUT4 in endocytosis. J Cell Sci *115*, 131-140.

Almers,W. (2001). Fusion needs more than SNAREs. Nature *409*, 567-568.

Andersen,G., Rose,C.S., Hamid,Y.H., Drivsholm,T., Borch-Johnsen,K., Hansen,T., and Pedersen,O. (2003). Genetic Variation of the GLUT10 Glucose Transporter (SLC2A10) and Relationships to Type 2 Diabetes and Intermediary Traits. Diabetes *52*, 2445-2448.

Antonin,W., Fasshauer,D., Becker,S., Jahn,R., and Schneider,T. (2002). Crystal structure of the endosomal SNARE complex reveals common structural principles of all SNAREs. Nat Struct Biol. *9*, 107-111.

Augustine,GJ. (2001). How does calcium trigger neurotransmitter release? Curr Opin Neurobiol. *11*, 320-326.

Avery,J., Jahn,R., and Edwardson,J.M. (1999). Reconstitution of regulated exocytosis in cell-free systems: a critical appraisal. Annu. Rev. Physiol. *61*, 777-807.

Bae,S.S., Han,C., Mu,J., and Birnbaum,M.J. (2003). Isoform-specific regulation of insulin-dependent glucose uptake by Akt/PKB. J. Biol. Chem. *278*, 49530-49536.

Bai,J., Tucker,W., and Chapman,ER. (2004a). PIP2 increases the speed of response of synaptotagmin and steers its membrane-penetration activity toward the plasma membrane. Nat Struct Mol Biol. *11*, 36-44.

Bai,J., Wang,C., Richards,D., Jackson,M., and Chapman,E. (2004b). Fusion pore dynamics are regulated by synaptotagmin-t-SNARE interactions. Neuron *41*, 929-942.

Bai,L., Zhu,D., Zhou,K., Zhou,W., Li,D., Wang,Y., Zhang,R., and Xu,T. (2006). Differential Properties of GTP- and Ca2+-Stimulated Exocytosis from Large Dense Core Vesicles. Traffic *7*, 416-428.

Bailey,A. and Cullis,P. (1994). Modulation of membrane fusion by asymmetric transbilayer distributions of amino lipids. Biochemistry *33*, 12573-12580.

Basu,S., Goldstein,JL., Anderson,R., and Brown,M. (1981). Monensin interrupts the recycling of low density lipoprotein receptors in human fibroblasts. Cell. *24*, 493-502.

Baumann,C., Ribon,V., Kanzaki,M., Thurmond,D., Mora,S., Shigematsu,S., Bickel,P., Pessin,J., and Saltiel,A. (2000). CAP defines a second signalling pathway required for insulin-stimulated glucose transport. Nature *407*, 202-207.

Bayer,M.J., Reese,C., Buhler,S., Peters,C., and Mayer,A. (2003). Vacuole membrane fusion: V0 functions after trans-SNARE pairing and is coupled to the Ca2+-releasing channel. J. Cell Biol. *162*, 211-222.

Beckers,C.J., Block,M.R., Glick,B.S., Rothman,J.E., and Balch,W.E. (1989). Vesicular transport between the endoplasmic reticulum and the Golgi stack requires the NEM-sensitive fusion protein. Nature *339*, 397-398.

Bell,G., Kayano,T., and Buse,J. (1990). Molecular biology of mammalian glucose transporters. Diabetes Care *13*, 198-208.

Bennett,PH. (1994). Definition, Diagnosis, and Classification of Diabetes Mellitus and the Imparied Glucose Tolerance. Joslin's Diabetes Mellitus 329-531.

Berwick,D.C., Dell,G.C., Welsh,G.I., Heesom,K.J., Hers,I., Fletcher,L.M., Cooke,F.T., and Tavare,J.M. (2004). Protein kinase B phosphorylation of PIKfyve regulates the trafficking of GLUT4 vesicles. J Cell Sci *117*, 5985-5993.

Beyenbach,K.W. and Wieczorek,H. (2006). The V-type H+ ATPase: molecular structure and function, physiological roles and regulation. J Exp Biol *209*, 577-589.

Bhalla,A., Tucker,W.C., and Chapman,E.R. (2005). Synaptotagmin Isoforms Couple Distinct Ranges of Ca2+, Ba2+, and Sr2+ Concentration to SNARE-mediated Membrane Fusion. Mol. Biol. Cell *16*, 4755-4764.

Birnbaum,MJ. (1989). Identification of a novel gene encoding an insulin-responsive glucose transporter protein. Cell *57*, 305-315.

Blumenthal,R., Gallo,S., Viard,M., Raviv,Y., and Puri,A. (2002). Fluorescent lipid probes in the study of viral membrane fusion. Chem Phys Lipids *116*, 39-55.

Bonifacino,J. and Glick,B. (2004). The mechanisms of vesicle budding and fusion. Cell *116*, 153-156.

Bose,A., Guilherme,A., Robida,S.I., Nicoloro,S.M., Zhou,Q.L., Jiang,Z.Y., Pomerleau,D.P., and Czech,M.P. (2002). Glucose transporter recycling in response to insulin is facilitated by myosin Myo1c. Nature *420*, 821-824.

Bose,A., Guilherme,A., Huang,S., Hubbard,A.C., Lane,C.R., Soriano,N.A., and Czech,M.P. (2005). The v-SNARE Vti1a Regulates Insulin-stimulated Glucose Transport and Acrp30 Secretion in 3T3-L1 Adipocytes. J. Biol. Chem. *280*, 36946-36951.

Bose,A., Robida,S., Furcinitti,P.S., Chawla,A., Fogarty,K., Corvera,S., and Czech,M.P. (2004). Unconventional Myosin Myo1c Promotes Membrane Fusion in a Regulated Exocytic Pathway. Mol. Cell. Biol. *24*, 5447-5458.

Bowen,M.E., Weninger,K., Brunger,A.T., and Chu,S. (2004). Single Molecule Observation of Liposome-Bilayer Fusion Thermally Induced by Soluble N-Ethyl Maleimide Sensitive-Factor Attachment Protein Receptors (SNAREs). Biophys. J. *87*, 3569-3584.

Bowman,E.J., Graham,L.A., Stevens,T.H., and Bowman,B.J. (2004). The Bafilomycin/Concanamycin Binding Site in Subunit c of the V-ATPases from Neurospora crassa and Saccharomyces cerevisiae. J. Biol. Chem. *279*, 33131-33138.

Brochier,G. and Morel,N. (1993). The same 15 kDa proteolipid subunit is a constituent of two different proteins in Torpedo, the acetylcholine releasing protein mediatophore and the vacuolar H+ ATPase. Neurochem Int. *23*, 525-539.

Bron,R., Ortiz,A., and Wilschut,J. (1994). Cellular cytoplasmic delivery of a polypeptide toxin by reconstituted influenza virus envelopes (virosomes). Biochemistry *33*, 9110-9117.

Bron,R., Wahlberg,J., Garoff,H., and Wilschut,J. (1993). Membrane fusion of Semliki Forest virus in a model system: correlation between fusion kinetics and structural changes in the envelope glycoprotein. EMBO J. *12*, 693-701.

Brose,N., Petrenko,AG., Sudhof,T., and Jahn,R. (1992). Synaptotagmin: a calcium sensor on the synaptic vesicle surface. Science *256*, 1021-1025.

Bruton,J., Katz,A., and Westerblad,H. (2001). The role of Ca2+ and calmodulin in insulin signalling in mammalian skeletal muscle. Acta Physiol Scand. *171*, 259-265.

Bruton,J.D., Katz,A., and Westerblad,H. (1999). Insulin increases near-membrane but not global Ca2+ in isolated skeletal muscle. PNAS *96*, 3281-3286.

Bryant,N., Govers,R., and James,D. (2002). Regulated transport of the glucose transporter GLUT4. Nat Rev Mol Cell Biol. *3*, 267-277.

Calderhead,D.M., Kitagawa,K., Tanner,L.I., Holman,G.D., and Lienhard,G.E. (1990). Insulin regulation of the two glucose transporters in 3T3-L1 adipocytes. J. Biol. Chem. *265*, 13800-13808.

Camacho,M., Machado,J., Montesinos,M., Criado,M., and Borges,R. (2006). Intragranular pH rapidly modulates exocytosis in adrenal chromaffin cells. J Neurochem. *96*, 324-334.

Carayannopoulos,M., Schlein,A., Wyman,A., Chi,M., Keembieyhetti,C., and Moley,K. (2004). GLUT 9 is differentially expressed and targeted in the preimplantation embryo. Endocrinology. *145*, 1435-1443.

Carruthers,A. (1990). Facilitated diffusion of glucose. Physiol Rev. *70*, 1135-1176.

Cartee,G., Douen,A., Ramlal,T., Klip,A., and Holloszi,J. (1991). Stimulation of glucose transport in skeletal muscle by hypoxia. J Appl Physiol. *70*, 1593-1600.

Chanturiya,A., Chernomordik,L.V., and Zimmerberg,J. (1997). Flickering fusion pores comparable with initial exocytotic pores occur in protein-free phospholipid bilayers. PNAS *94*, 14423-14428.

Chapman,E.R. and Davis,A.F. (1998). Direct Interaction of a Ca2+-binding Loop of Synaptotagmin with Lipid Bilayers. J. Biol. Chem. *273*, 13995-14001.

Chapman,ER. (2002). Synaptotagmin: a Ca(2+) sensor that triggers exocytosis? Nat Rev Mol Cell Biol. *3*, 498-508.

Charron,M.J., Brosius,F.C., Alper,S.L., and Lodish,H.F. (1989). A Glucose Transport Protein Expressed Predominately in Insulin-Responsive Tissues. PNAS *86*, 2535-2539.

Cheatham,B., Volchuk,A., Kahn,C.R., Wang,L., Rhodes,C.J., and Klip,A. (1996). Insulin-stimulated translocation of GLUT4 glucose transporters requires SNARE-complex proteins. Proc. Natl. Acad. Sci. U. S. A *93*, 15169-15173.

Cheetham,J., Nir,S., Johnson,E., Flanagan,T., and Epand,R. (1994). The effects of membrane physical properties on the fusion of Sendai virus with human erythrocyte ghosts and liposomes. Analysis of kinetics and extent of fusion. J Biol Chem. *269*, 5467-5472.

Chernomordik,L., Melikyan,G., and Chizmadzhev,Y. (1987). Biomembrane fusion: a new concept derived from model studies using two interacting planar lipid bilayers. Biochim Biophys Acta. 309-352.

Chien,K., Chiang,C., Hseu,Y., Vyas,A., Rule,GS., and Wu,W. (1994). Two distinct types of cardiotoxin as revealed by the structure and activity relationship of their interaction with zwitterionic phospholipid dispersions. J. Biol. Chem. *269*, 14473-14483.

Chieregatti,E., Chicka,M.C., Chapman,E.R., and Baldini,G. (2004). SNAP-23 Functions in Docking/Fusion of Granules at Low Ca2+. Mol. Biol. Cell *15*, 1918-1930.

Chunqiu,H.J. and Pessin,J.E. (2003). Lipid Raft targeting of the TC10 amino terminal domain is responsible for disruption of adipocyte cortical actin. Mol. Biol. Cell *14*, 3578-3591.

Civelek,V.N., Hamilton,J.A., Tornheim,K., Kelly,K.L., and Corkey,B.E. (1996). Intracellular pH in adipocytes: Effects of free fatty acid diffusion across the plasma membrane, lipolytic agonists, and insulin. PNAS *93*, 10139-10144.

Cushman,S.W. and Wardzala,L.J. (1980). Potential mechanism of insulin action on glucose transport in the isolated rat adipose cell. Apparent translocation of intracellular transport systems to the plasma membrane. J. Biol. Chem. *255*, 4758-4762.

Czech,M.P. and Corvera,S. (1999). Signaling Mechanisms That Regulate Glucose Transport. J. Biol. Chem. *274*, 1865-1868.

Davis,A., Bai,J., Fasshauer,D., Wolowick,MJ., Lewis,J., and Chapman,E. (1999). Kinetics of synaptotagmin responses to Ca2+ and assembly with the core SNARE complex onto membranes. Neuron *24*, 363-376.

Di Guan,C., Li,P., Riggs,P., and Inouye,H. (1988). Vectors that facilitate the expression and purification of foreign peptides in Escherichia coli by fusion to maltose-binding protein. Gene *67*, 21-30.

Doege,H., Bocianski,A., Joost,H.-G., and Schurmann,A. (2000a). Activity and genomic organization of human glucose transporter 9 (GLUT9), a novel member of the family of sugar transport facilitators predominantly expressed in brain and leucocytes. Biochem J. *350*, 771-776.

Doege,H., Bocianski,A., and Scheepers,A. (2001). Characterization of the human glucose transporter GLUT11, a novel sugar transport facilitator specifically expressed in heart and skeletal muscle. Biochem J. *359*, 443-449.

Doege,H., Schurmann,A., Bahrenberg,G., Brauers,A., and Joost,H.-G. (2000b). GLUT8, a novel member of the sugar transport facilitator family with glucose transport activity. J Biol Chem. *275*, 16275-16280.

Doege,H., Schurmann,A., Ohnimus,H., Monser,V., Holman,G.D., and Joost,H.G. (1998). Serine 294 and threonine 295 in the exofacial loop domain between helices 7 and 8 of glucose transporters (GLUT) are involved in the conformational alterations during the transport process. Biochemical Journal, *329*, 289-293.

Dohm,G., Tapscott EB, Pories WJ, Dabbs DJ, Flickinger EG, Meelheim D, Fushiki T, Atkinson SM, Elton CW, and Caro JF (1988). An in vitro human muscle preparation suitable for metabolic studies. Decreased insulin stimulation of glucose transport in muscle from morbidly obese and diabetic subjects. J Clin Invest. *82*, 486-494.

Draznin,B., Sussman,K., Kao,M., Lewis,D., and Sherman,N. (1987). The existence of an optimal range of cytosolic free calcium for insulin- stimulated glucose transport in rat adipocytes. J. Biol. Chem. *262*, 14385-14388.

Dugani,C. and Klip,A. (2005). Glucose transporter 4: cycling, compartments and controversies. EMBO Rep. *6*, 1137-1142.

Duplay,P., Bedouelle,H., Fowler,A., Zabin,I., Saurin,W., and Hofnung,M. (1988). Sequence of male gene and of its product, the maltose-binding protein of Escherichia coli K12. J Biol Chem *259*, 10606-10613.

Duzgunes,N. and Wilschut,J. (1993). Fusion assays monitoring intermixing of aqueous contents. Methods Enzymol *220*, 3-14.

Eguez,L., Lee,A., Chavez,J., Miinea,C., Kane,S., Lienhard,G., and McGraw,T. (2005). Full intracellular retention of GLUT4 requires AS160 Rab GTPase activating protein. Cell Metab. *2*, 263-272.

Emans,N., Biwersi,J., and Verkman,A.S. (1995). Imaging of endosome fusion in BHK fibroblasts based on a novel fluorimetric avidin-biotin binding assay. Biophys. J *69*, 716-728.

Epand,R., Nir,S., Parolin,M., and Flanagan,T. (1995). The role of the ganglioside GD1a as a receptor for Sendai virus. Biochemistry *34*, 1084-1089.

Etter,E.F., Kuhn,M.A., and Fay,F.S. (1994). Detection of changes in near-membrane Ca2+ concentration using a novel membrane-associated Ca2+ indicator. J. Biol. Chem. *269*, 10141-10149.

Ey,P.L., Prowse,S.J., and Jenkin,C.R. (1978). Isolation of Pure IgG1, IgG2a and IgG2b Immunoglobulins from Mouse Serum using Protein A-sepharose. Immunochemistry. *15*, 429-436.

Falk-Vairant,J., Correges,P., Eder-Colli,L., Salem,N., Roulet,E., Bloc,A., Meunier,F., Lesbats,B., Loctin,F., Synguelakis,M., Israel,M., and Dunant,Y. (1996). Quantal acetylcholine release induced by mediatophore transfection. PNAS *93*, 5203-5207.

Fasshauer,D. (2003). Structural insights into the SNARE mechanism. Biochim Biophys Acta *1641*, 87-97.

Fisher,R., Pevsner,J., and Burgoyne,R. (2001). Control of fusion pore dynamics during exocytosis by Munc18. Science *291*, 875-878.

Fix,M., Melia,T.J., Jaiswal,J.K., Rappoport,J.Z., You,D., Sollner,T.H., Rothman,J.E., and Simon,S.M. (2004). Imaging single membrane fusion events mediated by SNARE proteins. PNAS *101*, 7311-7316.

Fletcher,L., Welsh,G., Oatey,P., and Tavare,J. (2000). Role for the microtubule cytoskeleton in GLUT4 vesicle trafficking and in the regulation of insulin-stimulated glucose uptake. Biochem J. *352*, 267-276.

Foran,P.G.P., Fletcher,L.M., Oatey,P.B., Mohammed,N., Dolly,J.O., and Tavare,J.M. (1999). Protein Kinase B Stimulates the Translocation of GLUT4 but Not GLUT1 or Transferrin Receptors in 3T3-L1 Adipocytes by a Pathway Involving SNAP-23, Synaptobrevin-2, and/or Cellubrevin. J. Biol. Chem. *274*, 28087-28095.

Foster,L.J. and Klip,A. (2000). Mechanism and regulation of GLUT-4 vesicle fusion in muscle and fat cells. Am J Physiol Cell Physiol *279*, C877-C890.

Foster,L., Yeung,B., Mohtashami,M., Ross,K., Trimble,W., and Klip,A. (1998). Binary interactions of the SNARE proteins syntaxin4, SNAP23, and VAMP2 and their regulation by phosphoralation. Biochemistry *37*, 11089-11096.

Fukumoto,H., Kayano,T., and Buse,J. (1989). Cloning and characterization of the major insulin-responsive glucose transporter expressed in human skeletal muscle and other insulin-responsive tissues. J Biol Chem. *264*, 7776-7779.

Fukumoto,H., Seino,S., and Imura,H. (1988). Sequence, tissue distribution, and chromosomal localization of mRNA encoding a human glucose transporter-like protein. Proc Natl Acad Sci U S A. *85*, 5434-5438.

Fuldner,H. and Stadler,H. (1982). 31P-NMR analysis of synaptic vesicles. Status of ATP and internal pH. Eur J Biochem. *121*, 519-524.

Garcia,J.C., Strube,M., Leingang,K., Keller,K., and Mueckler,M.M. (1992). Amino acid substitutions at tryptophan 388 and tryptophan 412 of the HepG2 (GLUT1) glucose transporter inhibit transport activity and targeting to the plasma membrane in *xenopus* oocytes. Journal of Biological Chemistry, *267*, 7770-7776.

Garippa,R.J., Judge,T.W., James,D.E., and McGraw,T.E. (1994). The amino terminus of GLUT4 functions as an internalization motif but not an intracellular retention signal when substituted for the transferrin receptor cytoplasmic domain. J. Cell Biol. *124*, 705-715.

Garippa,R.J., Johnson,A., Park,J., Petrush,R.L., and McGraw,T.E. (1996). The Carboxyl Terminus of GLUT4 Contains a Serine-Leucine-Leucine Sequence That Functions as a Potent Internalization Motif in Chinese Hamster Ovary Cells. J. Biol. Chem. *271*, 20660-20668.

Glaser,P. and Gross,RW. (1994). Plasmenylethanolamine facilitates rapid membrane fusion: a stopped-flow kinetic investigation correlating the propensity of a major plasma membrane constituent to adopt an HII phase with its ability to promote membrane fusion. Biochemistry *33*, 5805-5812.

Goding,J.W. (1978). Use of Staphylococcal Protein A as an Immunological Reagent. Journal of Immunological Methods, *20*, 241-253.

Goncharova,E., Goncharov,D., Noonan,D., and Krymskaya,V.P. (2004). TSC2 modulates actin cytoskeleton and focal adhesion through TSC1-binding domain and the Rac1 GTPase. J. Cell Biol. *167*, 1171-1182.

Gonzalez,E., McGraw, and Timothy E. (2006). Insulin Signaling Diverges into Akt-dependent and -independent Signals to Regulate the Recruitment/Docking and the Fusion of GLUT4 Vesicles to the Plasma Membrane. Mol. Biol. Cell *17*, 4484-4493.

Gould,G. and Holman,GD. (1993). The glucose transporter family: structure,function and tissue-specific expression. Biochem J. *295*, 329-341.

Govers,R., Coster,A.C., and James,D.E. (2004). Insulin increases cell surface GLUT4 levels by dose dependently discharging GLUT4 into a cell surface recycling pathway. Mol. Cell Biol. *24*, 6456-6466.

Graham,M., Washborne,P., Wilson,MC., and Burgoyne,RD. (2002). Molecular Analysis of SNAP-25 Function in Exocytosis. Ann NY Acad Sci *971*, 210-221.

Gridley,S., Lane,W., Garner,C., and Lienhard,G. (2005). Novel insulin-elicited phosphoproteins in adipocytes. Cell Signal. *17*, 59-66.

Han,X., Wang,C., Bai,J., Chapman,E., and Jackson,MB. (2004). Transmembrane segments of syntaxin line the fusion pore of Ca2+-triggered exocytosis. Science *304*, 282-292.

Han,X., Jackson., and Meyer B (2005). Electrostatic Interactions between the Syntaxin Membrane Anchor and Neurotransmitter Passing through the Fusion Pore. Biophys. J. *88*, L20-L22.

Hara,K., Yonezawa,K., Sakaue,H., Ando,A., Kotani,K., Kitamura,T., Kitamura,Y., Ueda,H., Stephens,L., Jackson,T.R., Hawkins,P.T., Dhand,R., Clark,A.E., Holman,G.D., Waterfield,M.D., and Kasuga,M. (1994). 1-phosphatidylinositol 3-kinase activity is required for insulin- stimulated glucose-transport but not for Ras activation in CHO cells. Proc. Natl. Acad. Sci. U. S. A. *91*, 7415-7419.

Hashimoto,M., Yang,J., and Holman,G.D. (2001). Cell-surface recognition of biotinylated membrane proteins requires very long spacer arms: An example from glucose transporter probes. ChemBioChem *2*, 52-59.

Hausdorff,S.F., Fingar,D.C., Morioka,K., Garza,L.A., Whiteman,E.L., Summers,S.A., and Birnbaum,M.J. (1999). Identification of wortmannin-sensitive targets in 3T3-L1 adipocytes. Dissociation of insulin-stimulated glucose uptake and GLUT4 translocation. J. Biol. Chem. *274*, 24677-24684.

Hiesinger,P., Fayyazuddin,A., Mehta,S., Rosenmund,T., Schulze,K., Zhai,R., Verstreken,P., Cao,Y., Zhou,Y., Kunz,J., and Bellen,H. (2005). The v-ATPase V0 subunit a1 is required for a late step in synaptic vesicle exocytosis in Drosophila. Cell *121*, 607-620.

Hodgkinson,C., Mander,A., and Sale,GJ. (2005). Protein kinase-zeta interacts with munc18c: role in GLUT4 trafficking. Diabetologia *48*, 1627-1636.

Hoekstra D. (1990). Fluorescence assays to monitor membrane fusion: potential application in biliary lipid secretion and vesicle interactions. Hepatology *12*, 61-66.

Hoekstra,D., de Boer,T., Klappe,K., and Wilschut,J. (1984). Fluorescence method for measuring the kinetics of fusion between biological membranes. Biochemistry *23*, 5675-5681.

Hoekstra,D. (1990). Fluorescence assays to monitor membrane fusion: potential application in biliary lipid secretion and vesicle interactions. Hepatology *12*, 61-66.

Holloszy,J.O. (2003). A forty-year memoir of research on the regulation of glucose transport into muscle. Am J Physiol Endocrinol Metab *284*, E453-E467.

Holloszy,J.O. (2005). Exercise-induced increase in muscle insulin sensitivity. J Appl Physiol *99*, 338-343.

Holman,G.D. and Kasuga,M. (1997). From receptor to transporter: insulin signalling to glucose transport. Diabetologia *40*, 991-1003.

Holman,G.D., Kozka,I.J., Clark,A.E., Flower,C.J., Saltis,J., Habberfield,A.D., Simpson,I.A., and Cushman,S.W. (1990a). Cell-surface labeling of glucose transporter isoform GLUT4 by Bis-Mannose photolabel: Correlation with stimulation of glucose transport in rat adipose cells by insulin and phorbol ester. J. Biol. Chem. *265*, 18172-18179.

Holman,G., Kozka,I., Clark,A., Flower,C., Saltis,J., Habberfield,A., Simpson,I., and Cushman,S. (1990b). Cell surface labeling of glucose transporter isoform GLUT4 by bis-mannose photolabel. Correlation with stimulation of glucose transport in rat adipose cells by insulin and phorbol ester. J Biol Chem. *265*, 18172-18179.

Holman,G. and Sandoval,IV. (2001). Moving the insulin-regulated glucose transporter GLUT4 into and out of storage. Trends Cell Biol. *11*, 173-179.

Holroyd,C., Kistner,U., Annaert,W., and Jahn,R. (1999). Fusion of Endosomes Involved in Synaptic Vesicle Recycling. Mol. Biol. Cell *10*, 3035-3044.

Hong,W. (2005). SNAREs and traffic. Biochim Biophys Acta *1744*, 493-517.

Hu,C., Ahmed,M., Melia,T., Sollner,TH., Mayer,T., and Rothman,J. (2003). Fusion of cells by flipped SNAREs. Science *300*, 1745-1749.

Ibberson,M., Uldry M, and Thorens B. (2000). GLUTX1, a novel mammalian glucose transporter expressed in the central nervous system and insulin-sensitive tissues. J Biol Chem. *275*, 4607-4612.

Ikonomov,O.C., Sbrissa,D., Mlak,K., and Shisheva,A. (2002). Requirement for PIKfyve Enzymatic Activity in Acute and Long-Term Insulin Cellular Effects. Endocrinology *143*, 4742-4754.

Inoue,G., Cheatham,B., and Kahn,C.R. (1999). Development of an in vitro reconstitution assay for glucose transporter 4 translocation. PNAS *96*, 14919-14924.

Israel,M., Morel,N., Lesbats,B., Birman,S., and Manaranche,R. (1986). Purification of a Presynaptic Membrane Protein that Mediates a Calcium-Dependent Translocation of Acetylcholine. PNAS *83*, 9226-9230.

Jahn,R., Lang,T., and Sudhof,T. (2003). Membrane fusion. Cell *112*, 519-533.

Jahn,R. and Scheller,R. (2006). SNAREs - engines for membrane fusion. Nat Rev Mol Cell Biol. *7*, 631-643.

Jahn,R. and Sudhof,T. (1999). Membrane fusion and exocytosis. Annu Rev Biochem. *68*, 863-911.

Jahn,R. (2004). Principles of Exocytosis and Membrane Fusion. Ann NY Acad Sci *1014*, 170-178.

James,D., Strube,M., and Mueckler,M. (1989). Molecular cloning and characterization of an insulin-regulatable glucose transporter. Nature *338*, 83-87.

Jena,BP. (2004). Discovery of the Porosome: revealing the molecular mechanism of secretion and membrane fusion in cells. J Cell Mol Med. *8*, 1-21.

Jenkins,A. and Campbell,L. (2004). The genetics and pathophysiology of diabetes mellitus type II. J. Inherit. Metab. Dis. *27*, 331-347.

Jiang,Z.Y., Zhou,Q.L., Coleman,K.A., Chouinard,M., Boese,Q., and Czech,M.P. (2003). Insulin signaling through Akt/protein kinase B analyzed by small interfering RNA-mediated gene silencing. PNAS *100*, 7569-7574.

Johnson,L., Dunn,K., Pytowski,B., and McGraw,T. (1993). Endosome acidification and receptor trafficking: bafilomycin A1 slows receptor externalization by a mechanism involving the receptor's internalization motif. Mol Biol Cell. *4*, 1251-1266.

Jones,A.T., Mills,I.G., Scheidig,A.J., Alexandrov,K., and Clague,M.J. (1998). Inhibition of endosome fusion by wortmannin persists in the presence of activated Rab5. Mol. Biol. Cell *9*, 323-332.

Joost,H. and Thorens,B. (2001). The extended GLUT-family of sugar/polyol transport facilitators: nomenclature, sequence characteristics, and potential function of its novel members. Mol Membr Biol. *18*, 247-256.

Kaestner,K., Christy,R., McLenithan,J., Braiterman,L., Cornelius,P., Pekala,P., and Lane,M. (1989). Sequence, tissue distribution, and differential expression of mRNA for a putative insulin-responsive glucose transporter in mouse 3T3-L1 adipocytes. Proc Natl Acad Sci U S A. *86*, 3150-3154.

Kaiser,N., Leibowitz,G., and Nesher,R. (2003). Glucotoxicity and beta-cell failure in type 2 diabetes mellitus. J Pediatr Endocrinol Metab. *16*, 5-22.

Kanda,H., Tamori,Y., Shinoda,H., Yoshikawa,M., Sakaue,M., Udagawa,J., Otani,H., Tashiro,F., Miyazaki,J.i., and Kasuga,M. (2005). Adipocytes from Munc18c-null mice show increased sensitivity to insulin-stimulated GLUT4 externalization. J. Clin. Invest. *115*, 291-301.

Kane,S. and Lienhard,G. (2005). Calmodulin binds to the Rab GTPase activating protein required for insulin-stimulated GLUT4 translocation. Biochem Biophys Res Commun. *335*, 175-180.

Kane,S., Sano,H., Liu,S.C., Asara,J.M., Lane,W.S., Garner,C.C., and Lienhard,G.E. (2002). A method to identify serine kinase substrates. Akt phosphorylates a novel adipocyte protein with a Rab GTPase-activating protein (GAP) domain. J. Biol. Chem. *277*, 22115-22118.

Kanzaki,M. and Pessin,JE. (2003). Insulin signaling: GLUT4 vesicles exit via the exocyst. Curr Biol. *13*, 574-576.

Kapust,RB. and Waugh,D. (1999). Escherichia coli maltose-binding protein is uncommonly effective at promoting the solubility of polypeptides to which it is fused. Protein Sci. *8*, 1668-1674.

Karylowski,O., Zeigerer,A., Cohen,A., and McGraw,T.E. (2004). GLUT4 is retained by an intracellular cycle of vesicle formation and fusion with endosomes. Mol. Biol. Cell *15*, 870-882.

Kawasaki-Nishi,S., Bowers,K., Nishi,T., Forgac,M., and Stevens,T.H. (2001). The Amino-terminal Domain of the Vacuolar Proton-translocating ATPase a Subunit Controls Targeting and in Vivo Dissociation, and the Carboxyl-terminal Domain Affects Coupling of Proton Transport and ATP Hydrolysis. J. Biol. Chem. *276*, 47411-47420.

Kayano,T., Burant,C., and Fukumoto,H. (1990). Human facilitative glucose transporters: isolation, functional characterization, and gene localization of cDNAs encoding an isoform (GLUT5) expressed in small intestine, kidney, muscle, and adipose tissue and an unusual glucose transporter pseudogene-like sequence (GLUT6). J Biol Chem. *265*, 13276-13282.

Kayano,T., Fukumoto,H., and Eddy,R. (1988). Evidence for a family of human glucose transporter-like proteins: sequence and gene localization of a protein expressed in fetal skeletal muscle and other tissues. J Biol Chem. *263*, 15245-15248.

Kelly,K.L., Deeney,J.T., and Corkey,B.E. (1989). Cytosolic free calcium in adipocytes. Distinct mechanisms of regulation and effects on insulin action. J. Biol. Chem. *264*, 12754-12757.

Kessler,A., Tomas,E., Immler,D., Meyer,H., Zorzano,A., and Eckel,J. (2000). Rab11 is associated with GLUT4-containing vesicles and redistributes in response to insulin. Diabetologia *43*, 1518-1527.

Khayat,Z.A., Tong,P., Yaworsky,K., Bloch,R.J., and Klip,A. (2000). Insulin-induced actin filament remodeling colocalizes actin with phosphatidylinositol 3-kinase and GLUT4 in L6 myotubes. J. Cell Sci. *113*, 279-290.

Klip,A., Ramlal,T., and Koivisto,U. (1988). Stimulation of Na+/H+ exchange by insulin and phorbol ester during differentiation of 3T3-L1 cells. Relation to hexose uptake. Endocrinology *123*, 296-304.

Klip,A. and Ramlal,T. (1987). Cytoplasmic Ca2+ during differentiation of 3T3-L1 adipocytes. Effect of insulin and relation to glucose transport. J. Biol. Chem. *262*, 9141-9146.

Klip,A., Ramlal,T., and Cragoe,E.J., Jr. (1986). Insulin-induced cytoplasmic alkalinization and glucose transport in muscle cells. Am J Physiol Cell Physiol *250*, C720-C728.

Kobatake E, Ikariyama Y., Aizawa M, Miwa K, and Kato S (1990). Hyperproduction of a bifunctional hybrid protein, metapyrocatechase-protein A, by gene fusion. Journal of Biotechnology *16*, 87-96.

Kobatake,E., Ikariyama,Y., and Aizawa,M. (1995). Production of the chimeric-binding protein, maltose-binding protein-protein A, by gene fusion. Journal of Biotechnology *38*, 263-268.

Kono,T. (1983). Recycling of insulin-sensitive glucose transporter in rat adipocytes. Methods Enzymol. *98*, 431-444.

Koumanov,F., Jin,B., Yang,J., and Holman,G. (2005). Insulin signaling meets vesicle traffic of GLUT4 at a plasma-membrane-activated fusion step. Cell Metab. *2*, 179-189.

Kozlov,M. and Markin,V. (1983). Possible mechanism of membrane fusion. Biofizika. *28*, 242-247.

Langone,J.J. (1982). Applications of Immobilized Protein A in Immunochemical Techniques. J. Immunol. Methods. *55*, 277-296.

Lanner,J.T., Katz,A., Tavi,P., Sandstrom,M.E., Zhang,S.J., Wretman,C., James,S., Fauconnier,J., Lannergren,J., Bruton,J.D., and Westerblad,H. (2006). The Role of Ca2+ Influx for Insulin-Mediated Glucose Uptake in Skeletal Muscle. Diabetes *55*, 2077-2083.

Larance,M., Ramm,G., Stockli,J., van Dam,E.M., Winata,S., Wasinger,V., Simpson,F., Graham,M., Junutula,J.R., Guilhaus,M., and James,D.E. (2005). Characterization of the Role of the Rab GTPase-activating Protein AS160 in Insulin-regulated GLUT4 Trafficking. J. Biol. Chem. *280*, 37803-37813.

Lawe,D.C., Chawla,A., Merithew,E., Dumas,J., Carrington,W., Fogarty,K., Lifshtz,L., Tuft,R., Lambright,D., and Corvera,S. (2001). Sequential roles for phosphatidylinositol 3-phosphate and Rab5 in tethering and fusion of early endosomes via their interaction with EEA1. J Biol Chem *277*, 8611-8617.

Leabu,M. (2006). Membrane fusion in cells: molecular machinery and mechanisms. J Cell Mol Med. *10*, 423-427.

Lee,W., Ryu,J., Souto,R.P., Pilch,P.F., and Jung,C.Y. (1999). Separation and Partial Characterization of Three Distinct Intracellular GLUT4 Compartments in Rat Adipocytes. Subcellular fractionation without homogenization. J. Biol. Chem. *274*, 37755-37762.

Leng,X.H., Nishi,T., and Forgac,M. (1999). Transmembrane Topography of the 100-kDa a Subunit (Vph1p) of the Yeast Vacuolar Proton-translocating ATPase. J. Biol. Chem. *274*, 14655-14661.

Li,L., Omata,W., Kojima,I., and Shibata,H. (2001). Direct Interaction of Rab4 with Syntaxin 4. J. Biol. Chem. *276*, 5265-5273.

Li,Q., Manolescu,A., and Ritzel,M. (2004). Cloning and functional characterization of the human GLUT7 isoform (SLC2A7) from the small intestine. Am J Physiol Gastrointest Liver Physiol. *284*, G236-G242.

Lindau,M. and Almers,W. (1995). Structure and function of fusion pores in exocytosis and ectoplasmic membrane fusion. Curr Opin Cell Biol. *7*, 509-517.

Lindau,M. and de Toledo,G. (2003). The fusion pore. Biochim Biophys Acta. *1641*, 167-173.

Lindmark,R., Movitz,I., and Sjoquist,J. (1977). Extracellular protein A from a methicillin-resistant strain of Staphylococcus aureus. Eur. J. Biochem. *74*, 623-628.

Lindmark,R., Thoren-Tolling,K., and Sjoquist,J. (1983). Binding of Immunoglobulins to Protein A and Immunoglobulin Levels in Mammalian Sera. J. Immunol. Methods. *62*, 1-13.

Lizunov,V.A., Matsumoto,H., Zimmerberg,J., Cushman,S.W., and Frolov,V.A. (2005). Insulin stimulates the halting, tethering, and fusion of mobile GLUT4 vesicles in rat adipose cells. J. Cell Biol. *169*, 481-489.

Llinas,R., Steinberg,IZ., and Walton,K. (1981). Relationship between presynaptic calcium current and postsynaptic potential in squid giant synapse. Biophys J. *33*, 323-351.

Luiken,J., Coort,S., Koonen,D., van der Horst,D., Bonen,A., Zorzano,A., and Glatz,J. (2004). Regulation of cardiac long-chain fatty acid and glucose uptake by translocation of substrate transporters. Eur J Physiol *448*, 1-15.

Lund,S., Holman,G., Schmitz,O., and Pedersen,O. (1995). Contraction stimulates translocation of glucose transporter GLUT4 in skeletal muscle through a mechanism distinct from that of insulin. Proc Natl Acad Sci U S A. *92*, 5817-5821.

Luzio,J., Pryor,P., Gray,S., Gratian,M., Piper,R., and Bright,N. (2005). Membrane traffic to and from lysosomes. Biochem Soc Symp. *72*, 77-86.

Malide,D., Dwyer,N.K., BlanchetteMackie,E.J., and Cushman,S.W. (1997). Immunocytochemical evidence that GLUT4 resides in a specialized translocation post-endosomal VAMP2-positive compartment in rat adipose cells in the absence of insulin. Journal Of Histochemistry & Cytochemistry *45*, 1083-1096.

Malide,D., Ramm,G., Cushman,S.W., and Slot,J.W. (2000). Immunoelectron microscopic evidence that GLUT4 translocation explains the stimulation of glucose transport in isolated rat white adipose cells. J Cell Sci *113*, 4203-4210.

Martin,O.J., Lee,A., and McGraw,T.E. (2006). GLUT4 Distribution between the Plasma Membrane and the Intracellular Compartments Is Maintained by an Insulin-modulated Bipartite Dynamic Mechanism. J. Biol. Chem. *281*, 484-490.

Martin,S., Tellam,J., Livingstone,C., Slot,J.W., Gould,G.W., and James,D.E. (1996). The glucose transporter (GLUT-4) and vesicle-associated membrane protein-2 (VAMP-2) are segregated from recycling endosomes in insulin- sensitive cells. J. Cell Biol. *134*, 625-635.

Martinez-Arca,S., Lalioti,V.S., and Sandoval,I.V. (2000). Intracellular targeting and retention of the glucose transporter GLUT4 by the perinuclear storage compartment involves distinct carboxyl-tail motifs. J Cell Sci *113*, 1705-1715.

Mayer,A., Wickner,W., and Haas,A. (1996). Sec18p (NSF)-driven release of Sec17p (alpha-SNAP) can precede docking and fusion of yeast vacuoles. Cell. *85*, 83-94.

Mayer,A. (2002). Membrane fusion in eukaryotic cells. Annual Review of Cell and Developmental Biology *18*, 289-314.

Mayer,A. and Wickner,W. (1997). Docking of Yeast Vacuoles Is Catalyzed by the Ras-like GTPase Ypt7p after Symmetric Priming by Sec18p (NSF). J. Cell Biol. *136*, 307-317.

McNew,J., Parlati,F., Fukuda,R., Johnston,R., Paz,K., Paumet,F., Sollner,T., and Rothman,J. (2000). Compartmental specificity of cellular membrane fusion encoded in SNARE proteins. Nature *407*, 153-159.

McVie-Wylie,A., Lamson,D., and Chen,Y. (2001). Molecular cloning of a novel member of the GLUT family of transporters, SLC2A10 (GLUT10), localized on chromosome 20q13.1: a candidate gene for NIDDM susceptibility. Genomics. *72*, 113-117.

Meeusen,S., McCaffery,J., and Nunnari,J. (2004). Mitochondrial fusion intermediates revealed in vitro. Science *305*, 1747-1752.

Melvin DR, Marsh BJ, Walmsley AR., James DE, and Gould GW (1999). Analysis of amino and carboxy terminal GLUT-4 targeting motifs in 3T3-L1 adipocytes using an endosomal ablation technique. Biochemistry *38*, 1456-1462.

Michaelson,D. and Angel,I. (1980). Determination of delta pH in cholinergic synaptic vesicles: its effect on storage and release of acetylcholine. Life Sci. *27*, 39-44.

Miinea,C.P., Sano,H., Kane,S., Sano,E., Fukuda,M., Peranen,J., Lane,W.S., and Lienhard,G.E. (2005). AS160, the Akt substrate regulating GLUT4 translocation, has a functional Rab GTPase-activating protein domain. Biochem. J. *391*, 87-93.

Miller,T. and Stone,HO. (1978). The rapid isolation of ribonuclease-free immunoglobulin G by protein A-sepharose affinity chromatography. J Immunol Methods. *24*, 111-125.

Min,J., Okada,S., Kanzaki,M., Elmendorf,J., Coker,K., Ceresa,B., Syu,L., Noda,Y., Saltiel,A., and Pessin,J. (1999). Synip: a novel insulin-regulated syntaxin 4-binding protein mediating GLUT4 translocation in adipocytes. Mol Cell *3*, 751-760.

Moks,T., Abrahmsen,L., Nilsson,B., Hellman,U., Sjoquist,J., and Uhlen,M. (1986). Staphlycoccal Protein A consists of Five IgG-binding Domains. Eur. J. Biochem. *156*, 637-643.

Morel,N., Gerard,V., and Shiff,G. (1998). Vacuolar H+-ATPase domains are transported separately in axons and assemble in Torpedo nerve endings. J Neurochem. *71*, 1702-1708.

Morel,N. (2003). Neurotransmitter release: the dark side of the vacuolar-H+ATPase. Biol Cell. *95*, 453-457.

Morel,N., Dedieu,J.C., and Philippe,J.M. (2003). Specific sorting of the a1 isoform of the V-H+ATPase a subunit to nerve terminals where it associates with both synaptic vesicles and the presynaptic plasma membrane. J Cell Sci *116*, 4751-4762.

Mori,H., Hashiramoto,M., Clark,A.E., Yang,J., Muraoka,A., Tamori,Y., Kasuga,M., and Holman,G.D. (1994). Substitution of tyrosine 293 of GLUT1 locks the transporter in an outward facing conformation. Journal of Biological Chemistry, *269*, 11578-11583.

Mueckler,M., Caruso,C., and Baldwin,S. (1985). Sequence and structure of a human glucose transporter. Science *229*, 941-945.

Mueckler,M., Weng,W., and Kruse,M. (1994). Glutamine 161 of GLUT1 glucose transporter is critica l for transport activity and exofacial ligand binding. Journal of Biological Chemistry, *269*, 20533-20538.

Mullock,B.M., Perez,J.H., Kuwana,T., Gray,S.R., and Luzio,J.P. (1994). Lysosomes can fuse with a late endosomal compartment in a cell-free system from rat liver. J. Cell Biol. *126*, 1173-1182.

Mullock,B.M., Bright,N.A., Fearon,C.W., Gray,S.R., and Luzio,J. (1998). Fusion of Lysosomes with Late Endosomes Produces a Hybrid Organelle of Intermediate Density and Is NSF Dependent. J. Cell Biol. *140*, 591-601.

Murata,H., Hresko,R.C., and Mueckler,M. (2003). Reconstitution of phosphoinositide 3-kinase-dependent insulin signaling in a cell-free system. J. Biol. Chem. *278*, 21607-21614.

Nelson,N. (2003). A journey from mammals to yeast with vacuolar H+-ATPase (V-ATPase). J Bioenerg Biomembr. *35*, 281-289.

Nelson,N. and Harvey,W.R. (1999). Vacuolar and Plasma Membrane Proton-Adenosinetriphosphatases. Physiol. Rev. *79*, 361-385.

Nielsen,E., Christoforidis,S., Uttenweiler-Joseph,S., Miaczynska,M., Dewitte,F., Wilm,M., Hoflack,B., and Zerial,M. (2000). Rabenosyn-5, a Novel Rab5 Effector,

Is Complexed with hVPS45 and Recruited to Endosomes through a FYVE Finger Domain. J. Cell Biol. *151*, 601-612.

Nishi,T. and Forgac,M. (2002). The vacuolar (H+)-ATPases--nature's most versatile proton pumps. Nat Rev Mol Cell Biol. *3*, 94-103.

Nishi,T. and Forgac,M. (2000). Molecular Cloning and Expression of Three Isoforms of the 100-kDa a Subunit of the Mouse Vacuolar Proton-translocating ATPase. J. Biol. Chem. *275*, 6824-6830.

Oatey,P., Van Weering,D., Dobson,S., Gould,G., and Tavare,JM. (1997). GLUT4 vesicle dynamics in living 3T3 L1 adipocytes visualized with green-fluorescent protein. Biochem J. *327*, 637-642.

Oka,T., Murata,Y., Namba,M., Yoshimizu,T., Toyomura,T., Yamamoto,A., Sun-Wada,G.H., Hamasaki,N., Wada,Y., and Futai,M. (2001). a4, a Unique Kidney-specific Isoform of Mouse Vacuolar H+-ATPase Subunit a. J. Biol. Chem. *276*, 40050-40054.

Palacios,S., Lalioti,V., Martinez-Arca,S., Chattopadhyay,S., and Sandoval,I.V. (2001). Recycling of the Insulin-sensitive Glucose Transporter GLUT4. Access of surface internalized GLUT4 molecules to the perinuclear storage compartment is mediated by the Phe5-Gln6-Gln7-Ile8 motif. J. Biol. Chem. *276*, 3371-3383.

Palfreyman,R.W., Clark,A.E., Denton,R.M., Holman,G.D., and Kozka,I.J. (1992). Kinetic resolution of the separate Glut1 and Glut4 glucose- transport activities in 3t3-l1 cells. Biochem. J. *284*, 275-281.

Parlati,F., Weber,T., McNew,J.A., Westermann,B., Sollner,T.H., and Rothman,J.E. (1999). Rapid and efficient fusion of phospholipid vesicles by the alpha -helical core of a SNARE complex in the absence of an N-terminal regulatory domain. PNAS *96*, 12565-12570.

Patel,N., Huang,C., and Klip,A. (2005). Cellular location of insulin-triggered signals and implications for glucose uptake. European Journal of Physiology *451*, 499-510.

Peak,M., al-Habori,M., and Agius,L. (1992). Regulation of glycogen synthesis and glycolysis by insulin, pH and cell volume. Interactions between swelling and alkalinization in mediating the effects of insulin. Biochem J. *282*, 797-805.

Pedersen,O. and Gliemann,J. (1981). Hexose transport in human adipocytes: factors influencing the response to insulin and kinetics of methylglucose and glucose transport. Diabetologia. *20*, 630-635.

Pereira,L. and Lancha,A.J. (2004). Effect of insulin and contraction up on glucose transport in skeletal muscle. Prog Biophys Mol Biol. *84*, 1-27.

Perin,M., Fried,V., Mignery,G., Jahn,R., and Sudhof,TC. (1990). Phospholipid binding by a synaptic vesicle protein homologous to the regulatory region of protein kinase C. Nature *345*, 260-263.

Peters,C., Bayer,M., Buhler,S., Andersen,J., Mann,M., and Mayer,A. (2001). Trans-complex formation by proteolipid channels in the terminal phase of membrane fusion. Nature *409*, 581-588.

Peters,C. and Mayer,A. (1998). Ca2+/calmodulin signals the completion of docking and triggers a late step of vacuole fusion. Nature *396*, 575-580.

Phay,J., Hussain,H., and Moley,JF. (2000). Strategy for identification of novel glucose transporter family members by using internetbased genomic databases. Surgery. *128*, 946-951.

Ploug,T., Galbo,H., Vinten,J., Jorgensen,M., and Richter,E. (1987). Kinetics of glucose transport in rat muscle: effects of insulin and contractions. Am J Physiol. *253*, 12-20.

Poea-Guyon,S., Amar,M., Fossier,P., and Morel,N. (2006). Alternative Splicing Controls Neuronal Expression of v-ATPase Subunit a1 and Sorting to Nerve Terminals. J. Biol. Chem. *281*, 17164-17172.

Porat,A. and Elazar,Z. (2000). Regulation of Intra-Golgi Membrane Transport by Calcium. J. Biol. Chem. *275*, 29233-29237.

Presley,J.F., Mayor,S., McGraw,T.E., Dunn,K.W., and Maxfield,F.R. (1997). Bafilomycin A1 Treatment Retards Transferrin Receptor Recycling More than Bulk Membrane Recycling. J. Biol. Chem. *272*, 13929-13936.

Pryor,P.R., Mullock,B.M., Bright,N.A., Gray,S.R., and Luzio,J.P. (2000). The Role of Intraorganellar Ca2+ in Late Endosome-Lysosome Heterotypic Fusion and in the Reformation of Lysosomes from Hybrid Organelles. J. Cell Biol. *149*, 1053-1062.

Rea,S., Martin,L.B., McIntosh,S., Macaulay,S.L., Ramsdale,T., Baldini,G., and James,D.E. (1998). Syndet, an Adipocyte Target SNARE Involved in the Insulin-induced Translocation of GLUT4 to the Cell Surface. J. Biol. Chem. *273*, 18784-18792.

Reaves,B. and Banting,G. (1994). Vacuolar ATPase inactivation blocks recycling to the trans-Golgi network from the plasma membrane. FEBS Lett. *345*, 61-66.

Ribe,D. (2005). Insulin signalling and membrane fusion in adipose cells. PhD thesis, University of Bath.

Riggs,P. (2000). Expression and purification of recombinant proteins by fusion to maltose-binding protein. Molecular Biotechnology *15*, 51-63.

Rizzoli,S., Bethani,I., Zwilling,D., Wenzel,D., Siddiqui,T., Brandhorst,D., and Jahn,R. (2006). Evidence for early endosome-like fusion of recently endocytosed synaptic vesicles. Traffic *7*, 1163-1176.

Rogers,S., Chandler,J., Clarke,A., Petrou,S., and Best.JD (2003). Glucose transporter GLUT12-functional characterization in *Xenopus laevis* oocytes. Biochem Biophys Res Commun. *308*, 422-426.

Rothman,J.E. and Sollner,T.H. (1997). Throttles and dampers: controlling the engine of membrane fusion. Science *276*, 1212-1213.

Rothman,J. (1994). Mechanisms of intracellular protein transport. Nature *372*, 55-63.

Rothman,J. and Orci,L. (1992). Molecular dissection of the secretory pathway. Nature *355*, 409-415.

Rudich A, Konrad D., Torok D, Ben-Romano R, Huang C, Niu W, Garg RR, Wijesekara N, Germinario RJ, Bilan PJ, and Klip A (2003). Indinavir uncovers different contributions of GLUT4 and GLUT1 towards glucose uptake in muscle and fat cells and tissues. Diabetologia *46*, 649-658.

Sabatini,B. and Regehr,W. (1996). Timing of neurotransmission at fast synapses in the mammalian brain. Nature *384*, 170-172.

Sambrook,J., Fritsch,E.F., and Maniatis,T. (1989). Molecular Cloning: A Laboratory Manual.

Sandoval,I.V., Martinez-Arca,S., Valdueza,J., Palacios,S., and Holman,G.D. (2000). Distinct Reading of Different Structural Determinants Modulates the Dileucine-mediated Transport Steps of the Lysosomal Membrane Protein LIMPII and the Insulin-sensitive Glucose Transporter GLUT4. J. Biol. Chem. *275*, 39874-39885.

Sano,H., Kane,S., Sano,E., and Lienhard,G. (2005). Synip phosphorylation does not regulate insulin-stimulated GLUT4 translocation. Biochem Biophys Res Commun *332*, 880-884.

Sano,H., Kane,S., Sano,E., Miinea,C., Asara,J., Lane,W., Garner,C., and Lienhard,G. (2003). Insulin-stimulated phosphorylation of a Rab GTPase-activating protein regulates GLUT4 translocation. J Biol Chem. *278*, 14599-14602.

Sato,M. and Mueckler,M. (1999). A conserved amino acid motif (RXGRR) in the GLUT1 glucose transporter is an important determinant of membrane topology. Journal of Biological Chemistry, *274*, 24721-24725.

Satoh,S., Nishimura,H., Clark,A.E., Kozka,I.J., Vannucci,S.J., Simpson,I.A., Quon,M.J., Cushman,S.W., and Holman,G.D. (1993). Use of bismannose photolabel to elucidate insulin-regulated GLUT4 subcellular trafficking kinetics in rat adipose cells. Evidence that exocytosis is a critical site of hormone action. J. Biol. Chem. *268*, 17820-17829.

Scheepers,A., Joost,H.G., and Schurmann,A. (2004). The glucose transporter families SGLT and GLUT: molecular basis of normal and aberrant function. JPEN J Parenter Enteral Nutr *28*, 364-371.

Schimmoller,F., Simon,I., and Pfeffer,S.R. (1998). Rab GTPases, Directors of Vesicle Docking. J. Biol. Chem. *273*, 22161-22164.

Schuette,C.G., Hatsuzawa,K., Margittai,M., Stein,A., Riedel,D., Kuster,P., Konig,M., Seidel,C., and Jahn,R. (2004). Determinants of liposome fusion mediated by synaptic SNARE proteins. PNAS *101*, 2858-2863.

Schurmann,A., Rosenthal W, Hinsch KD, and Joost HG (1989). Differential sensitivity to guanine nucleotides of basal and insulin-stimulated glucose transporter activity reconstituted from adipocyte membrane fractions. FEBS Lett. *255*, 259-264.

Schurmann,A., Doege,H., Ohnimus,H., Monser,V., Buchs,A., and Joost,H.G. (1997). Role of conserved arginine and glutamate residues on the cytosolic surface of glucose transporters (GLUT) for transporter function. Biochemistry *36*, 12897-12902.

Schurmann,A., Keller,K., Monden,I., Brown,F.M., Wandel,S., Shanahan,M.F., and Joost,H.G. (1993). Glucose transport activity and photolabelling with 3-[125]iodo-4-azidophenethylamido-7-0-succinyldeacetyl (IAPS)-forskolin of two mutants at tryptophan-388 and -412 of the glucose transporter GLUT1: dissociation of the binding domains of forskolin and glucose. BiochemicalJournal, *290*, 497-501.

Semiz,S., Park,J., Nicoloro,S., Furcinitti,P., Zhang,C., Chawla,A., Leszyk,J., and Czech,M. (2003). Conventional kinesin KIF5B mediates insulin-stimulated GLUT4 movements on microtubules. EMBO J. *22*, 2387-2399.

Sheffield,P., Garrard,S., and Derewenda,Z. (1999). Overcoming Expression and Purification Problems of RhoGDI Using a Family of "Parallel" Expression Vectors. Protein Expression and Purification *15*, 34-39.

Shewan,A., Marsh,B., Melvin,D., Martin,S., Gould,G., and James,DE. (2000). The cytosolic C-terminus of the glucose transporter GLUT4 contains an acidic cluster endosomal targeting motif distal to the dileucine signal. Biochem J. *350*, 99-107.

Shewan,A.M., van Dam,E.M., Martin,S., Luen,T.B., Hong,W., Bryant,N.J., and James,D.E. (2003). GLUT4 Recycles via a trans-Golgi Network (TGN) Subdomain Enriched in Syntaxins 6 and 16 But Not TGN38: Involvement of an Acidic Targeting Motif. Mol. Biol. Cell *14*, 973-986.

Shi,J. and Kandror,K. (2005). Sortilin is essential and sufficient for the formation of Glut4 storage vesicles in 3T3-L1 adipocytes. Dev Cell. *9*, 99-108.

Silhavy,T., Szmelcman,S., Boos,W., and Schwartz,M. (1975). On the significance of the retention of ligand by protein. Proc Natl Acad Sci U S A. *72*, 2120-2124.

Simpson,I.A., Yver,D.R., Hissin,P.J., Wardzala,L.J., Karnieli,E., Salans,L.B., and Cushman,S.W. (1983). Insulin-stimulated translocation of glucose transporters in the isolated rat adipose cells. Characterization of subcellular fractions. Biochim. Biophys. Acta *763*, 393-407.

Slot,J.W., Geuze,H.J., Gigengack,S., Lienhard,G.E., and James,D.E. (1991). Immuno-localization of the insulin regulatable glucose transporter in brown adipose tissue of the rat. J. Cell Biol. *113*, 123-135.

Smolarsky,M., Teitelbaum,D., Sela,M., and Gitler,C. (1977). A simple fluorescent method to determine complement-mediated liposome immune lysis. J Immunol Methods *15*, 255-265.

Sorensen,JB. (2004). Formation, stabilisation and fusion of the readily releasable pool of secretory vesicles. Pflugers Arch. *448*, 347-362.

Srinivasakumar,N., Ogra,P., and Flanagan,TD. (1991). Characteristics of fusion of respiratory syncytial virus with HEpG-2 cells as measured by R18 fluorescence dequenching assay. J Virol *65*, 4063-4069.

St-Denis,J., Cabaniols,J., Cushman,S., and Roche,PA. (1999). SNAP-23 participates in SNARE complex assembly in rat adipose cells. Biochem J. *338*, 709-715.

Stegmann,T., Doms,R., and Helenius,A. (1989). Protein-mediated membrane fusion. Annu Rev Biophys Chem *18*, 187-211.

Stegmann,T. (2000). Membrane fusion mechanisms: the influenza hemagglutinin paradigm and its implications for intracellular fusion. Traffic. *1*, 598-604.

Struck,D., Hoekstra,D., and Pagano,RE. (1981). Use of resonance energy transfer to monitor membrane fusion. Biochemistry *20*, 4093-4099.

Subtil,A., Lampson,M.A., Keller,S.R., and McGraw,T.E. (2000). Characterization of the Insulin-regulated Endocytic Recycling Mechanism in 3T3-L1 Adipocytes Using a Novel Reporter Molecule. J. Biol. Chem. *275*, 4787-4795.

Sudhof,TC. (1995). The synaptic vesicle cycle: a cascade of protein-protein interactions. Nature *1995*, 645-653.

Sutton,R., Fasshauer,D., Jahn,R., and Brunger,AT. (1998). Crystal structure of a SNARE complex involved in synaptic exocytosis at 2.4 A resolution. Nature *395*, 347-353.

Suzuki,K. and Kono,T. (1980). Evidence that insulin causes translocation of glucose transport activity to the plasma membrane from an intracellular storage site. Proc Natl Acad Sci U S A. *77*, 2542-2545.

Tamori,Y., Kawanishi,M., Niki,T., Shinoda,H., Araki,S., Okazawa,H., and Kasuga,M. (1998). Inhibition of Insulin-induced GLUT4 Translocation by Munc18c through Interaction with Syntaxin4 in 3T3-L1 Adipocytes. J. Biol. Chem. *273*, 19740-19746.

Taylor,L.P. and Holman,G.D. (1981). Symmetrical kinetic parameters for 3-O-methyl-D-glucose transport in adipocytes in the presence and in the absence of insulin. Biochim. Biophys. Acta *642*, 325-335.

Tellam,J.T., Macaulay,S.L., McIntosh,S., Hewish,D.R., Ward,C.W., and James,D.E. (1997). Characterization of Munc-18c and Syntaxin-4 in 3T3-L1 Adipocytes: Putative role in insulin-dependent movement of GLUT4. J. Biol. Chem. *272*, 6179-6186.

Thurmond,D. and Pessin,J. (2000). Discrimination of GLUT4 vesicle trafficking from fusion using a temperature-sensitive Munc18c mutant. EMBO J. *19*, 3565-3575.

Timmers,K., Clark,A., Omatsu-Kanbe,M., Whiteheart,S., Bennett,M., Holman,G., and Cushman,S. (1996). Identification of SNAP receptors in rat adipose cell membrane fractions and in SNARE complexes co-immunoprecipitated with epitope-tagged N-ethylmaleimide-sensitive fusion protein. Biochem J. *320*, 429-436.

Tong,P., Khayat,Z.A., Huang,C., Patel,N., Ueyama,A., and Klip,A. (2001). Insulin-induced cortical actin remodeling promotes GLUT4 insertion at muscle cell membrane ruffles. J. Clin. Invest. *108*, 371-381.

Toyomura,T., Oka,T., Yamaguchi,C., Wada,Y., and Futai,M. (2000). Three Subunit a Isoforms of Mouse Vacuolar H+-ATPase: Preferential expression of the a3 isoform during osteoclast differentiation. J. Biol. Chem. *275*, 8760-8765.

Tuch,B., Dunlop,M., and Proietto,J. (2000). Diabetes Research: A Guide for Postgraduates. Harwood Academic Publishers).

Tucker,W. and Chapman,E. (2002). Role of synaptotagmin in Ca2+-triggered exocytosis. Biochem J. *366*, 1-13.

Tucker,W., Weber,T., and Chapman,E. (2004). Reconstitution of Ca2+-regulated membrane fusion by synaptotagmin and SNAREs. Science *304*, 435-438.

Uhlen,M., Guss,B., Nilsson,B., Gatenbeck,S., Philipson,L., and Lindberg,M. (1984). Complete sequence of the staphylococcal gene encoding protein A. A gene evolved through multiple duplications. J. Biol. Chem. *259*, 1695-1702.

Uldry,M., Ibberson,M., Horisberger,J.-D., Chatton,J.-Y., Riederer,B., and Thorens,B. (2001). Identification of a mammalian H^+ -myo-inositol symporter expressed predominantly in the brain. EMBO J. *20*, 4467-4477.

Uldry,M., Ibberson,M., Hosokawa,M., and Thorens,B. (2002). GLUT2 is a high affinity glucosamine transporter. FEBS Lett. *524*, 199-203.

Ungermann,C., Wickner,W., and Xu,Z. (1999). Vacuole acidification is required for trans-SNARE pairing, LMA1 release, and homotypic fusion. PNAS *96*, 11194-11199.

Uster,PS. (1993). In situ resonance energy transfer microscopy: monitoring membrane fusion in living cells. Methods Enzymol *221*, 239-246.

van Dam,E.M., Govers,R., and James,D.E. (2005). Akt Activation Is Required at a Late Stage of Insulin-Induced GLUT4 Translocation to the Plasma Membrane. Mol Endocrinol *19*, 1067-1077.

Vannucci,S.J., Nishimura,H., Satoh,S., Cushman,S.W., Holman,G.D., and Simpson,I.A. (1992). Cell-surface accessibility of Glut4 glucose transporters in insulin- stimulated rat adipose-cells - modulation by isoprenaline and adenosine. Biochem. J. *288*, 325-330.

Vicogne,J., Vollenweider,D., Smith,J.R., Huang,P., Frohman,M.A., and Pessin,J.E. (2006). Asymmetric phospholipid distribution drives in vitro reconstituted SNARE-dependent membrane fusion. PNAS *103*, 14761-14766.

Wandel,S., Schurmann,A., Becker,W., Summers,S.A., Shanahan,M.F., and Joost,H.G. (1994). Substitution of conserved tyrosine residues in helix 4 (Y143) and 7 (Y293) affects the activity, but not IAPS-forskolin binding, of the glucose transporter GLUT4. FEBS Letters, *348*, 114-118.

Warnock,D.G., Reenstra,W.W., and Yee,V.J. (1982). Na+/H+ antiporter of brush border vesicles: studies with acridine orange uptake. Am J Physiol Renal Physiol *242*, F733-F739.

Watson RT and Pessin JE. (2006). Bridging the GAP between insulin signaling and GLUT4 translocation. Trends Biochem Sci. *31*, 215-222.

Watson,R.T., Khan AH, Furukawa M, Hou JC, Li L, Kanzaki M, Okada S, Kandror KV, and Pessin JE (2004a). Entry of newly synthesized GLUT4 into the insulin-responsive storage compartment is GGA dependent. EMBO J. *23*, 2059-2070.

Watson,R.T., Kanzaki,M., and Pessin,J.E. (2004b). Regulated Membrane Trafficking of the Insulin-Responsive Glucose Transporter 4 in Adipocytes. Endocr Rev *25*, 177-204.

Watson,R. and Pessin,JE. (2006). Bridging the GAP between insulin signaling and GLUT4 translocation. Trends Biochem Sci. *31*, 215-222.

Weber,T., Zemelman,B., McNew,JA., Westermann,B., Gmachl,M., Parlati,F., Sollner,T., and Rothman,J. (1998). SNAREpins: minimal machinery for membrane fusion. Cell *92*, 759-772.

Weimer,R.M. and Jorgensen,E.M. (2003). Controversies in synaptic vesicle exocytosis. J Cell Sci *116*, 3661-3666.

Whitehead,J.P., Molero,J.C., Clark,S., Martin,S., Meneilly,G., and James,D.E. (2001). The Role of Ca2+ in Insulin-stimulated Glucose Transport in 3T3-L1 Cells. J. Biol. Chem. *276*, 27816-27824.

Whiteman,E.L., Cho,H., and Birnbaum,M.J. (2002). Role of Akt/protein kinase B in metabolism. Trends Endocrinol. Metab *13*, 444-451.

Whyte,J.R.C. and Munro,S. (2002). Vesicle tethering complexes in membrane traffic. J Cell Sci *115*, 2627-2637.

Widberg,C.H., Bryant,N.J., Girotti,M., Rea,S., and James,D.E. (2003). Tomosyn Interacts with the t-SNAREs Syntaxin4 and SNAP23 and Plays a Role in Insulin-stimulated GLUT4 Translocation. J. Biol. Chem. *278*, 35093-35101.

Wilschut,J., Duzgunes,N., Fraley,R., and Papahadjopoulos,D. (1980). Studies on the mechanism of membrane fusion: kinetics of calcium ion induced fusion of phosphatidylserine vesicles followed by a new assay for mixing of aqueous vesicle contents. Biochemistry *19*, 6011-6021.

Wilschut,J. and Papahadjopoulos,D. (1979). Ca2+-induced fusion of phospholipid vesicles monitored by mixing of aqueous contents. Nature *281*, 692.

Wilschut,J., Scholma,J., Eastman,S., Hope,M., and Cullis,P. (1992). Ca(2+)-induced fusion of phospholipid vesicles containing free fatty acids: modulation by transmembrane pH gradients. Biochemistry *31*, 2629-2636.

Wood,S. and Trayhurn,P. (2003). Glucose transporters (GLUT and SGLT): expanded families of sugar transport proteins. Br J Nutr. *89*, 3-9.

Woodbury,D. and Rognlien,K. (2000). The t-SNARE syntaxin is sufficient for spontaneous fusion of synaptic vesicles to planar membranes. Cell Biol Int. *24*, 809-818.

Worrall,D.S. and Olefsky,J.M. (2002). The Effects of Intracellular Calcium Depletion on Insulin Signaling in 3T3-L1 Adipocytes. Mol Endocrinol *16*, 378-389.

Wu,X. and Freeze,H. (2002). GLUT14, a duplicon of GLUT3, is specifically expressed in testis as alternative splice forms. Genomics. *80*, 553-557.

Xu,T., Rammner,B., Margittai,M., Artalejo,A., Neher,E., and Jahn,R. (1999). Inhibition of SNARE complex assembly differentially affects kinetic components of exocytosis. Cell *99*, 713-722.

Xu,Z., Huang,G., and Kandror,K.V. (2006). Phosphatidylinositol 4-kinase type II{alpha} is targeted specifically to cellugyrin-positive Glut4-vesicles. Mol Endocrinol me.

Yamada,E., Okada,S., Saito,T., Ohshima,K., Sato,M., Tsuchiya,T., Uehara,Y., Shimizu,H., and Mori,M. (2005). Akt2 phosphorylates Synip to regulate docking and fusion of GLUT4-containing vesicles. J. Cell Biol. *168*, 921-928.

Yang,J. and Holman,G.D. (1993). Comparison of GLUT4 and GLUT1 subcellular trafficking in basal and insulin-stimulated 3T3-L1 cells. J. Biol. Chem. *268*, 4600-4603.

Yang,J., Gillingham,A.K., Hodel,A., Koumanov,F., Woodward,B., and Holman,G.D. (2002a). Insulin-stimulated cytosol alkalinization facilitates optimal activation of glucose transport in cardiomyocytes. Am J Physiol Endocrinol Metab *283*, E1299-E1307.

Yang,J., Hodel,A., and Holman,G.D. (2002b). Insulin and Isoproterenol Have Opposing Roles in the Maintenance of Cytosol pH and Optimal Fusion of GLUT4 Vesicles with the Plasma Membrane. J. Biol. Chem. *277*, 6559-6566.

Yates,A. and Rampersaud,A. (1998). Sphingolipids as receptor modulators. An overview. Ann N Y Acad Sci. *845*, 57-71.

Youn,J.H., Gulve,E.A., Henriksen,E.J., and Holloszy,J.O. (1994). Interactions between effects of W-7, insulin, and hypoxia on glucose transport in skeletal muscle. Am J Physiol Regul Integr Comp Physiol *267*, R888-R894.

Zeigerer,A., McBrayer,M.K., and McGraw,T.E. (2004). Insulin Stimulation of GLUT4 Exocytosis, but Not Its Inhibition of Endocytosis, Is Dependent on RabGAP AS160. Mol. Biol. Cell *15*, 4406-4415.

Zeuzem,S., Feick,P., Zimmermann,P., Haase,W., Kahn,R.A., and Schulz,I. (1992). Intravesicular Acidification Correlates With Binding of ADP-Ribosylation Factor to Microsomal Membranes. PNAS *89*, 6619-6623.

Zhou,Q., Park,J., Jiang,Z., Holik,J., Mitra,P., Semiz,S., Guilherme,A., Powelka,A., Tang,X., Virbasius,J., and Czech,M. (2004). Analysis of insulin signalling by RNAi-based gene silencing. Biochem Soc Trans. *32*, 817-821.

Zimmet,P., Shaw,J., Murray,S., and Sicree,R. (2003). The diabetes epidemic in full flight: forecasting the future. Diabetes Voice *48*, 12-16.

Zueco,J. and Boyd,A. (1992). Protein A fusion vectors for use in combination with pEX vectors in the production and affinity purification of specific antibodies. Gene. *121*, 181-182.

Appendix

1) General buffers

Table 1 Compositions of the buffers used in the general experiments

Name of buffer	Composition
Phosphate Buffered Saline (PBS)	154 mM NaCl, 12.5 mM $Na_2HPO_4.12H_2O$, pH 7.2
Tris Buffered Saline (TBS)	10 mM Tris, pH 7.4, 154 mM NaCl
Tris Buffered Saline – Tween 20 (TBS-T)	10 mM Tris, pH 7.4, 154 mM NaCl, 0.1 % (v/v) Tween-20
Column Buffer for Amylose Resin	20 mM HEPES pH 7.4, 150 mM NaCl
High salt column buffer 1	20 mM HEPES pH 7.4, 500 mM NaCl
High salt column buffer 2	20 mM HEPES pH 7.4, 1 M NaCl
Ni-NTA Wash Buffer	300 mM NaCl, 50 mM sodium phosphate buffer, 20 mM imidazole, pH 8.0
Ni-NTA Elute Buffer	300 mM NaCl, 50 mM sodium phosphate buffer, 250 mM imidazole, pH 8.0
SDS Sample Buffer	Protein samples were solubilised in 2 % (w/v) SDS, 62.5 mM Tris HCl pH 6.8, 0.01 % (w/v) bromophenol blue, and 10 % (v/v) glycerol. The reducing agent was 20 mM Dithiothreitol (DTT) unless otherwise stated
Resolving Gel Buffer	1.5 M Tris HCl, 0.4 % (w/v) SDS, pH 8.8
Stacking Gel Buffer	0.5 M Tris HCl, 0.4 % (w/v) SDS, pH 6.1
Electrophoresis Running Buffer	25 mM Tris HCl, pH 6.3, 0.1 % (w/v) SDS, 0.2 M Glycine
Transfer Buffer	39 mM Glycine, 48 mM Tris, 0.0375 % SDS (w/v), 20 % methanol (v/v), pH 8.8 without adjusting
NUPAGE LDS Sample Buffer	Protein samples were solubilised in 2 % (w/v) LDS, 1.705 % (w/v) Tris Base, 1.665 % (w/v) Tris HCl, 0.015 % (w/v) EDTA, 0.01875 % (w/v) Serva Blue G250, 0.00625 % (w/v) Phenol Red and 10 % (v/v) glycerol, pH 8.5 without adjusting. The reducing agent was 20 mM Dithiothreitol (DTT) unless otherwise stated
NUPAGE MOPS SDS Running Buffer	50 mM MOPS, 50 mM Tris Base, 3.465 mM SDS, 1.025 mM EDTA, pH 7.7 without adjusting
NUPAGE MES SDS Running Buffer	50 mM MES, 50 mM Tris Base, 3.465 mM SDS, 1.025 mM EDTA, pH 7.3 without adjusting
NUPAGE Transfer Buffer	25 mM Bicine, 25 mM Bis-Tris, 1.025 mM EDTA, pH 7.2

	without adjusting
Ponceau S Stain	0.1 % (w/v) Ponceau S, 3 % (w/v) trichloroacetic acid
Stripping Buffer	100 mM β-Mercaptoethanol, 2 % SDS, 62.5 mM Tris HCl, pH 6.7
BCA Reagent B	4 % (w/v) $CuSO_4.5H_2O$
Luria Broth (LB)	1 % (w/v) Bacto™ Tryptone, 0.5 % (w/v) Bacto™ Yeast Extract, 0.5 % NaCl, pH 7.5, autoclaved
Agar Plates	1 % (w/v) Bacto™ Tryptone, 0.5 % (w/v) Bacto™ Yeast Extract, 0.5 % NaCl, 1.5 % (w/v) Agar, pH 7.5, autoclaved
Tris-acetate EDTA (TAE) buffer	40 mM Tris-acetate, pH 8, 1 mM EDTA
TFB1 medium	30 mM potassium acetate, 10 mM $CaCl_2$, 50 mM $MnCl_2$, 100 mM RbCl, 15 % (v/v) glycerol, pH 5.8 with 1 M acetic acid, 0.2 µm filter-sterilized
TFB2 medium	10 mM MOPS or PIPES, 75 mM $CaCl_2$, 10 mM RbCl, 15 % (v/v) glycerol, pH 6.5 with 1 M KOH, 0.2 µm filter-sterilized
IB Wash Buffer for recombinant t-SNAREs	50 mM Tris HCl pH 7.5, 1 mM EDTA, 1 % (w/v) octyl-ß-D-glucoside
Solubilisation buffer for recombinant t-SNAREs	6 M guanidine HCl, 10 mM DTT, 1 % (w/v) octyl-ß-D-glucoside

2) Rat adipocytes buffers

Table 2 Composition of buffers in rat adipocytes experiments

Name of buffer	Composition
Krebs-Ringer-HEPES (KRH) for Adipocytes	140 mM NaCl, 4.7 mM KCl, 2.5 mM $CaCl_2$, 1.25 mM $MgSO_4$, 0.2 mM NaH_2PO_4, 10 mM HEPES, pH 7.4
HEPES-EGTA-Sucrose I (HESI)	250 mM Sucrose, 0.5 mM EGTA, 20 mM HEPES, pH 7.0
HESI Sucrose Cushion	1.12 M Sucrose, 1 mM EDTA, 20 mM HEPES, pH 7.0
Adipocyte Digestion Buffer	3.5 % (w/v) BSA in KRH supplemented with 5 mM glucose and 500 µg/ml Collagenase type 1 from Clostridium histolyticum
Adipocyte Lysis Buffer	2 % (w/v) Nonaethylene glycol monododecyl ether (Thesit) ($C_{30}H_{62}O_{10}$), PBS
Intracellular Buffer (IC buffer)	20 mM HEPES pH 7.4, 140 mM K-glutamate, 5 mM NaCl, 1 mM EGTA

3) Fusion assay buffers

Table 3 Composition of buffers in plasma membrane liposomes and GLUT4 vesicles fusion assay

Name of buffer	Composition
Reconstitution Buffer (RB)	25 mM HEPES pH 7.4, 100 mM KCl, 10 % (w/v) glycerol or ddH_2O, 1 mM DTT
RB for pH fusion assay (low HEPES)	5 mM HEPES pH 7.4, 100 mM KCl, 10 % (w/v) glycerol or ddH_2O, 1 mM DTT
IC buffer for pH fusion assay (high HEPES)	50 mM HEPES pH 7.4 or pH 6 or pH 8.3, 140 mM K-glutamate, 5 mM NaCl, 1 mM EGTA

Table 4 Composition of buffers in SNARE protein reconstituted liposomes fusion assay

Name of buffer	Composition
Reconstitution Buffer for SNARE fusion assay (sRB)	25 mM HEPES pH 7.4, 100 mM NaCl, 1 mM DTT, 1 % (w/v) octyl-glucoside
t-SNARE liposome buffer	25 mM HEPES pH 7.4, 100 mM NaCl, 15 mM $EuCl_3$, 150 mM citrate, 1 mM DTT
v-SNARE liposome buffer	25 mM HEPES pH 7.4, 100 mM NaCl, 150 mM 2,6-pyridinedicaroxylic Acid (dipicolinic Acid, DPA)
Dialysis Buffer	25 mM HEPES pH 7.4, 100 mM NaCl, 1 mM DTT

4) Compositions for resolving and stacking gels

Table 5 Quantities of stock solutions required for 2 mini-gels (Bio-Rad).

Stock Solutions	Resolving gel		Stacking gel
	10 %	15 %	6 %
Acylamide stock solution (ml)	5	7.5	3.4
Resovling gel buffer (ml)	5	5	-
Stacking gel buffer (ml)	-	-	5
Double-distilled water (ml)	5	2.5	7.5
Ammonium persulphate (µl)	100	100	100
TEMED (µl)	8	8	20

Related publication

Koumanov,F., Jin,B., Yang,J., and Holman,G. (2005). Insulin signaling meets vesicle traffic of GLUT4 at a plasma-membrane-activated fusion step. Cell Metab. *2*, 179-189.